

UNCLASSIFIED

AD NUMBER
ADB084976
NEW LIMITATION CHANGE
TO Approved for public release, distribution unlimited
FROM Distribution authorized to U.S. Gov't. agencies only; Proprietary Info.; May 1984. Other requests shall be referred to Air Force Wright Aeronautical Laboratories, Attn: POSF, Wright-Patterson AFB, OH 45433.
AUTHORITY
AFWAL ltr, 27 Mar 1985

THIS PAGE IS UNCLASSIFIED

AD BD 84 976

AUTHORITY:

AFWPL

100, 27 MAR 85-

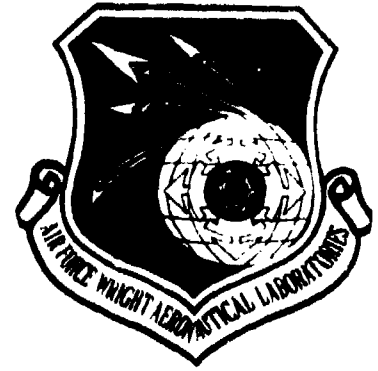


AFWAL-TR-84-2063

EXPERIMENTS AND MODELING OF MULTI-COMPONENT FUEL  
BEHAVIOR IN COMBUSTION

Peter R. Solomon

ADVANCED FUEL RESEARCH, INC.  
87 CHURCH STREET  
EAST HARTFORD, CONNECTICUT 06108



MAY 1984

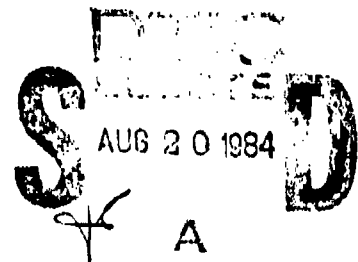
FINAL REPORT FOR PERIOD 30 SEPTEMBER 1983 - 31 MARCH 1984

Distribution limited to U.S. Government agencies only;  
Proprietary Information, May 1984. Other requests for  
this document must be referred to the Aero Propulsion  
Laboratory, AFWAL/POSF, Wright-Patterson AFB, OH 45433.

SUBJECT TO EXPORT CONTROL LAWS

This document contains information for manufacturing or using munitions of war. Export of the information contained herein, or release to foreign nationals within the United States, without first obtaining an export license, is a violation of the International Traffic-in-Arms Regulations. Such violation is subject to a penalty of up to 2 years imprisonment and a fine of \$100,000 under 22 USC 2778.

Include this notice with any reproduced portion of this document.



DTIC FILE COPY

AERO PROPULSION LABORATORY  
AIR FORCE WRIGHT AERONAUTICAL LABORATORIES  
AIR FORCE SYSTEMS COMMAND  
WRIGHT-PATTERSON AIR FORCE BASE, OHIO 45433

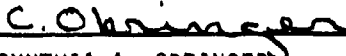
84 08 09 08

AD-B084 976

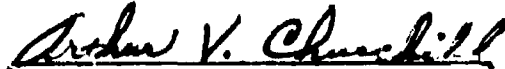
## NOTICE

When Government drawings, specifications, or other data are used for any purpose other than in connection with a definitely related Government procurement operation, the United States Government thereby incurs no responsibility nor any obligation whatsoever; and the fact that the government may have formulated, furnished, or in any way supplied the said drawings, specifications, or other data, is not to be regarded by implication or otherwise as in any manner licensing the holder or any other person or corporation, or conveying any rights or permission to manufacture, use, or sell any patented invention that may in any way be related thereto.

This technical report has been reviewed and is approved for publication.



CYNTHIA A. OBRINGER  
Fuels Branch  
Fuels and Lubrication Division  
Aero Propulsion Laboratory



ARTHUR V. CHURCHILL  
Chief, Fuels Branch  
Fuels and Lubrication Division  
Aero Propulsion Laboratory

FOR THE COMMANDER:



ROBERT D. SHERRILL  
Chief, Fuels and Lubrication Division  
Aero Propulsion Laboratory

"If your address has changed, if you wish to be removed from our mailing list, or if the addressee is no longer employed by your organization please notify AFWAL/POSF, W-P AFB, OH 45433 to help maintain a current mailing list".

Copies of this report should not be returned unless return is required by security considerations, contractual obligations, or notice on a specific document.

## REPORT DOCUMENTATION PAGE

1a. REPORT SECURITY CLASSIFICATION UNCLASSIFIED			1b. RESTRICTIVE MARKINGS			
2a. SECURITY CLASSIFICATION AUTHORITY N/A			3. DISTRIBUTION/AVAILABILITY OF REPORT Distribution limited to U.S. Government agencies only. (Continued)			
2b. DECLASSIFICATION/DOWNGRADING SCHEDULE N/A						
4. PERFORMING ORGANIZATION REPORT NUMBER(S)			5. MONITORING ORGANIZATION REPORT NUMBER(S) AFWAL-TR-84-2063			
6a. NAME OF PERFORMING ORGANIZATION Advanced Fuel Research, Inc.		6b. OFFICE SYMBOL (if applicable)	7a. NAME OF MONITORING ORGANIZATION Aero Propulsion Laboratory Fuels and Lubrication Div (AFWAL/POSF)			
6c. ADDRESS (City, State and ZIP Code) 87 Church Street East Hartford CT 06108			7b. ADDRESS (City, State and ZIP Code) AFWAL/POSF Wright-Patterson AFB OH 45433			
8a. NAME OF FUNDING/SPONSORING ORGANIZATION		8b. OFFICE SYMBOL (if applicable)	9. PROCUREMENT INSTRUMENT IDENTIFICATION NUMBER F33615-83-C-2371			
8c. ADDRESS (City, State and ZIP Code)			10. SOURCE OF FUNDING NOS.			
			PROGRAM ELEMENT NO.	PROJECT NO.	TASK NO.	WORK UNIT NO.
11. TITLE (Include Security Classification) Experiments and Modeling of Multi-Component Fuel Behavior in Combustion			65502F	3005	20	08
12. PERSONAL AUTHOR(S) Peter R. Solomon						
13a. TYPE OF REPORT Phase I Final Report		13b. TIME COVERED FROM Sep 83 to Mar 84		14. DATE OF REPORT (Yr., Mo., Day) May 1984		15. PAGE COUNT 61
16. SUPPLEMENTARY NOTATION						
17. COSATI CODES			18. SUBJECT TERMS (Continue on reverse if necessary and identify by block number)			
FIELD	GROUP	SUB. GR.	Fourier Transform Infrared Spectroscopy			
2102			Field Ionization Mass Spectroscopy			
2104			Fuel Characterization (continued)			
19. ABSTRACT (Continue on reverse if necessary and identify by block number) An important Air Force objective is to develop technology to allow the utilization of aviation fuels with a broader range of properties including lower hydrogen content and higher aromaticity. The objectives of this program are to develop a data base and modeling capabilities to relate vaporization, pyrolysis, and soot formation to the properties of the fuel, the atomizer and combustion conditions. The benefits of reduced soot in jet engines are significant: increased life, improved reliability of combustor liners and reduced pollution. In addition, reduction of the IR emission from military jet engines is important for lowering an aircraft's visibility for tracking and targeting. During Phase I, excellent results were obtained using FT-IR emission and transmission for on-line monitoring of soot and gas concentrations and temperatures. A particularly important feature of the experimental work is the capability of measuring the formation of soot under conditions where the concentration of fuel and oxygen and the temperature are independently controlled, thus eliminating the complications of separating these factors when soot (continued)						
20. DISTRIBUTION/AVAILABILITY OF ABSTRACT UNCLASSIFIED/UNLIMITED <input checked="" type="checkbox"/> SAME AS RPT. <input type="checkbox"/> DTIC USERS <input type="checkbox"/>			21. ABSTRACT SECURITY CLASSIFICATION UNCLASSIFIED			
22a. NAME OF RESPONSIBLE INDIVIDUAL C. A. Obringer			22b. TELEPHONE NUMBER (Include Area Code) (513) 255-7487		22c. OFFICE SYMBOL AFWAL/POSF	

Block 18 continued

Gas Turbine Combustion	Pyrolysis
Droplet Vaporization	Soot Production
High Pressure Entrained Flow Reactor	Combustion Modeling

Block 19 continued

measurements are performed under combustion conditions. The study of four fuels has led to the identification of a controlling factor in soot formation which provides a better correlation with sooting behavior than total hydrogen or aromaticity. A major focus of future work will be to identify how this parameter can be measured, the mechanisms by which it affects soot production and methods for controlling soot.

Block 3 continued

Proprietary information, May 1984. Other requests for this document must be referred to the Aero Propulsion Laboratory, AFWAL/POSF, Wright-Patterson AFB OH 45433.

Table of Contents

<u>Section</u>	<u>Title</u>	<u>Page</u>
1.	INTRODUCTION .....	1
	1.1 The Problem .....	1
	1.2 The Solution .....	1
	1.3 Phase I - Technical Objectives .....	2
	1.4 Summary of Phase I Accomplishments .....	2
2.	DISCUSSION OF PHASE I RESULTS .....	4
	2.1 Measurements of Vaporization, Pyrolysis, Combustion and Radiative Emission Behavior of a Fuel Droplet Stream in the Entrained Flow Reactor (Phase I - Task I) .....	4
	2.2 Fuel Characterization (Phase I - Task II) .....	22
	2.3 Droplet Generation and Vaporization .....	26
	2.4 Application of Vaporization and Pyrolysis Model in Conjunction with Literature Models to Simulate the Experimental Results (Phase I - Task III) .....	31
3.	DISCUSSION .....	44
4.	CONCLUSIONS AND RECOMMENDATIONS .....	53
5.	REFERENCES .....	54



B-3	
-----	--

## 1. INTRODUCTION

### 1.1 The Problem

An important Air Force objective is to develop technology to allow the utilization of aviation fuels with a broader range of properties including lower hydrogen content and higher aromaticity. Such fuels will be increasingly important as the sources shift to heavier petroleum, oil shale, tar sands and coal derived fuels. The combustion of such fuels adds substantial complexities to fuel volatilization and pyrolysis, and increases the potential for higher radiative emission from soot, reducing the useful life of turbine combustors (1,2). Also, the smoke emitted from an engine, resulting from unburned soot, is both a pollutant and a problem due to increased visibility for detecting and targeting of military aircraft.

Current research suggests that the sooting potential of an aircraft fuel increases with decrease in hydrogen (1) or alternatively, increases with increasing aromatic content (2). The problem is, therefore, to provide fuel specification, fuel processing strategies and combustion design concepts to reduce soot, but which still allow utilization of readily available fuels. While many trends have been established, there is no accepted model for soot formation. This lack of understanding hinders our ability to provide combustor design and fuel specifications. For example, Lefebvre (2) points out that "it is quite possible that not all of the various types of aromatics (1-ring, 2-ring, etc) are equally effective in producing soot and thus a better correlation of smoke emission might be achieved by neglecting certain aromatic constituents of the fuel."

To develop the appropriate technology to utilize such fuels, it is desirable to develop capabilities to experimentally study and theoretically model the combustion of sprays of multi-component fuels, including fuels with higher boiling fractions and aromatic and heteroatom components. Such models will be necessary input to the large computer codes which calculate the characteristics of two phase reacting flows in two and three dimensions (3-7). The current level of understanding of droplet and spray combustion is discussed in several reviews (8-13). For the simplest case of isolated, single component, volatile paraffin drops, the " $d^2$ "-Law model has been well established. For this case it is assumed that the fuel vaporizes from a homogeneous fuel drop and diffuses to the flame zone without cracking and without radiative absorption or emission. For higher molecular weight fuels with aromatic components, separation of components during vaporization, pyrolysis of the fuel, soot formation, and radiative absorption and emission by the soot become important.

### 1.2 The Solution

\* The objectives of this program were to develop a data base and modeling capabilities  
\* to relate vaporization, pyrolysis, and soot formation to the properties of the fuel,  
\* the atomizer and combustion conditions. It is soot generation and its radiation  
\* which appears to be the major problem. Based on the Phase I results, it appears  
\* that the "hydrogen available for release" in pyrolysis controls soot production. A  
\* major focus of the further work will be to identify how this parameter can be  
\* measured, the mechanisms by which it affects soot production and methods based on  
\* these mechanisms for controlling soot. The relation between soot production and  
\* "available hydrogen" is discussed in more detail in Sec. 2.

\* The Phase I program has demonstrated that substantial progress can be made in  
\* developing a general fuel combustion model by employing successful experimental and  
\* theoretical methods already developed at Advanced Fuel Research, Inc. for  
\* characterization of complex hydrocarbons in combustion and gasification. The  
\* development of the experimental and modeling techniques have been sponsored by the

"Use or disclosure of the proposal data on lines specifically identified by asterisk (\*) are subject to the restriction on the cover page of this proposal."



United States Department of Energy (14,15), the National Science Foundation (16,17), the Electric Power Research Institute (18,19), and the Gas Research Institute (20,21). Successful application of these techniques for fuel studies was demonstrated in Phase I.

### 1.3 Phase I - Technical Objective

- Demonstrate the capabilities of a high temperature entrained flow reactor with on-line, in-situ analysis by FT-IR to measure pyrolysis species temperature and radiation characteristics.
- Provide data on vaporization and pyrolysis of a multi-component liquid drop stream.
- Perform characterization of the fuel by quantitative FT-IR, FIMS and programmed pyrolysis/FT-IR.
- Correlate volatile amounts and rates with fuel characteristics.
- Select appropriate models for various elements of fuel volatilization.
- Answer questions on amount of distillation in vaporization, pyrolysis of volatiles, soot formation and coking.

### 1.4 Summary of Phase I Accomplishments

- \* ● Excellent results obtained using FT-IR emission and transmission for on-line monitoring of soot and gas concentrations and temperatures. (See Section 2.1).
- \* ● Quantitative data obtained for vaporization, pyrolysis, and soot formation for JP-4, JP-7, dodecane and ERBS at temperatures up to 1573K. (See Section 2.1).
- \* ● Good correlation obtained between radiative emission intensity and weight of soot collected. (See Sec. 2.1).
- \* ● Observation of substantially different soot production for three multi-component and four pure hydrocarbon fuels. The variation correlates with aromatic content but not with hydrogen content (JP-4 which has a higher hydrogen content than JP-7 produced substantially more soot). (See Section 2.1).
- \* ● Good correlation of soot radiative emission intensity under pyrolysis conditions with smoke point and soot produced in a jet engine at take-off conditions (see Sec. 3).
- \* ● Possible identification of a controlling factor in soot formation ("hydrogen released during pyrolysis") which provides a better correlation with sooting behavior than total hydrogen or aromaticity. (See Section 3 for discussion of results).
- \* ● Observation of the effect of oxygen in increasing soot at low concentrations and decreasing soot at high concentrations. (This effect is discussed in Sec. 2.1 and Sec. 3).

\*Use or disclosure of the proposal data on lines specifically identified by asterisk (\*) are subject to the restriction on the cover page of this proposal.\*

- ★ ● Demonstration of FT-IR and FIMS for quantitative characterization of fuel including factors controlling soot production. (See Section 2.2).
- ★ ● Observation of fuel composition changes in vaporization and pyrolysis by FT-IR. The changes fall between the results expected for distillation and for complete mixing. (See Section 2.3).
- ★ ● Development of gas phase cracking model for fuel components. (See Section 2.4).
- ★ ● Demonstration of temperature programmed/FIMS for fuel characterization. (See Section 2.2).

"Use or disclosure of the proposal data on lines specifically identified by asterisk (\*) are subject to the restriction on the cover page of this proposal."

## 2. PHASE I RESULTS

### 2.1. Measurements of Vaporization, Pyrolysis, Combustion and Radiative Emission Behavior of a Fuel Droplet Stream in the Entrained Flow Reactor. (Phase I - Task I)

The objective of Phase I, Task I, was to elucidate the coupled vaporization, pyrolysis and soot production behavior of a series of increasingly complicated fuels in an entrained flow reactor with on-line, in-situ FT-IR spectroscopy. The fuel series consisted of: i) a single component paraffin (dodecane); ii) a multi-component aviation fuel with low aromaticity (JP-7); iii) a jet fuel with higher aromaticity (JP-4); and iv) a heavy multi-component fuel (ERBS).

#### Experimental

The entrained flow reactor is shown in Fig. 1. It employs a Nicolet 7199 FT-IR for in-situ analysis of gas species and gas temperature and quantitative analysis of the gas composition after cooling. To operate the reactor, a gas stream of predetermined composition is heated during transit through the heat exchanger (maintained at furnace temperature). The gas stream then turns through the U-tube and enters a 5 cm diameter test section, maintained at the furnace temperature. Fuel was introduced into the test section at variable positions through a movable water cooled injector. The fuel was injected as a droplet stream by passing the liquid through a section of 100 micron ID hypodermic tubing and mechanically vibrating the feed tube assembly at the natural drop formation frequency. After a variable residence time, the reacting stream passes optical access ports and, immediately downstream, is quenched in a water cooled collector. There are five optical access ports, of which two are presently employed for the FT-IR beam. The other three ports are available for additional diagnostics.

After quenching, the product stream is passed through a cyclone to separate out particulates larger than 4 microns. The remaining stream of gas, condensed oil mist and soot is collected in a bag. A gas sample is drawn from the bag for analysis by FT-IR spectroscopy. Solids are collected on the bag walls and in a filter when the bag is pumped out. The bag can be used to study the settling time of the suspended solids as a means of determining particle size distributions.

Figure 2 compares the spectra from the in-situ analysis and room temperature gas cell analysis for the furnace at 1100°C. In transmission measurements, radiation from a globar source passes through the interferometer before traversing the reactor to the detector. In passage through the interferometer the radiation gets amplitude modulated as a function of wavelength, and it is only modulated radiation that is detected. In this way the transmission experiment measures the extinction, independent of emission from the furnace. Easily seen in the hot spectrum are CO, CO<sub>2</sub>, H<sub>2</sub>O, CH<sub>4</sub>, and heavy paraffins. The lower noise of the room temperature spectrum permits the measurement of additional species including C<sub>2</sub>H<sub>2</sub>, C<sub>2</sub>H<sub>4</sub>, C<sub>2</sub>H<sub>6</sub>, C<sub>3</sub>H<sub>6</sub>, HCN, NH<sub>3</sub>, COS, CS<sub>2</sub>, SO<sub>2</sub>, and heavy olefins. This spectrum is used for quantitative analysis. A typical gas analysis together with the yield of solids and liquids is presented in Table I.

The relative intensities of the hot CO absorption lines can be used for measuring gas temperature (22). Figure 3 compares the in-situ CO spectra at measured furnace temperatures of 20°C and 950°C; the calculated temperatures from line intensities are 30°C and 1050°C.

The FT-IR can be operated to measure emission (35). Radiation from emission within the entrained flow reactor emerges through a KBr window, and is directed by mirrors

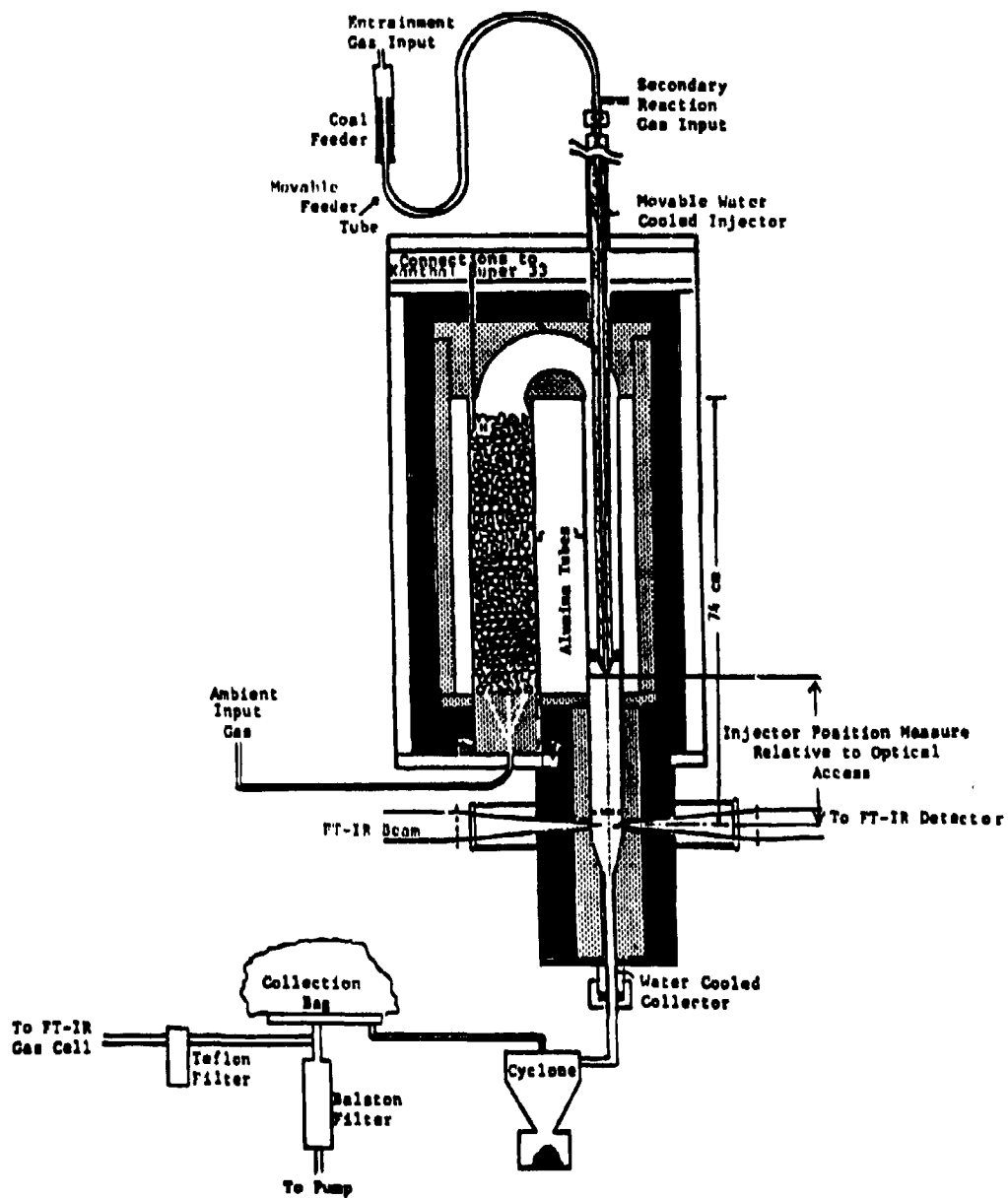


Figure 1. Schematic of Entrained Flow Reactor.

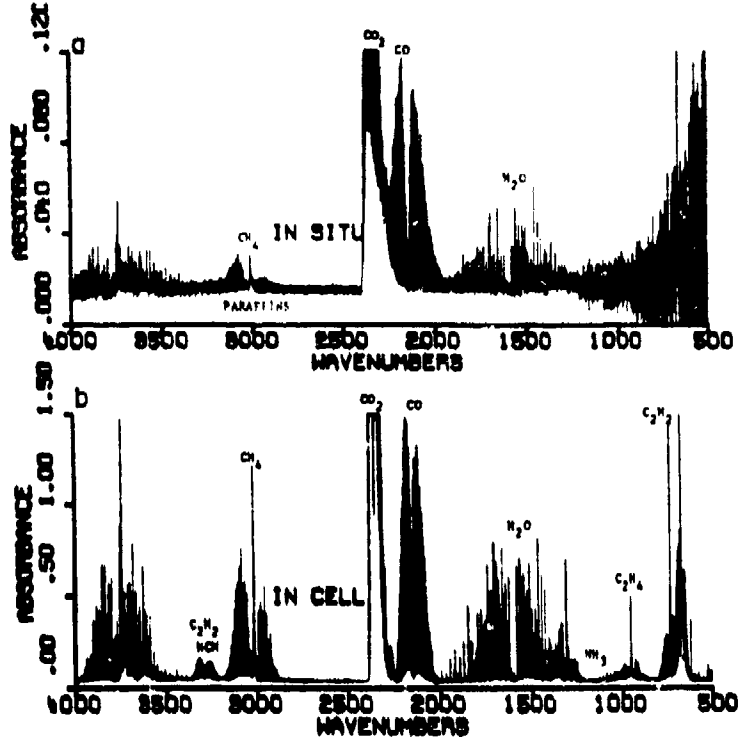


Figure 2. FT-IR Spectra of Pyrolysis Gases from Seulah, North Dakota Lignite at 1100°C. a) In-situ Spectrum, b) Room Temperature Cell Spectrum.

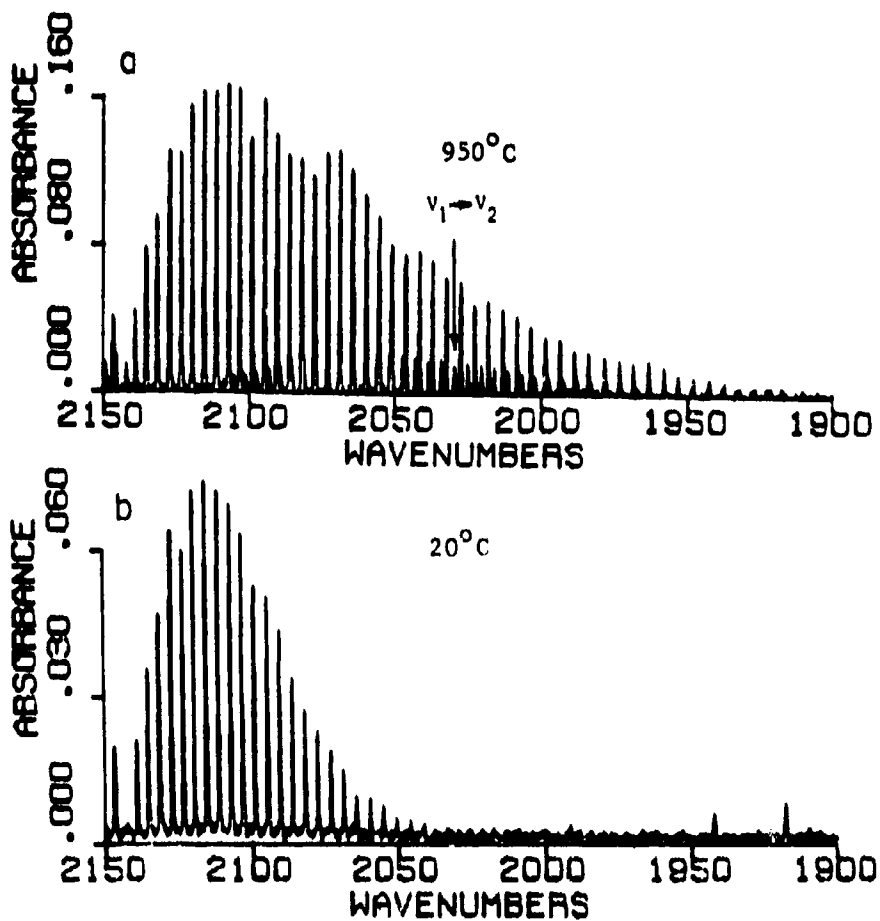


Figure 3. Spectra of Carbon Monoxide in Furnace at 950 and 20°C.

TABLE I

## Quantitative Analysis of Pyrolysis Products

## PYROLYSIS SUMMARY REPORT - FAFRUN 19

## RUN CONDITIONS

3600 mg. NO COAL

1300 Degrees c.

754.500 mm. Final Pressure for 82.8524 liters

## Fuel

Name : JP7 - 24

## PYROLYSIS PRODUCT DISTRIBUTION

	Wt. %
Soot	44.3660
Oil	0
Gas	32.1700
Water	2.05846
Missing	21.4054

## GAS COMPOSITION

	Wt. %	Volume %
Methane	2.75819	.28523
CO	1.22922	.07263
Hydrogen	0	0
CO2	7.62343E-4	2.86680E-5
Acetylene	2.92771	.18631
Ethylene	4.21738	.24922
Ethane	.32221	1.77713E-2
Propylene	2.37902	.09372
Benzene	4.29908	.09119
Paraffins	4.59319	.09047
Olefins	9.14044	.18004
HCN	.25326	1.55208E-2
Ammonia	1.43669E-3	1.39835E-4
COS	-5.15781E-4	-1.42237E-5
CS2	4.77412E-2	1.03939E-3
SO2	8.30467E-4	2.14705E-5
Water	2.05846	.13099
Other	0	98.5856
Gas Total:	34.2284	100

onto the FT-IR spectrometer, from which it passes to a HgCdTe detector. The overall detection efficiency for this path is wavelength dependent, and must be corrected for. This is done by placing a "black-body" standard, a blackened stainless steel rod of known temperature, within the reactor, and measuring its spectra. The path correction at each wavelength is found by dividing the observed intensity, corrected for background, by the theoretical "black-body" curve appropriate to the rod temperature measured with a thermocouple.

It has been shown that the use of the outer surface of a blackened stainless steel rod as a gray body standard can lead to systematic errors in temperature determinations of up to 20 K (36). This deficiency in the present measurements will be corrected in future studies by the use of a cavity emitter.

Measurements of soot emission have been made previously by Vervisch and Coppalle (37) and by Buckius and Tien (38) in oxidizing atmospheres. The advantage of the present method is speed, (a spectrum can be obtained in less than 1 sec) and both spectral and spatial resolution. A single spectrum of lower resolution presented by Vervisch and Coppalle required three hours to obtain (37).

### Pyrolysis Results

Figure 4a shows a series of emission spectra taken from pyrolysis of JP-4 fuel in the reactor at 1300°C. The spectra were accumulated over a series of reaction distances from 6 to 66 cm, all in under 6 minutes. The gas velocity is 1 meter/sec giving a maximum residence time of 660 msec. At short reaction distances there is evidence of the paraffinic fuel. As the distances increase, the paraffins crack to form olefins and the olefins crack to form acetylene until at 36 cm there appears a broad emission due to soot.

Figure 4b shows the corresponding transmission spectra. The absorption of radiation by soot results in the sloping spectra for 46 and 66 cm. Figure 5 shows data for 1100°C for the same fuel. The data show cracking of paraffins to methane, olefins and acetylene, but no soot formation. At 800°C (Fig. 6) there is little cracking at all.

Quantitative product distributions obtained from collection of solids and liquids and analysis of the gas in a room temperature cell are compared for JP-7 and JP-4 fuels at 1300°C in Figs. 7 and 8. The general trend validates the observation from the emission spectra. First vaporization of the fuel, followed by cracking to light paraffins, olefins, and benzene, and further cracking to methane and acetylene accompanied by soot formation. The trends are similar for the two fuels except that JP-4 produces more methane than JP-7. Both fuels show substantial benzene production.

Data for JP4 at 1100 and 800°C are presented in Figs. 9 and 10. At 1100°C (Fig. 9) the cracking pattern is similar to that at 1300°C but occurs at longer residence times. Also, the drop off in the concentration at longer residence times seen for 1300°C occurs later and is not as severe for 1100°C. This drop off coincides with soot production and as can be seen from the emission in Figs. 5 and 6, soot production at 800°C and 1100°C is minimal. The 1100°C case also show substantial benzene. At 800°C (Fig. 10), little cracking occurs. The fact that no benzene is observed at 800°C indicates that the 6-8% benzene observed at 1100 and 1300°C is a pyrolysis product.

### Soot Formation in Pyrolysis

Tests using variable drop feed vibration frequencies showed that with our apparatus

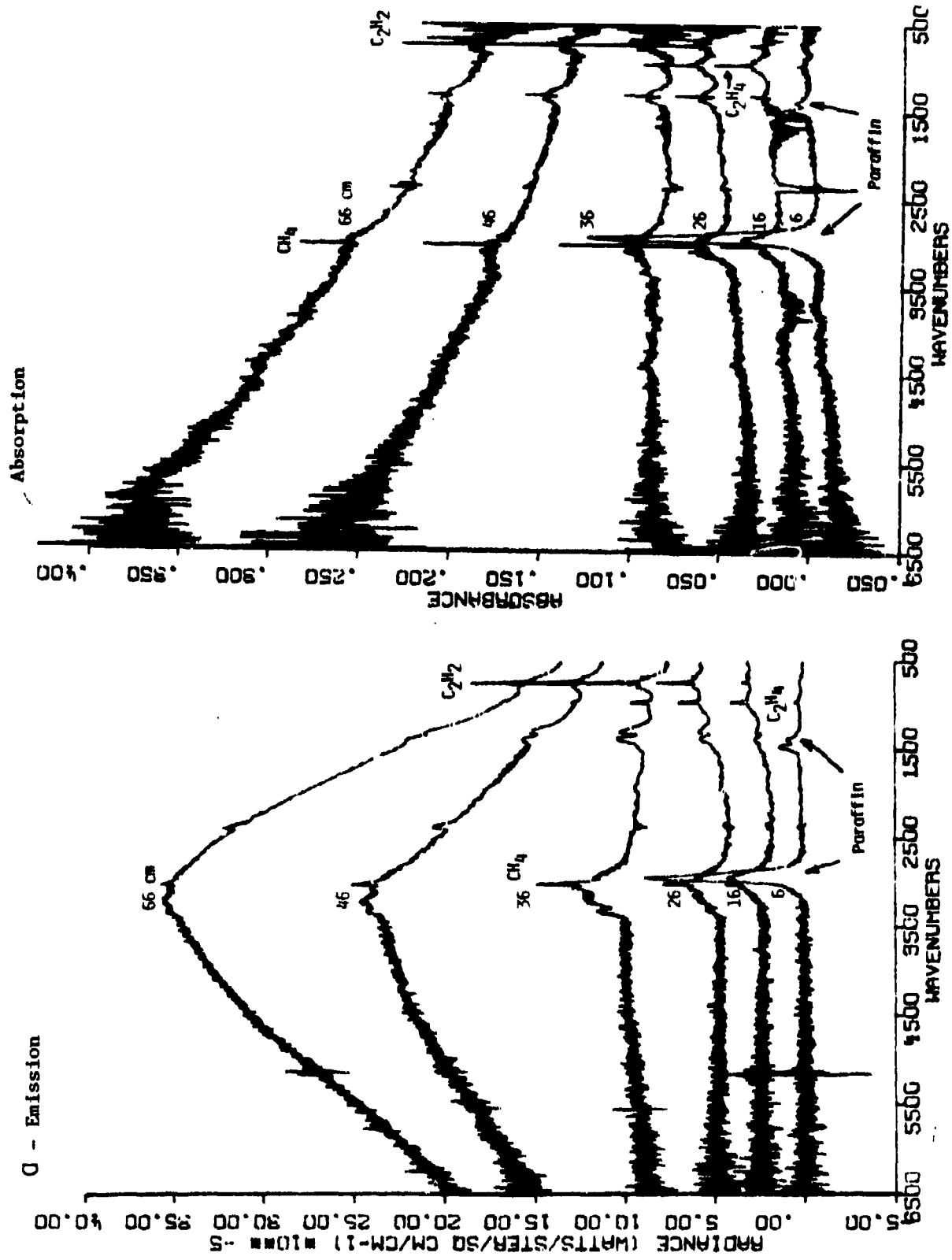


Figure 4. FT-IR Emission and Absorption Spectra for JP-4 Fuel at 1300°C at Several Reaction Distances.



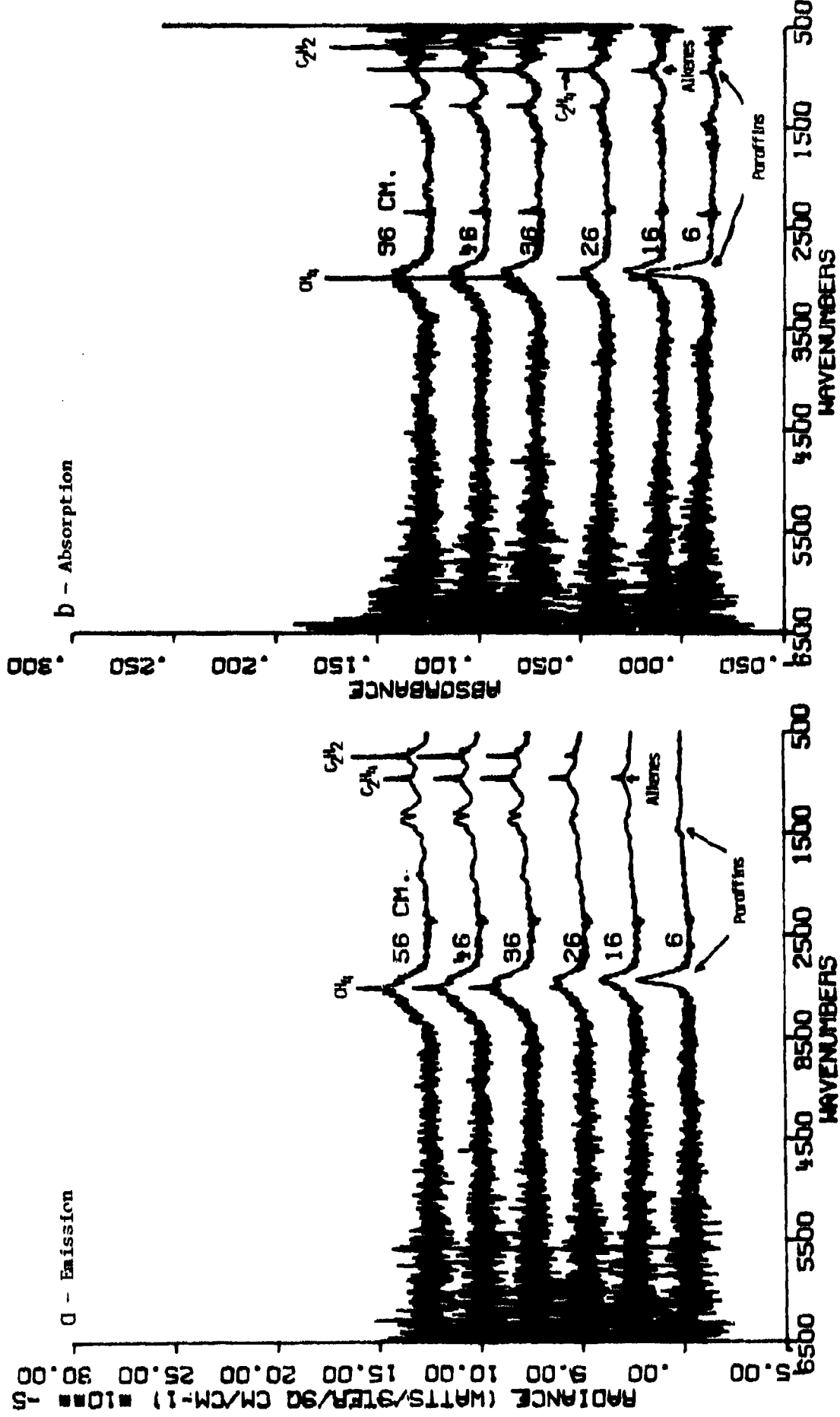


Figure 5. FT-IR Emission and Absorption Spectra for JP-4 Fuel at 1100°C at Several Reaction Distances.

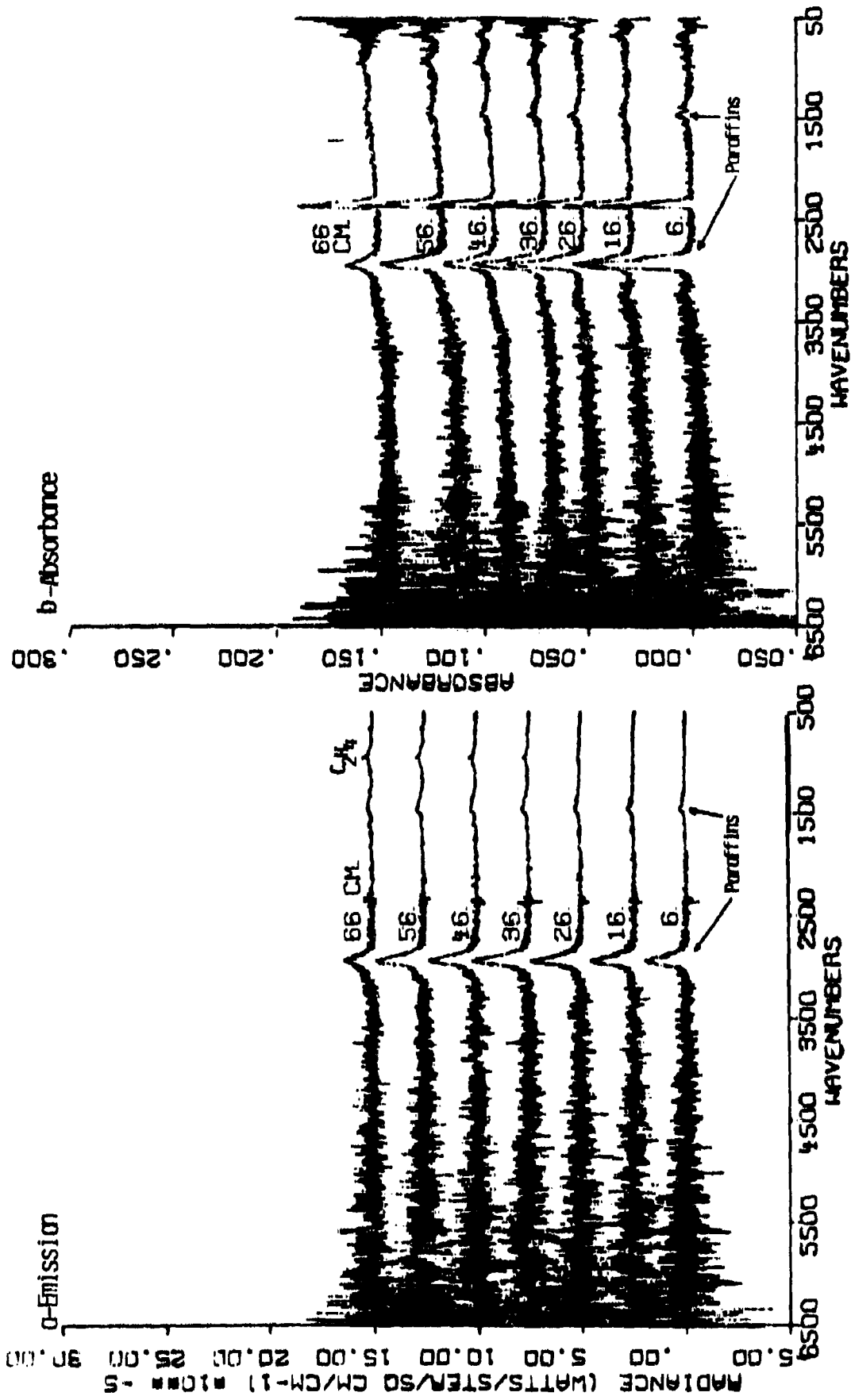


Figure 6. FT-IR Emission and Absorption Spectra for JP-4 Fuel at 800°C at Several Reaction Distances.

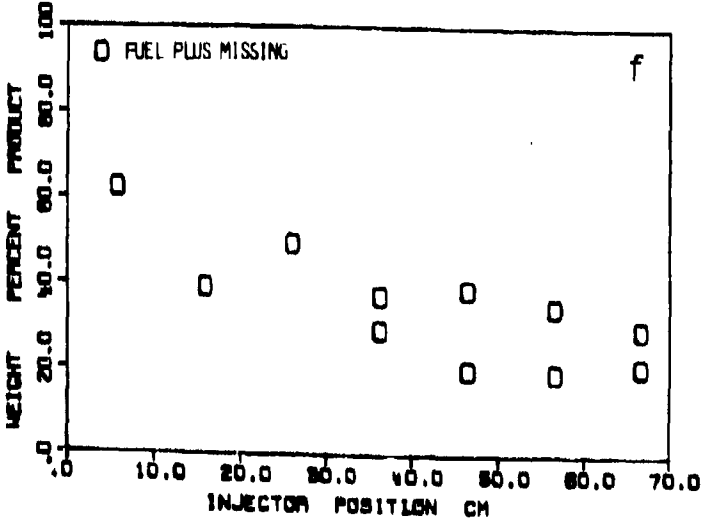
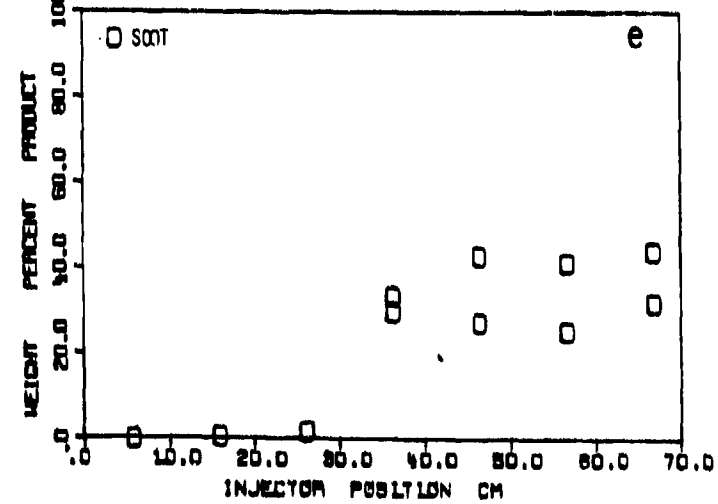
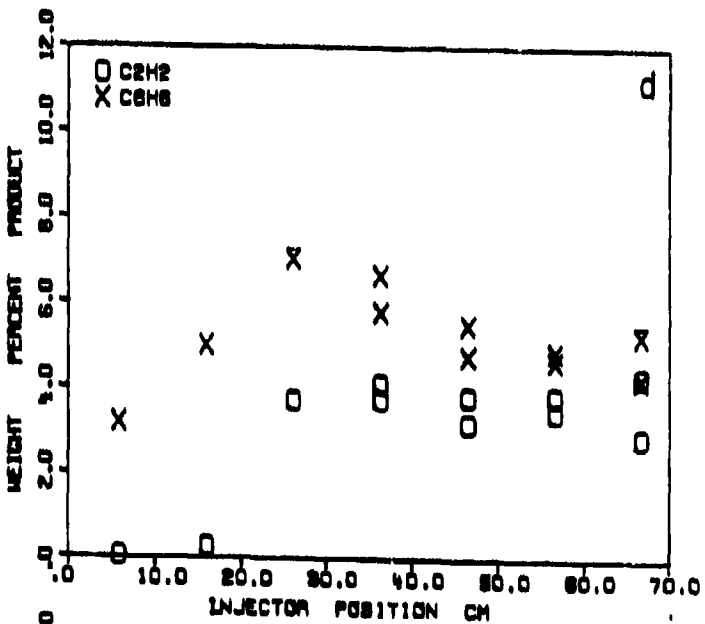
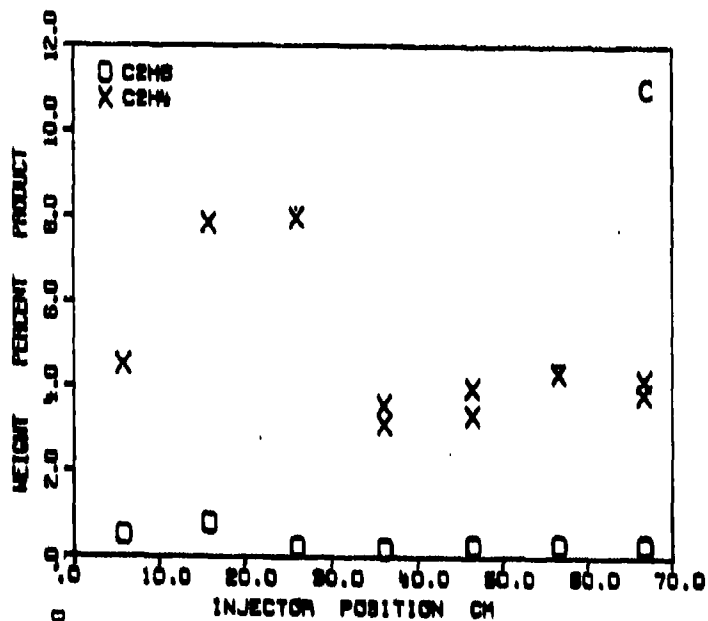
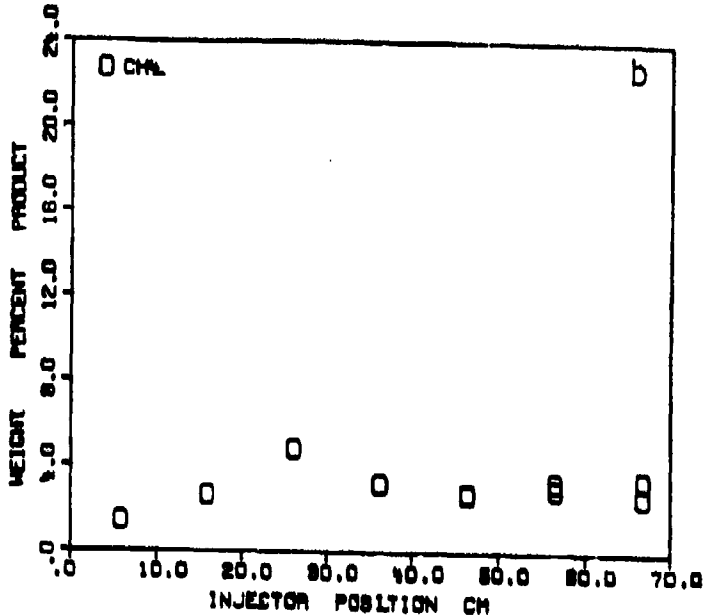
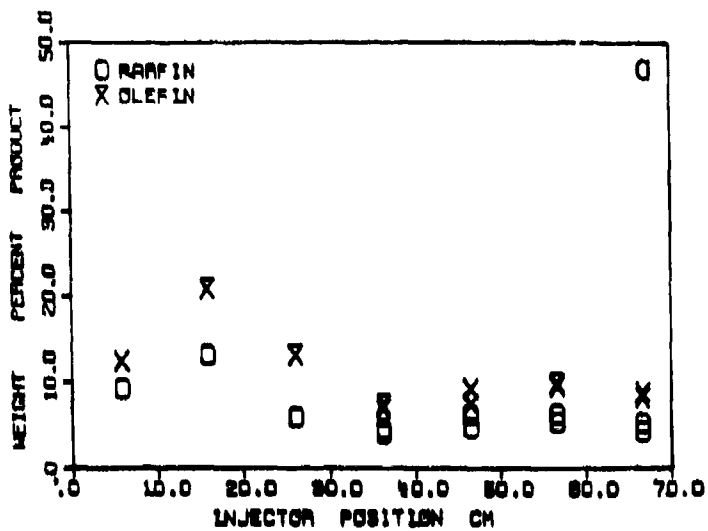


Figure 7. Pyrolysis Products from JP-7 in Nitrogen at 1300°C at Variable Reaction Distances. Gas Velocity is 1 m/sec.

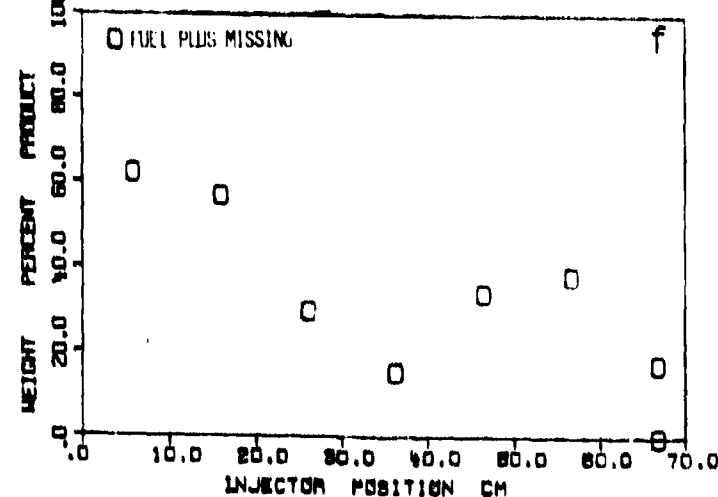
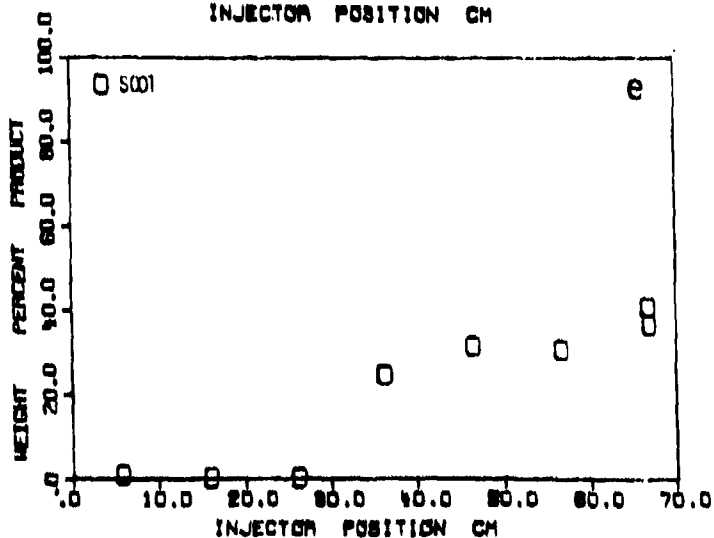
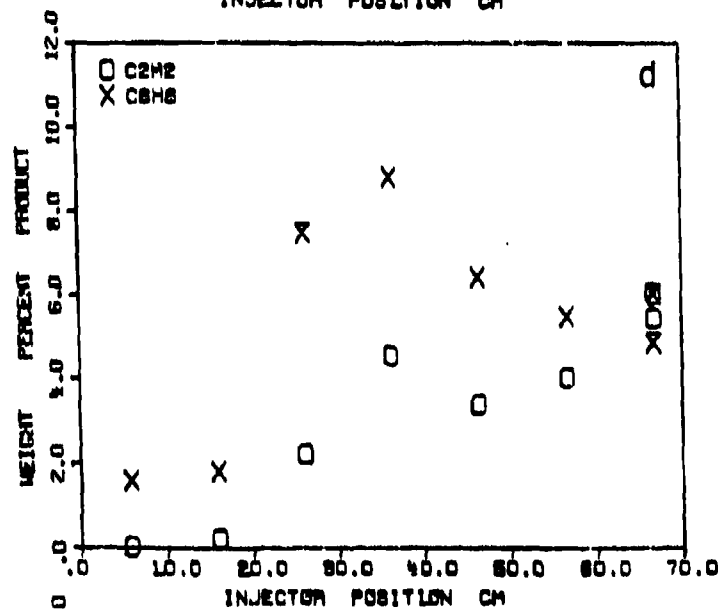
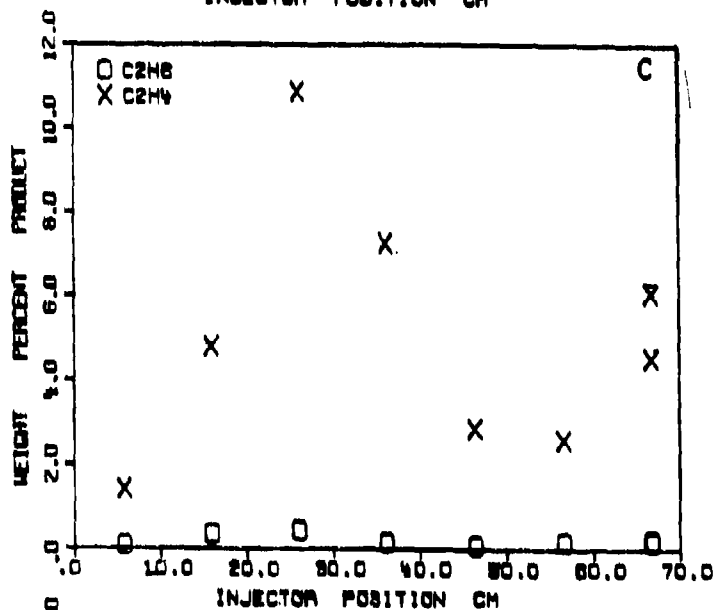
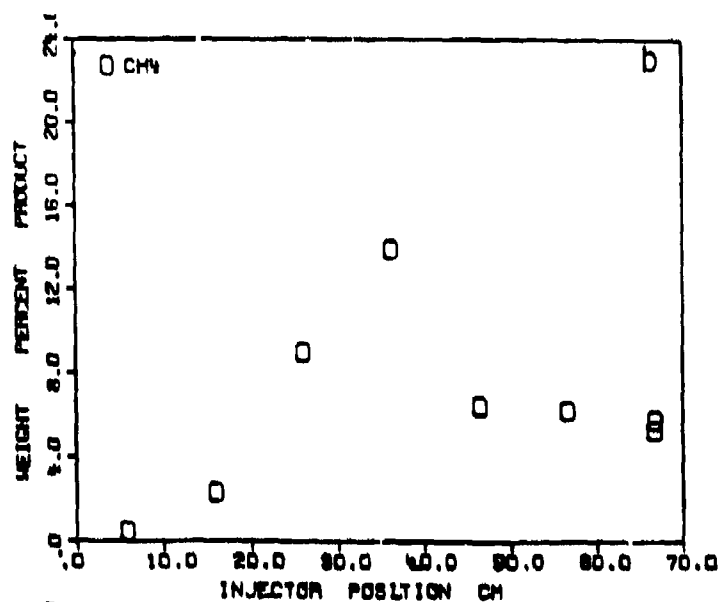
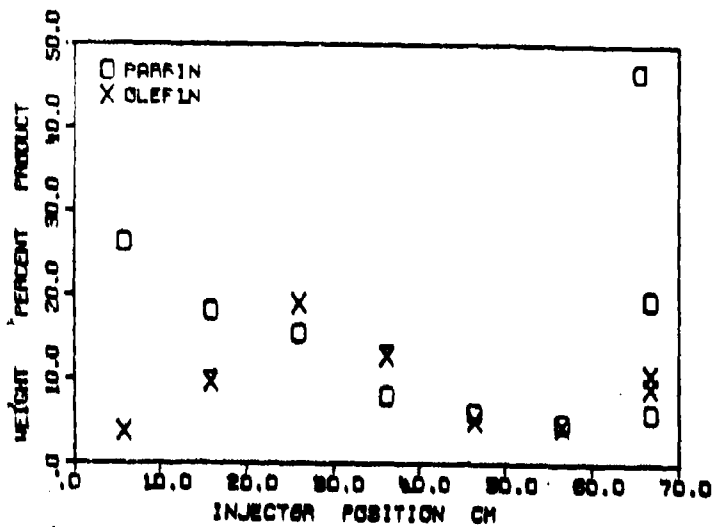


Figure 8. Pyrolysis Products from JP-4 in Nitrogen at 1300°C at Variable Reaction Distances. Gas Velocity is 1 m/sec.

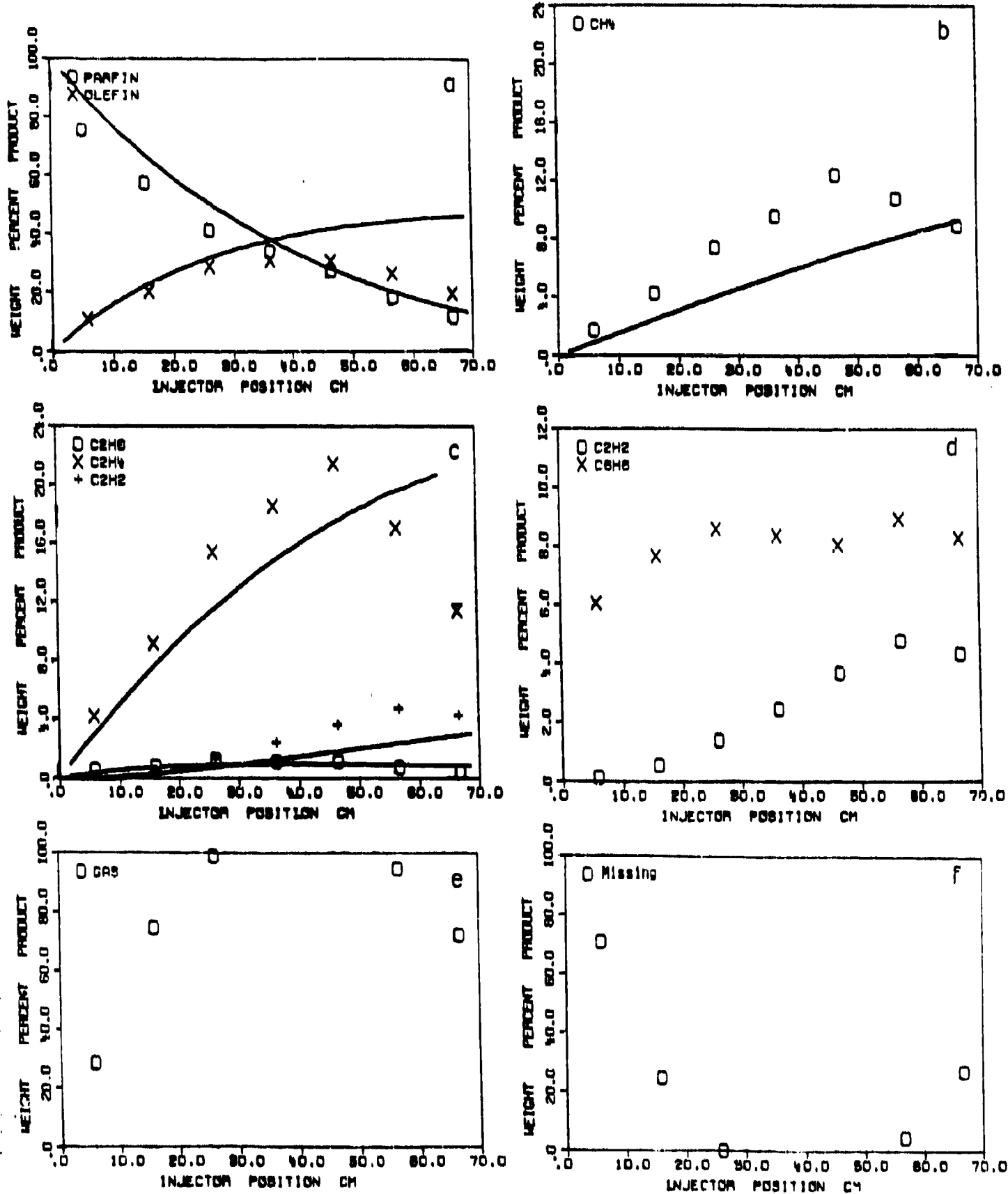


Figure 9. Pyrolysis Products from JP-4 in Nitrogen at 1100°C at Variable Reaction Distances. Gas Velocity is 1 m/sec.

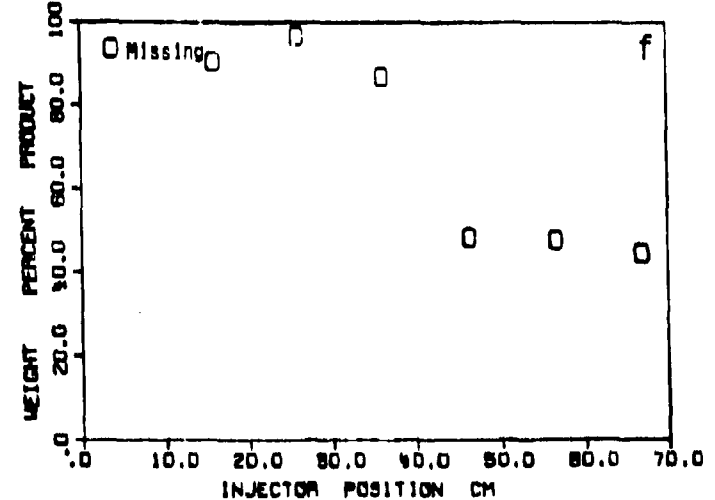
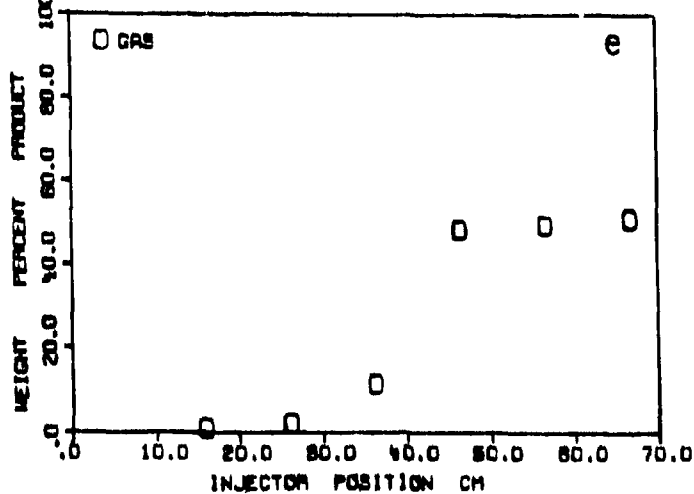
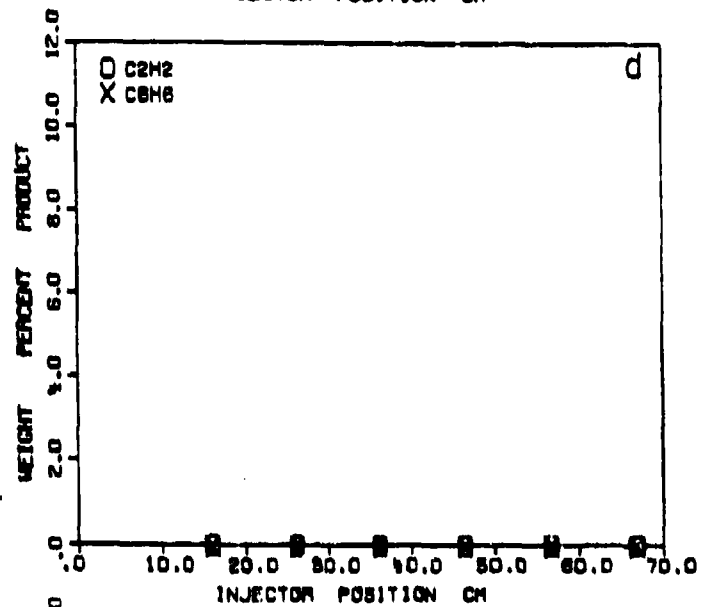
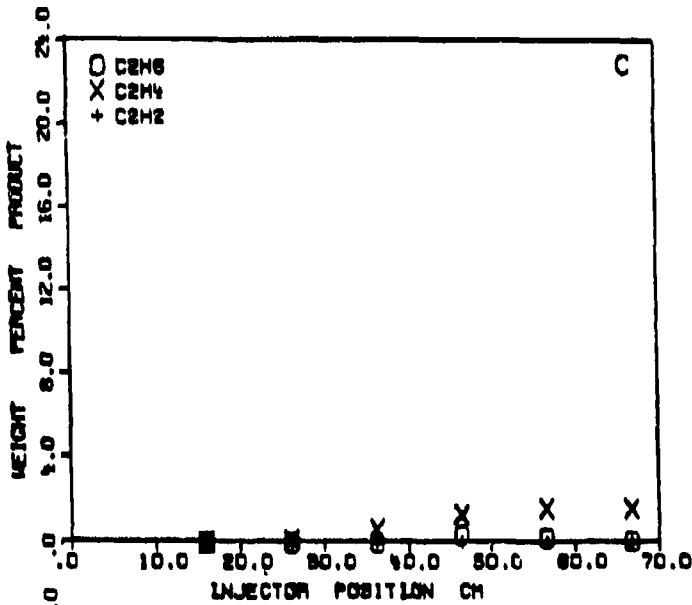
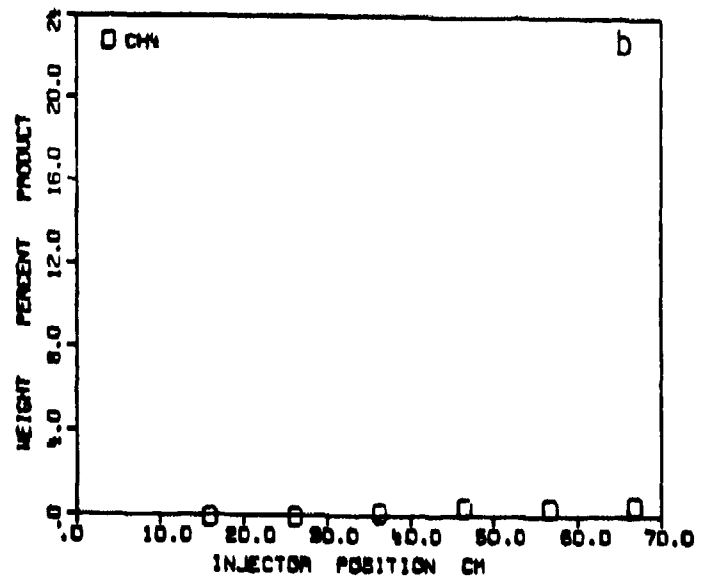
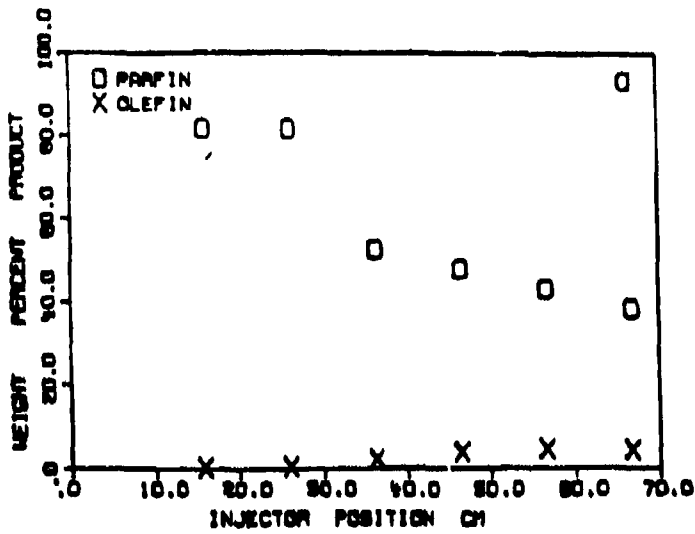


Figure 10. Pyrolysis Products from JP-4 in Nitrogen at 800°C at Variable Reaction Distances. Gas Velocity is 1 m/sec.

soot formation was not sensitive to details of drop formation, but it was found that there were some variations in the emission spectra which were related to the position and angle of the injector with respect to the reaction tube center-line. To make a meaningful comparison of the 4 fuels, measurements were made without moving the injector. The results are shown in Fig. 11. Results for 3 pure hydrocarbons are shown in Fig. 12 for comparison. The emission intensity appears to be a good measure of soot density as shown in Fig. 13 where the intensity is plotted as a function of soot collected. The emission intensity correlates roughly with the aromatic content of the fuels. The emission does not correlate well with hydrogen content. ERBS and JP-7 both have a lower hydrogen content than JP-4 but one is higher and one lower in soot emission. The relation between soot formation in pyrolysis and in combustion is discussed in Sec. 3.

### Soot Characteristics

A distinguishing feature of the soot spectra is their non black-body appearance. This shape depends on the soot temperature, size-distribution, density and optical properties (37,39-41).

Quantitative analysis of soot spectra is discussed for the spectra shown in Fig. 14, which are from ERBS fuel at the onset of sooting (36 cm injector height), and at a longer residence time (66 cm). In Fig. 15 the spectra have been scaled for comparison to each other, and to the appropriate black-body curve for the measured temperature.

The transmission spectra for these two cases has also been measured. The soot emission spectrum of higher intensity in Fig. 14 apparently suffers from self-absorption effects. As shown by Stull and Plass (42), at sufficiently high density-pathlength products, all soot spectra will have black-body form. To extract information about the soot particle size distribution one should use extinction-pathlength products ( $kL$ ), or emission spectra corrected for self-absorption. The 66 cm soot spectrum has been corrected back to an optically thin sample form in Fig. 15 by multiplying by  $\ln T/(1-T)$ , where  $T$  is the measured transmission (43). The behavior shown in the raw data persists; both soot spectra are of non black-body form, but that from the shorter residence time has a cut-off at higher wavenumber.

Other information concerning the sample has been obtained. A log-log plot of  $kL$  versus wavelength is approximately a straight line; there is no break in the curve. Scanning electron micrographs (SEM) have been measured of the soot generated over the 66 cm distance (Fig.16). These soot particles, of order 200 nm, have agglomerated into chains. The particles generated at 36 cm were too small to be distinguished in our SEM.

In trying to understand the difference between the spectral properties of soot at 36 cm and 66 cm respectively, there are two pieces of background information that must be considered. First, in the Rayleigh limit,  $\lambda \gg$  diameter, the absorption is much greater than scattering, and the extinction coefficient is indistinguishable from the absorption coefficient (39,43,43). There is no explicit dependence of the spectral shape on particle size in this regime (39).

Also in the Rayleigh limit, it is found that log-log plots of extinction-pathlength products versus wavelength are straight lines in the region 1.5 to 10 microns (37). This line becomes noticeably segmented only for larger particle sizes, for diameters greater than about 0.3 microns, where the Rayleigh approximation breaks down. An explicit dependence of extinction on particle size is expected for these large particle diameters (37,41).

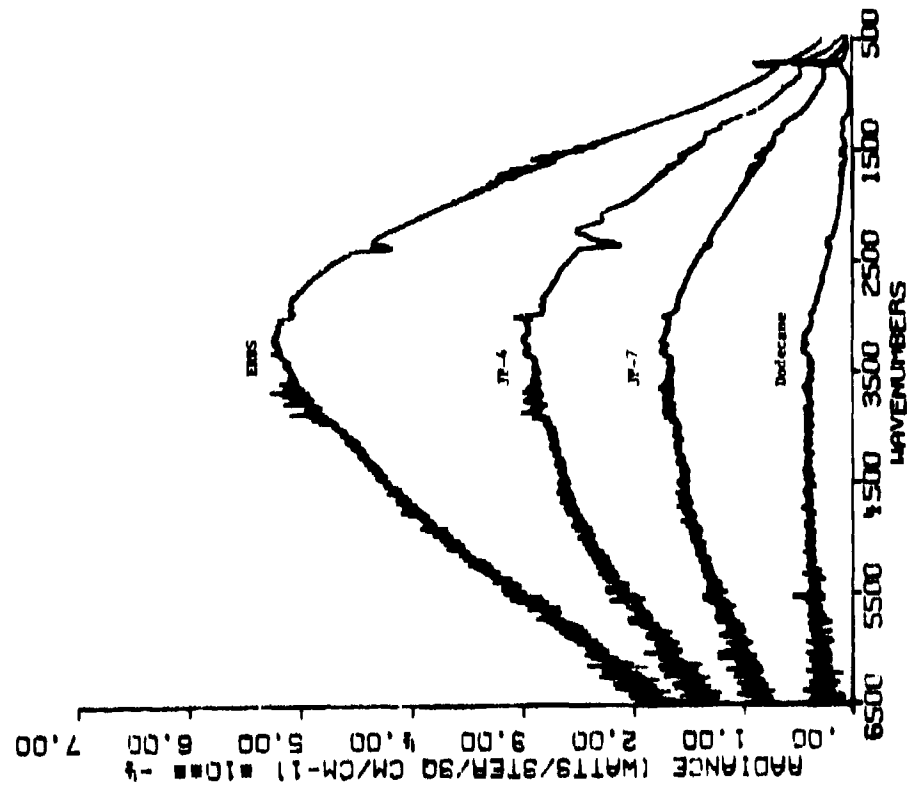


Figure 11. Emission Spectra for 4 Fuels at 1300°C in Nitrogen at 56 cm Reaction Distance.

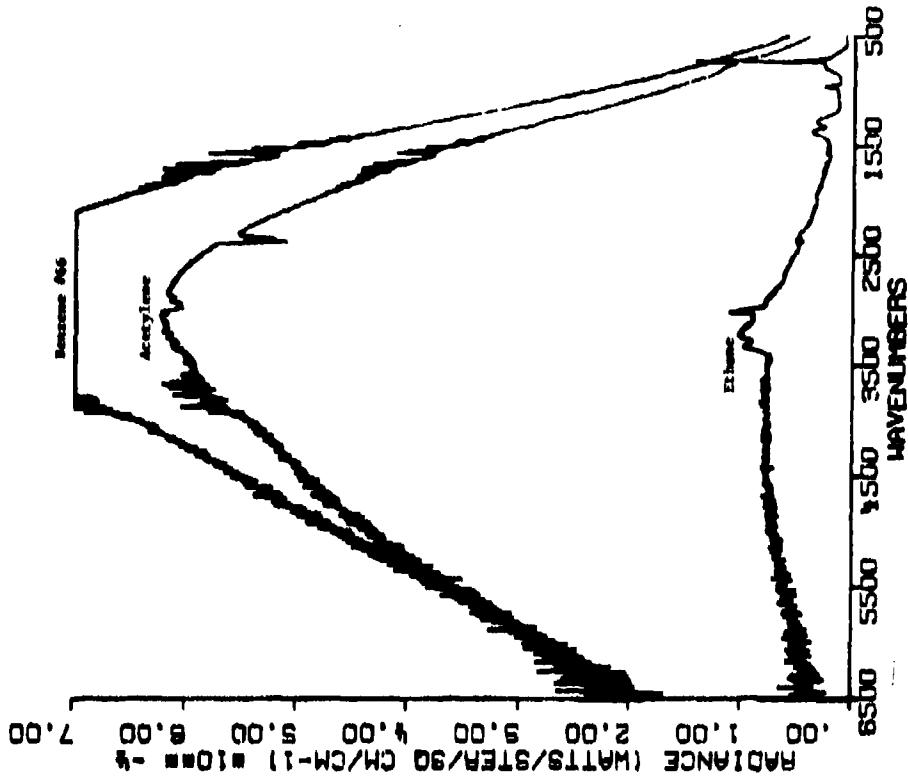


Figure 12. Emission Spectra for 3 Pure Hydrocarbons in Nitrogen at 56 cm Reaction Distance.



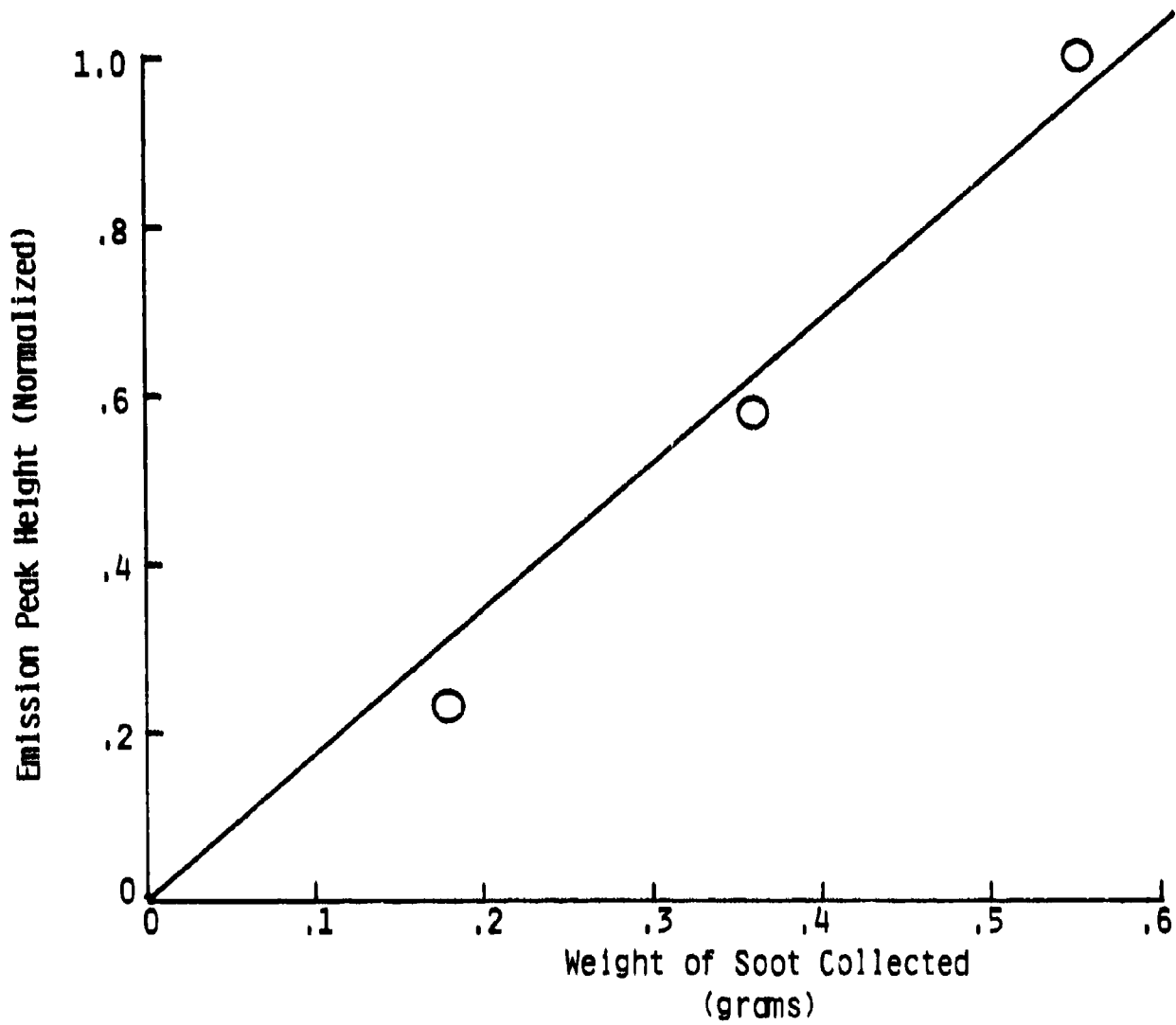


Figure 13. Correlation of Soot Emission Intensity from the Entrained Flow Reactor with Soot Collected.

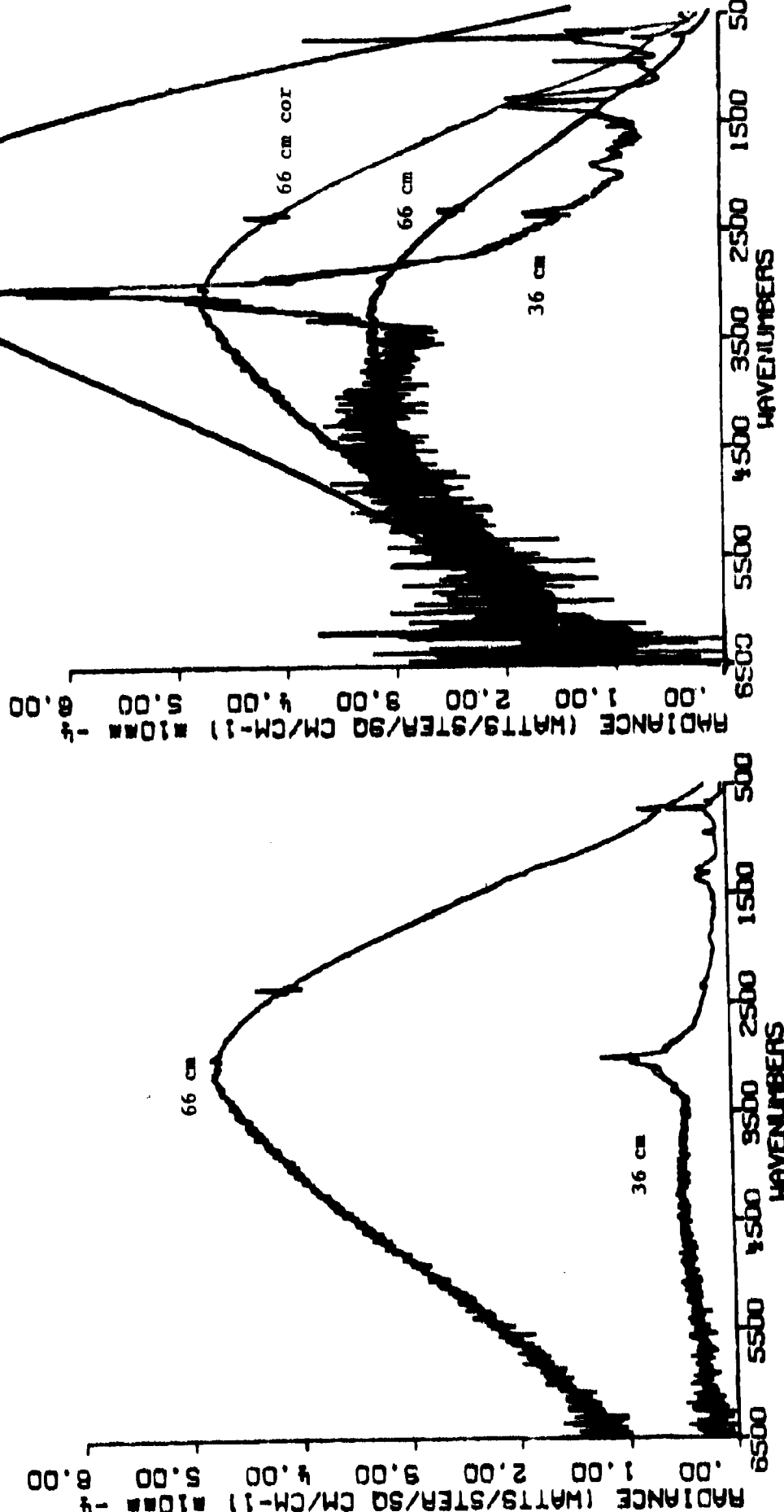


Figure 14. Emission Spectra from the Products of ERBS Fuel Pyrolyzing at 1300°C for 36 cm and 66 cm Reactor Distances.

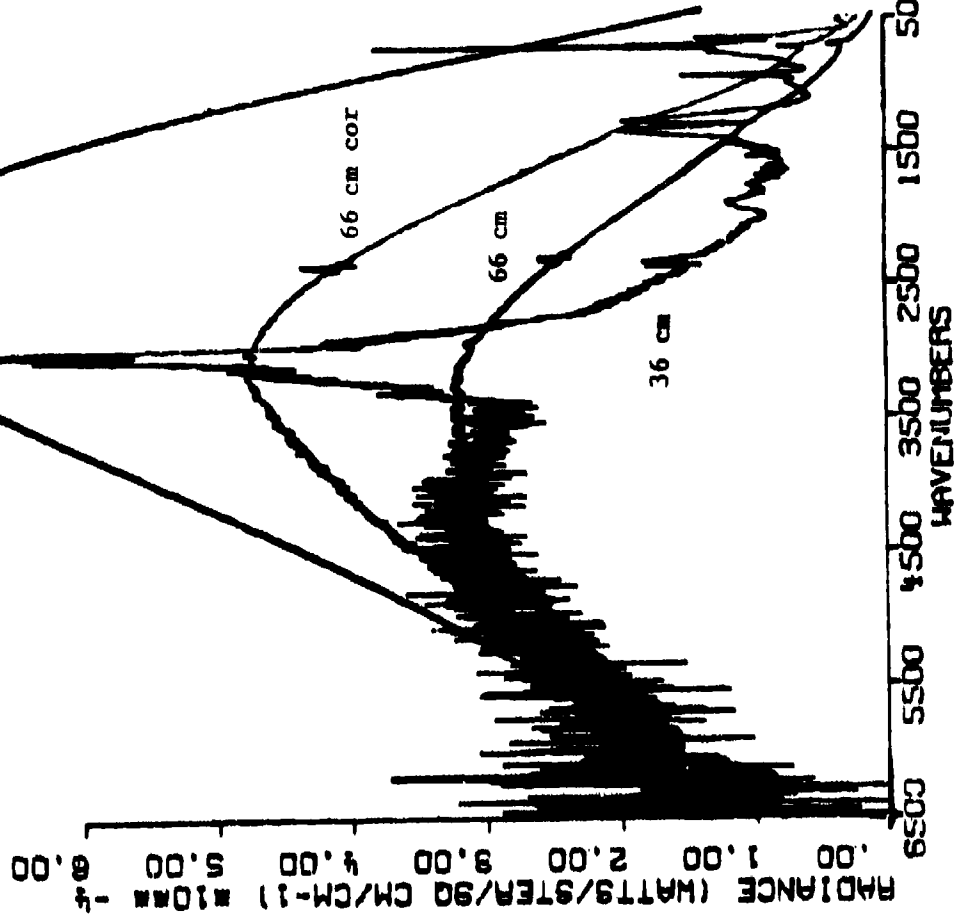


Figure 15. Spectra from Figure 14 Normalized to the Same Sample Amplitude at 6500 Wavenumbers. The 66 cm Spectrum has been Corrected to the Optically Thin Spectrum and a Black Body Curve at the Measured Temperature has been included for Comparison.

For the 66 cm spectra the log-log plot is linear, and the spherical particles of the collected soot have diameters less than 0.3 microns. It seems probable, then, that both spectra in Figs. 14 and 15 are from samples for which the Rayleigh limit is applicable. However, the corrected spectra from the 36 and 66 cm injector positions do not have the same shape. The problem posed by these data is that soot particles of different size from the same fuel and essentially the same temperature have different spectral shapes, a difference which cannot be ascribed to the explicit appearance of particle dimension in the Mie formula (39). We conclude that in this region of the spectrum the optical constants of the soot vary with particle size. Whether the variation is due only to size, or is related to soot H/C ratio, cannot be determined from these data alone. Vervisch and Coppalle note that the slope of the log-log plot of  $kL$  versus  $\lambda$  depends on the soot H/C ratios, (37) so it is probable that the marked variation that we see in the shape of the emissivity has this same origin.

Coupling FT-IR measurements with the microscopic examination of collected soot should enable us to determine whether there is a reproducible correspondence between particle size and spectral shape. Such correspondence would enable the determination of fine soot particle size distributions from FT-IR measurements. These measurements would also give new information about the optical constants of soot (41).

For emission from larger particles, computer programs like that being used by Lee and Tien (41) and by Vervisch and Coppalle (37) can be used to determine particle size distributions from FT-IR measurements.

#### Soot Temperature Determination

For carbonaceous particles, and for wavelengths greater than the particle diameters, radiation scattering is negligible compared with absorption (42,44). Neglect of scattering is therefore a valid approximation for the wavenumber region of interest.

For an array of non-opaque particles, the particle temperature can be deduced from a combination of emission and transmission measurements by the application of Kirchoff's Laws, as used by Vervisch and Coppalle (37).

$$E_p = C_b(T) [1 - \exp(-k_p L)] \quad (1)$$

$$I_T/I_0 = \exp(-k_p L) \quad (2)$$

where  $E_p$  is the emission,  $C_b(T)$  the black-body emission at temperature  $T$ ,  $k_p$  is the wavenumber dependent absorption coefficient,  $L$  is the path length,  $\nu$  is wavenumber and  $I_T$  and  $I_0$  are the transmitted and incident intensities in the transmission experiment, respectively.

For the 66 cm case for which the emission is shown in Fig. 14 the absorbance was also measured. It can be seen from Eq. 1 and 2 above that  $E_p$  divided by  $(1 - I_T/I_0)$  should give a black-body curve appropriate to the temperature of the soot. The result of this calculation for the 66cm case of Fig. 14 is shown in Fig. 17, where it is overlaid with a black-body curve for a temperature of 1250K. It can be seen that the quotient curve is of excellent black-body shape, and from this and comparisons with other black-body curves, it can be concluded that the particle temperature is  $1250 \pm 15K$ .

In the case appropriate to Fig. 17 a suction pyrometer was inserted into the gas stream, yielding a temperature measurement within  $10^\circ C$  of that deduced above. It is

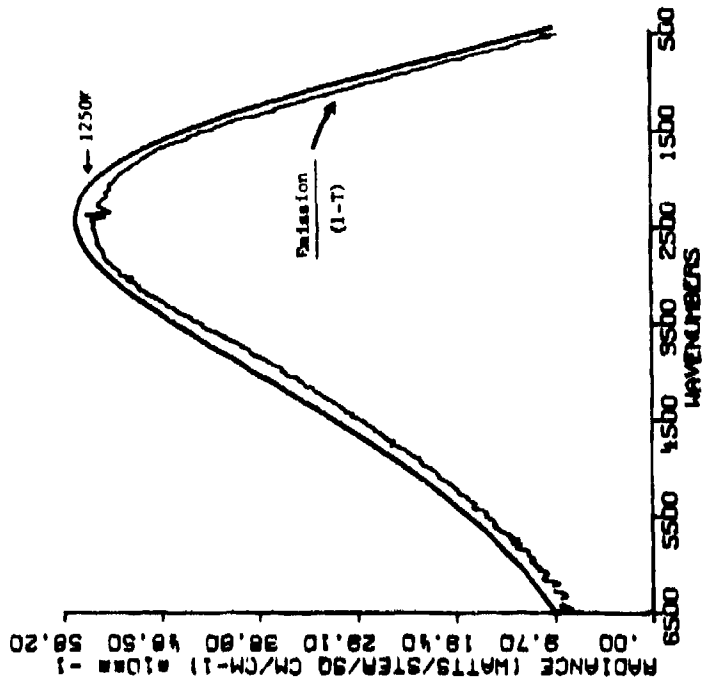


Figure 17. Emission Spectrum at 66 cm from Figure 13 Divided by (1-Transmission) Compared with Planck Curve for a Temperature of 1250 K.

Figure 16. SEM Photograph of Soot from Pyrolysis of ERBS Fuel at 1300°C with a Reaction Distance of 66 cm.

expected that soot and gas temperatures are essentially the same for the case where reactions are not occurring at the soot surfaces (45).

### Combustion

Data for JP-4 were taken as a function of oxygen concentration for a furnace temperature of 1300°C. Figure 18 shows the emission spectra. It can be seen that the addition of oxygen first increases and then decreases the radiation intensity. The intensity increases without much change in shape and the absorption increases suggesting that there is more soot at the same temperature. The increase of sooting with small amounts of oxygen was discussed by Glassman (26). His explanation is that small amounts of oxygen enhance the fuel pyrolysis rate (46) which leads to a higher soot formation rate. The oxygen will also reduce the "available hydrogen."

The reduction of the broad based emission above 6% oxygen occurs as the soot is oxidized, and is accompanied by an increase in CO<sub>2</sub> and H<sub>2</sub>O.

The quantitative gas composites are shown in Fig. 19. Oxidation of the gas species starts for oxygen concentrations greater than 2%. This contrasts with the observation that 2% oxygen substantially enhanced the soot concentration (Fig. 18). The oxidation of the gas species is substantially complete at 8% oxygen at which point, oxidation of the soot is beginning.

### 2.2 Fuel Characterization - (Phase I - Task II)

The objective of Phase I, Task II was to obtain characteristics of the fuels in terms of the functional group and molecular weight components, and the relative volatility of these components. The four were analyzed by quantitative FT-IR, FIMS, and programmed temperature distillation/FT-IR. FT-IR and FIMS provided the most useful information.

### FT-IR

Four fuels of increasing complexity were studied in this program. The fuels and their hydrogen content, aromaticity and naphthalene content are listed in Table II.

Quantitative FT-IR spectra were obtained using a liquid cell of known dimensions. Compositions are obtained from FT-IR spectra using automated computer data-reduction routines which perform baseline correction, solvent subtraction, spectral synthesis, peak area determination, library searches and factor analysis. A quantitative determination can be made of hydroxyl, aliphatic, hydroaromatic and aromatic hydrogen. From these data, the aliphatic and aromatic carbon may also be calculated. Moreover, information can be obtained on the types of ether linkages, and the distribution of aromatic hydrogen. The techniques have been described in several previous publications (28-30). The spectra are presented in Fig. 20. Important differences in the four fuels can be seen. The ERBS fuel and JP-4 have the highest aromatic hydrogen content (peaks near 850 wavenumbers). The dodecane has the highest aliphatic chain length (sharp peak near 720 wavenumbers) and JP-4 has the highest methyl group concentration (1375 wavenumbers). Some of the compositions derived by FT-IR are compared to the ASTM determination in Table II. It should be pointed out that the ASTM method includes in the aromatic percent, aliphatic components attached to an aromatic ring, while FT-IR determines aromatic C-H concentrations. The latter may be a better property to correlate with soot production.

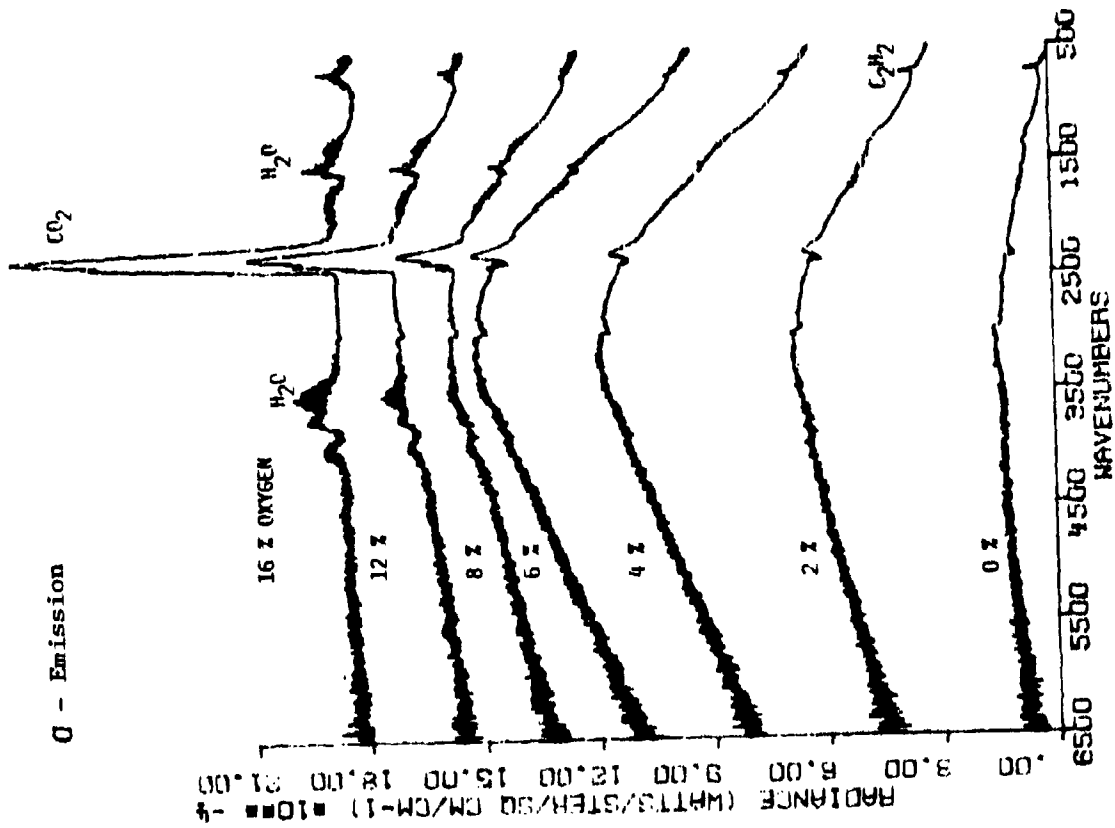
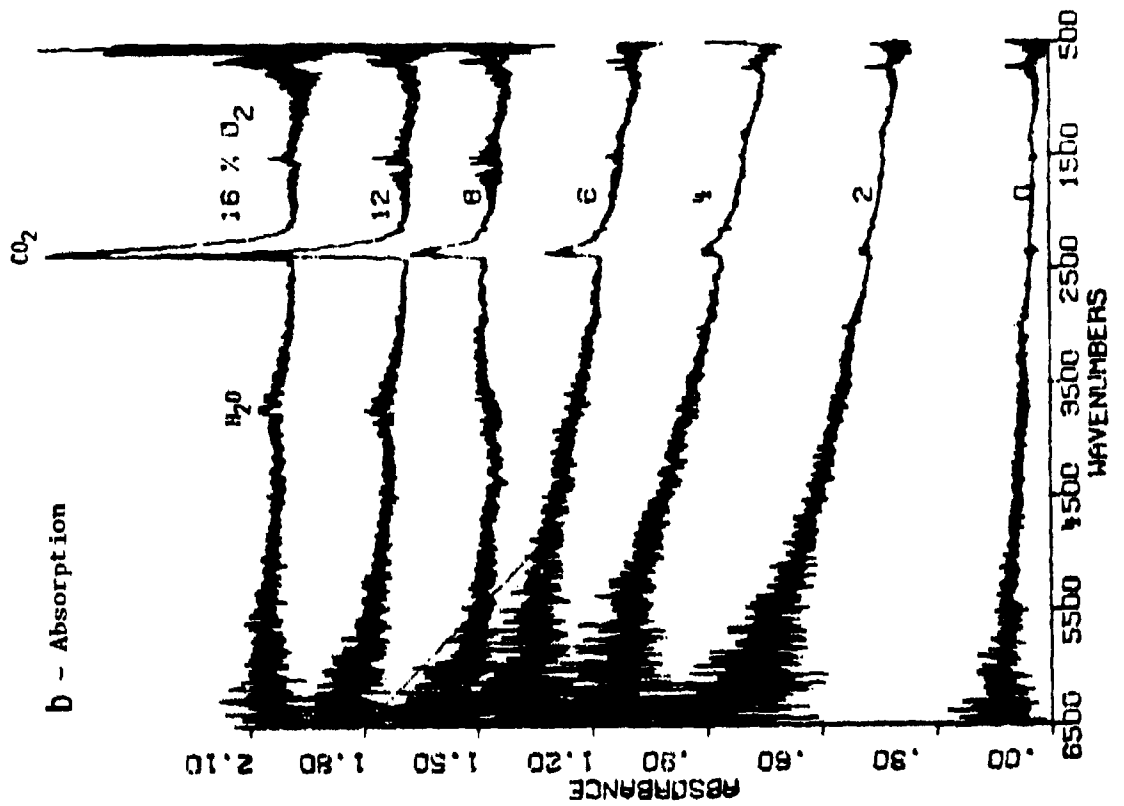


Figure 18. FT-IR Emission and Absorption Spectra for JP-4 at 1300°C with Variable Oxygen Concentration.

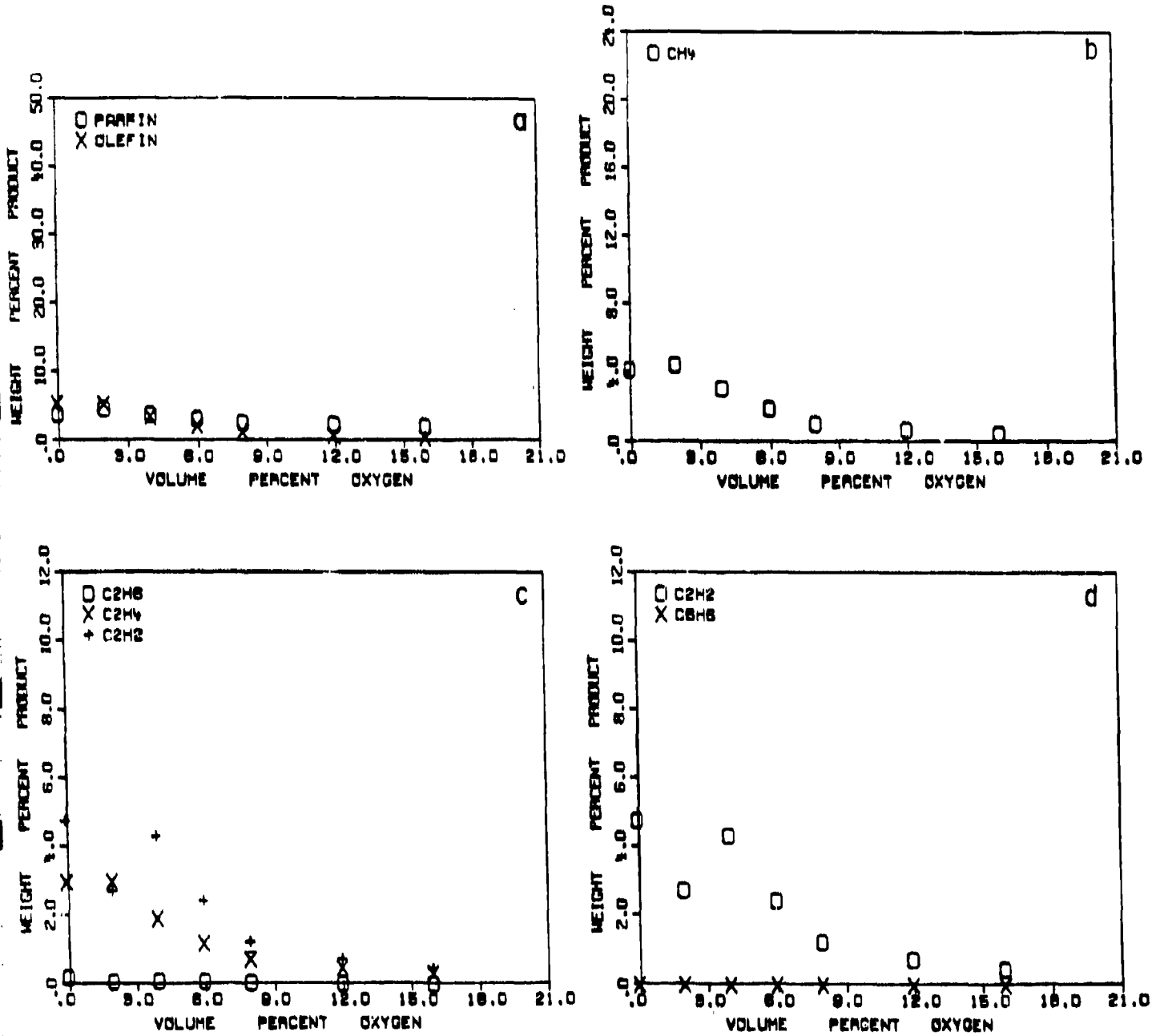


Figure 19. Pyrolysis Products from JP-4 in Nitrogen at 1300°C with Variable Oxygen Concentration.

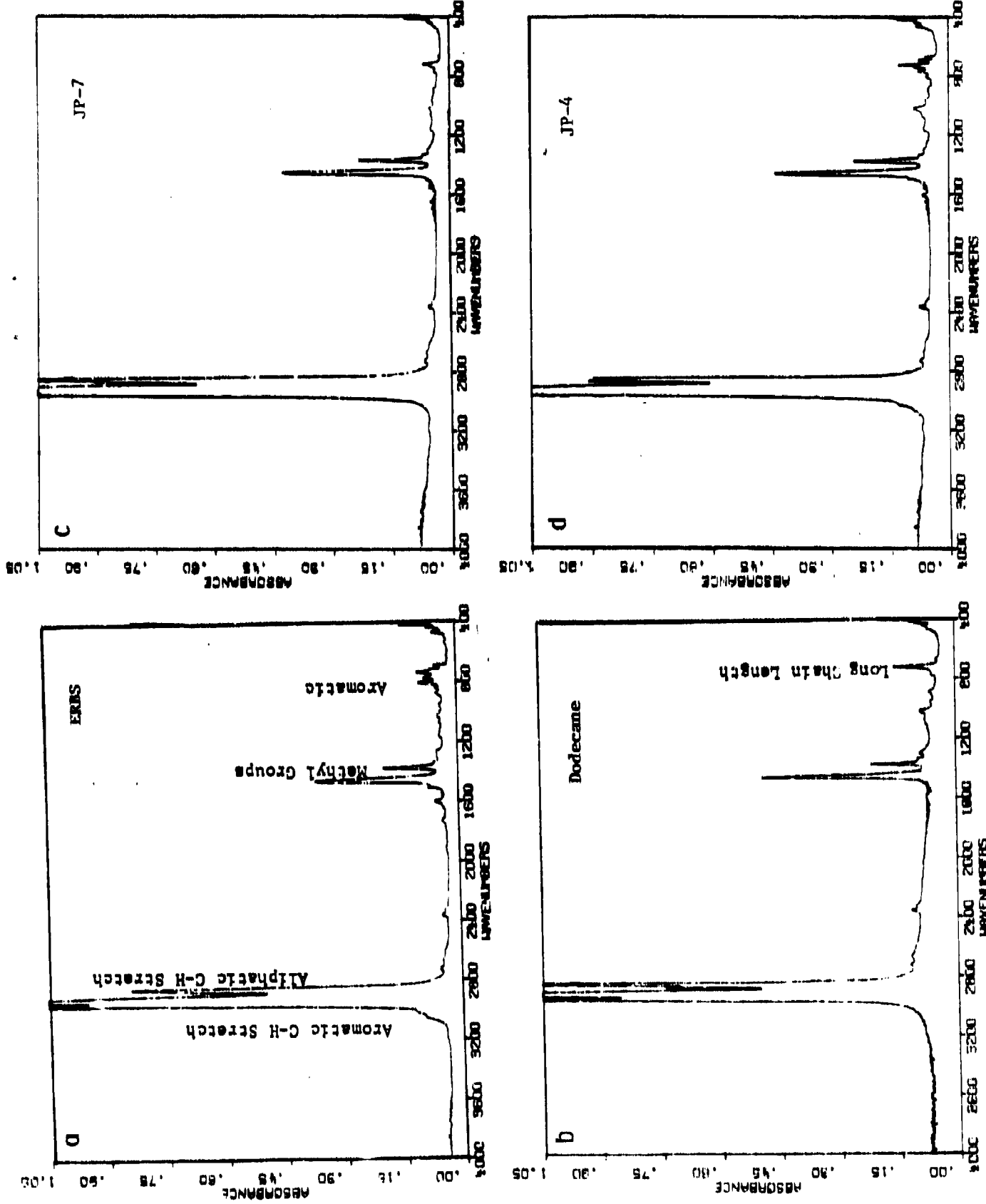


Figure 20. Quantitative FT-IR Spectra of Four Fuels.



## COMPARISON OF FT-IR AND ASTM METHODS FOR FUEL CHARACTERIZATION

FUEL	FT-IR			ASTM		
	%Hal	%Har	H(calc)	H <sub>T</sub> (Meas)	%Aromatics	%Naphthalene
Dodecane	14.8	.12	14.9	15.3	0	0
JP-7	14.9	.18	15.1	14.4	2.5	0
JP-4	15.0	.41	15.4	14.6	15.7	0.5
ERBS	10.7	1.2	11.9	12.8	30.2	16.0

Molecular Weight Distribution of Fuel Components by FIMS

Experiments to determine molecular weight distributions in fuels and hydrocarbon pyrolysis products have been performed for AFR with a Field Ionization Mass Spectrometer (FIMS) at Stanford Research Institute. The technique was described by St. John et al. (47). FIMS is unique in its ability to produce unfragmented molecular ions from almost all classes of compounds.

Figure 21 compares the batch inlet FIMS spectra of JP-4, JP-7 and ERBS. Compared to the JP-4, the JP-7 spectra appears to have substantial quantities of alkanes, alkenes and dienes with few phenyl compounds. This is in agreement with the low aromatic content measured by ASTM or FT-IR. The ERBS fuel has substantial quantities of phenyl compounds and naphthalenes in agreement with its high aromaticity. The JP-4 spectrum was obtained using the batch inlet at 500°C. The low molecular weight (150-250) alkanes and alkenes appear to result from cracking, suggesting that the batch inlet temperature was too high. Subsequent runs on ERBS and JP-7 were made at lower temperatures.

Distillation/FT-IR

A new technique was tried for fuel characterization. The fuel was heated at approximately 30°C/min inside an FT-IR cell swept with nitrogen, as FT-IR spectra were recorded. The spectra obtained during heating from 0 to 700°C are shown in Fig. 22. Specific regions of the spectra which are related to different functional groups may be integrated and plotted as a function of time. Results for a dodecane/phenanthrene mixture are shown in Fig. 23. The spectra show the evolution of the more volatile dodecane at earlier (low temperature) than the phenanthrene.

2.3 Droplet Generation and VaporizationGeneration

The study of the droplet generation and vaporization was originally planned to be performed in the entrained flow reactor as part of Phase I-Task I. The optical access was not good for photography and the temperatures used for the pyrolysis and soot studies were too high to study vaporization. A duplicate of the droplet injector assembly used in the entrained flow reactor was, therefore, installed in an apparatus (Fig. 24) which allows the droplets to pass through an electrically heated tube. The injection point and length of the heated section can be varied to obtain different residence times. A microscope focused at the tube exit allows photography

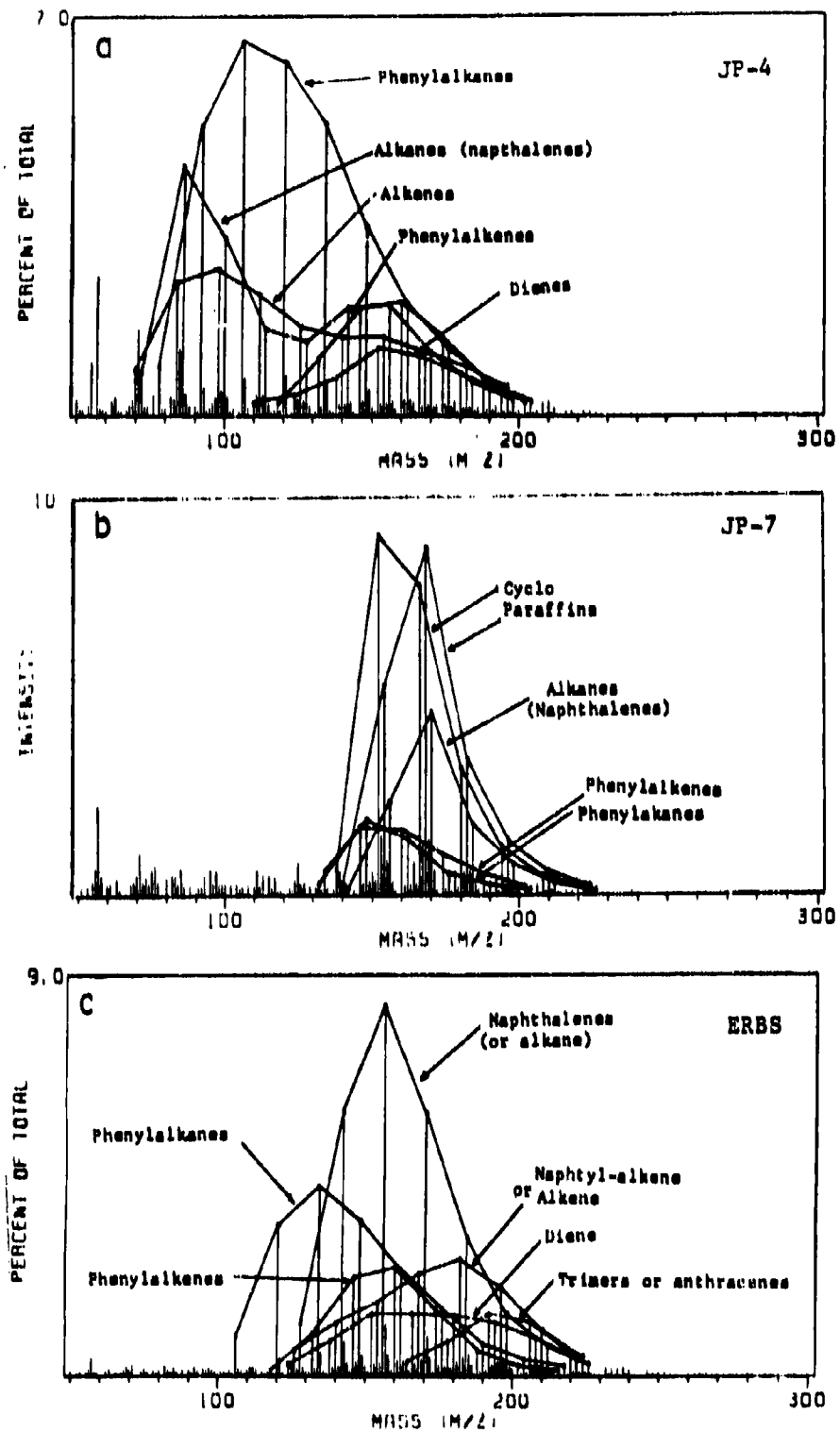


Figure 20. Comparison of FIMS Spectra for Three Fuels using Batch Inlet.

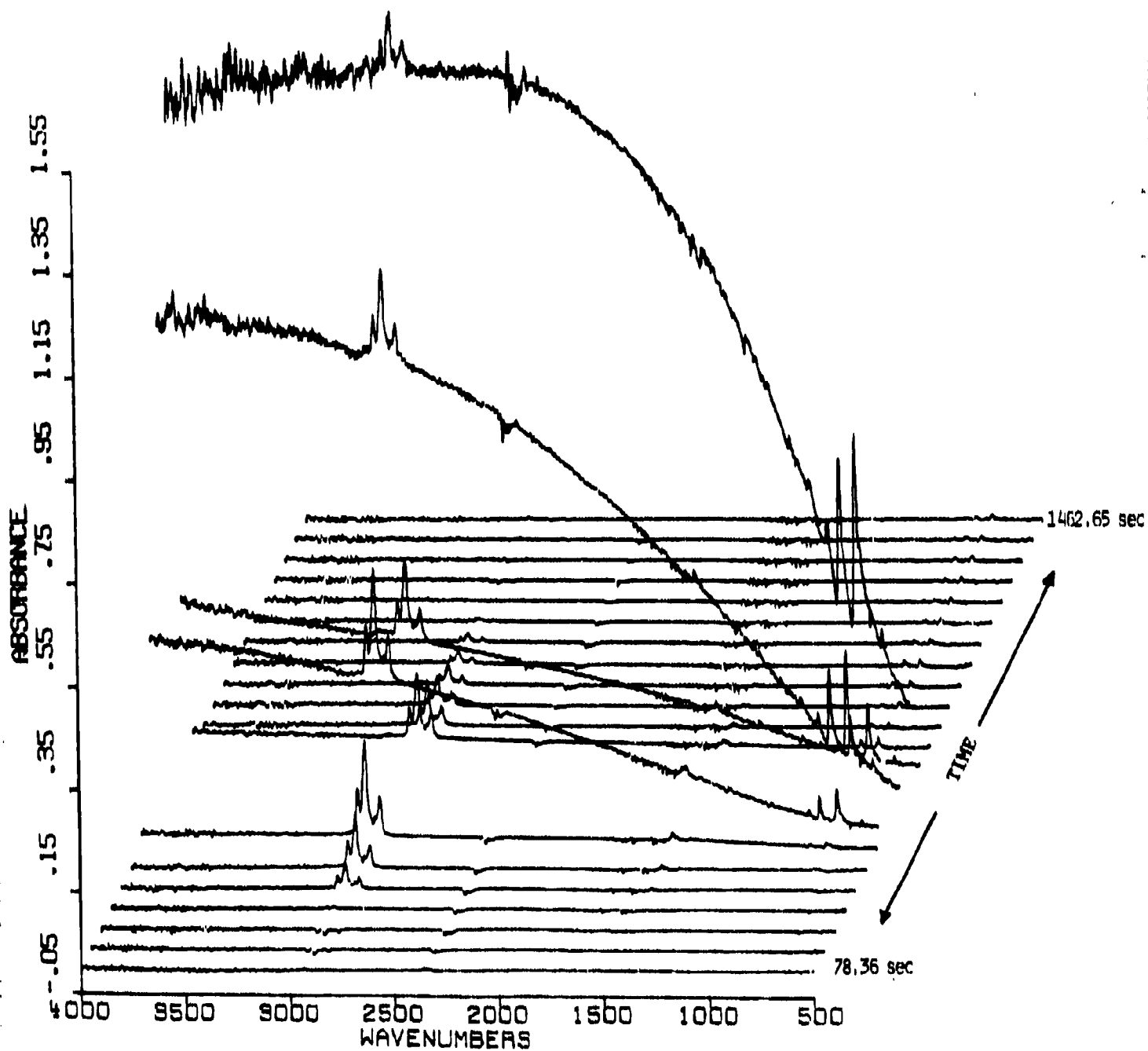


Figure 22. FT-IR Spectra taken during Distillation of Phenathrene/Dodecane. The Drastic increase in the Absorbance Starting at Spectrum #8 is caused by Scattering of the IR due to the Mist of Fuel which is being Vaporized from the Screen.

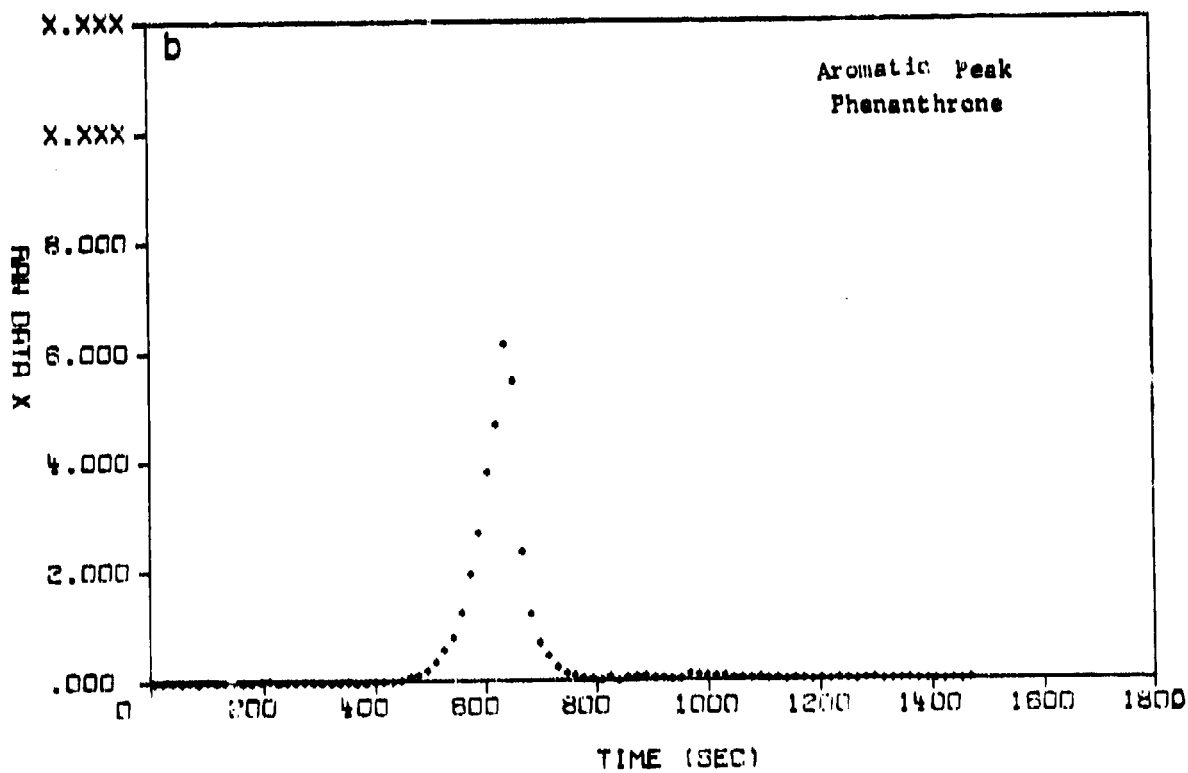
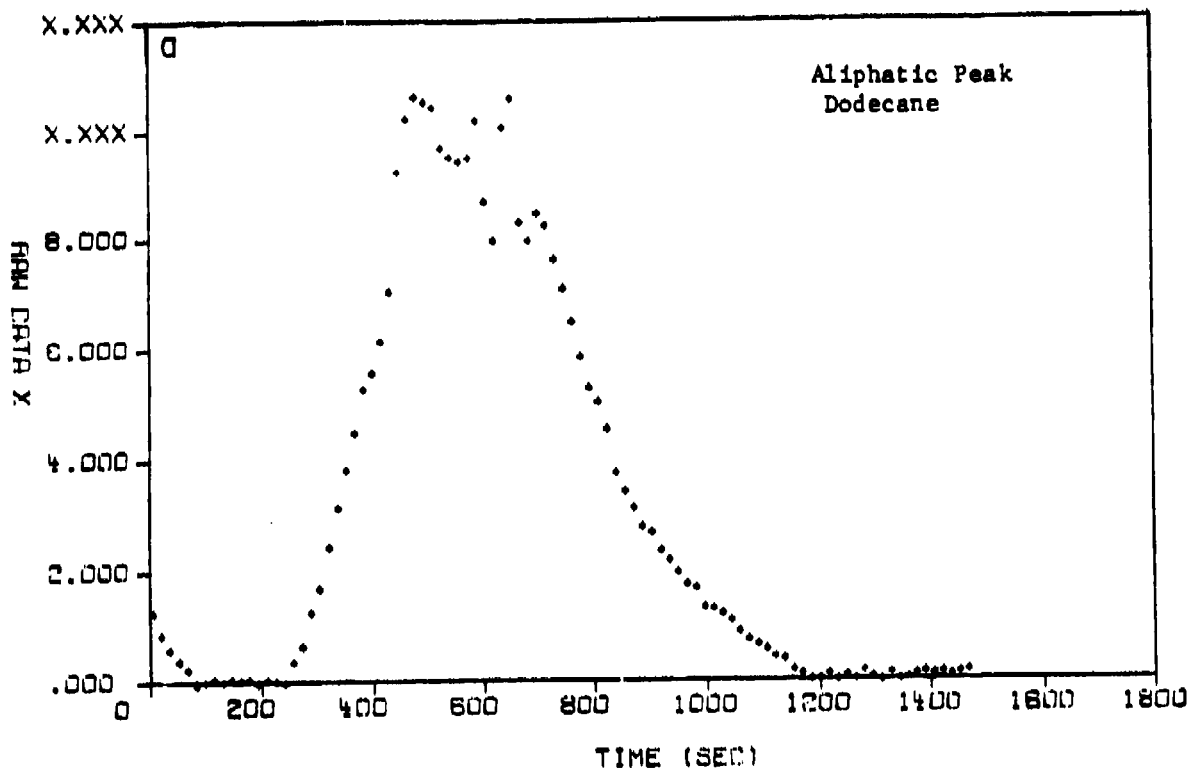


Figure 23. Integral over Specific Regions of the Spectra from Fig. 22 as a Function of Time.

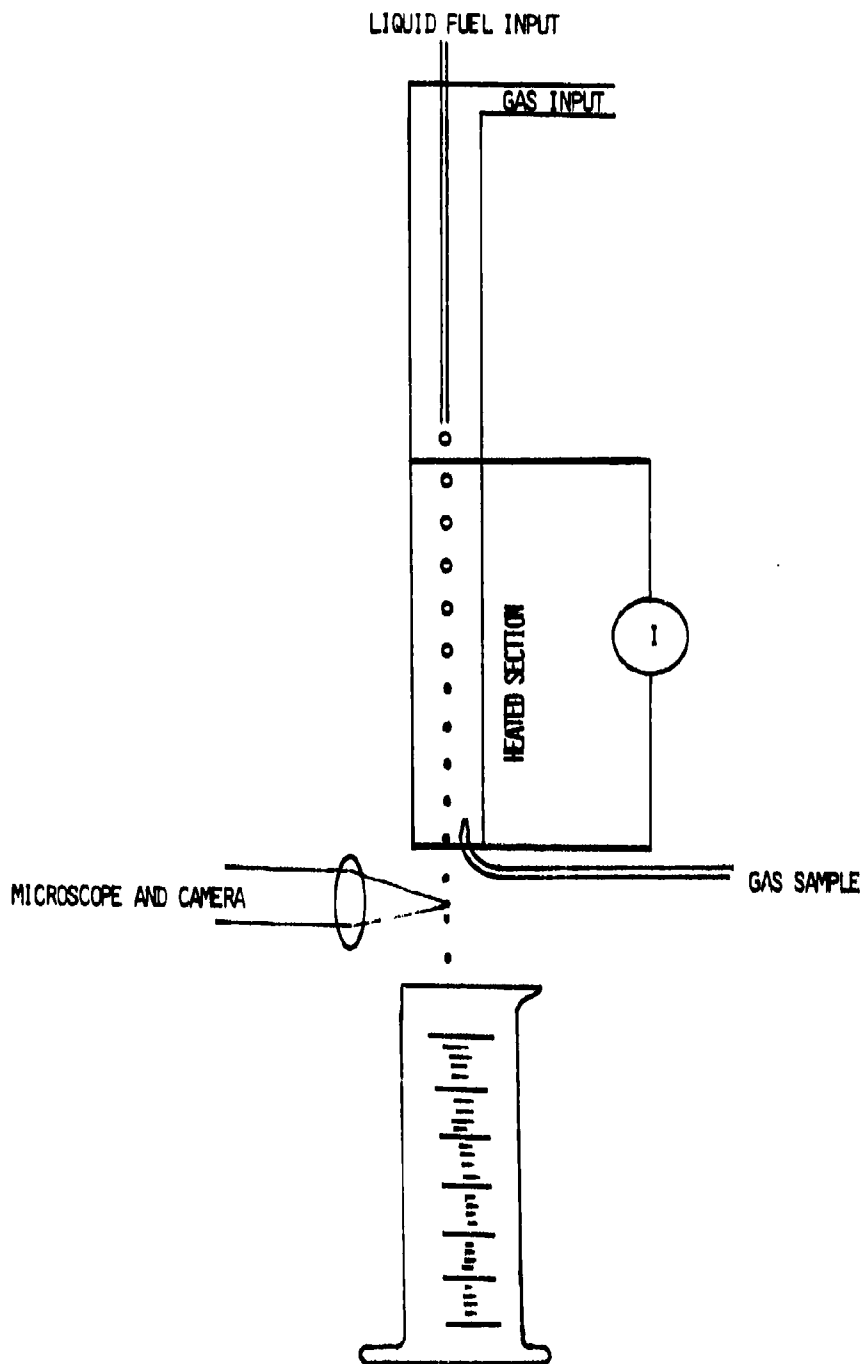


Figure 24. Schematic of Droplet Vaporization Apparatus.

of the droplet stream at various stages of pyrolysis. The liquids are collected, weighed, and analyzed by FT-IR. Gas is also collected for analysis.

The evolution of a drop stream is illustrated in Fig. 25. Figure 25a shows the stream emerging from the hypodermic tube (250 micron OD). After a short distance, the stream starts to break up (Fig. 25b) due to the Rayleigh instability. Droplets form, but are not spherical (Fig. 25c and d) due to shape oscillation. The shape finally settles down and a regular stream of spheres of about 200 micron diameter is observed (Bottom of Fig. 25d). The drops are shown in higher magnification in Fig. 26 where the effect of drop collisions can be seen (Fig. 26d).

#### Mass Loss

Figure 27 shows the droplets appearing after 20 and 50 cm, within the tube. The droplets at 20 cm are larger than in Fig. 25. Investigations indicated that droplet collisions were taking place at longer distances, leading to larger droplets. The droplets at 50 cm (Fig. 27c) are clearly smaller than those at 20 cm (Fig. 27a and b).

The droplets were quantitatively collected at the tube exit to determine the amount vaporized. The results are presented in Fig. 28. Assuming that the number of drops is constant, the volume collected to the 2/3 power should follow the "d<sup>2</sup>" law. The results are in reasonable agreement with the "d<sup>2</sup>" law.

#### Fuel Component Separation

The composition of the collected liquid was analyzed by FT-IR to determine whether separation of the fuel components occurs during vaporization. Figure 29 compares the initial fuel with the collected fuel after 51 msec (69% volume loss). The major change is in the chain length indicator near 720 wavenumbers. The shorter components appear to be leaving first. Figure 30 shows a similar comparison for the ERBS fuel. Here the aromatic components increase as vaporization occurs.

To get a quantitative measure of the separation, a blend of dodecane and benzene (50/50 by volume) was analyzed in a manner similar to the above. The FT-IR spectra were used to determine the composition as a function of reaction time. As vaporization proceeds, the aliphatic components increase relative to benzene. The calculated percentages are shown in Fig. 31a as a function of extent of vaporization. Data from Hansen et al (48) are presented for comparison. It was expected that the results would look like those for pyridine as the boiling point of benzene is similar. Instead they are closer to the quinoline data. The lower than expected evolution of benzene suggests that there is not much mixing within the drop. This investigation will have to be carried further to study the effects of relative velocity.

#### 2.4. Application of Vaporization and Pyrolysis Model in Conjunction with Literature Models to Simulate the Experimental Results (Phase I - Task III)

The objective of Phase I, Task III was to test the predictions of various models for droplet heating, vaporization, pyrolysis, and transport against the data. Progress was made in two areas. A program to calculate the vaporization from droplets in AFR's two reactors was implemented on a PDP 11/23 computer. The program will allow testing and improvements of the assumptions used in the heat transfer calculations and the addition of component separation. A cracking model has been developed and programmed to describe the pyrolysis of large paraffins. Sufficient data were not collected on component separation in vaporization to test critically the predictions



Figure 25. Photomicrographs of Fuel Stream Emerging from Hypodermic Tube and Breakup into Droplets. The Tube OD is 250 Microns. The average Droplet Size is about 200 Microns.

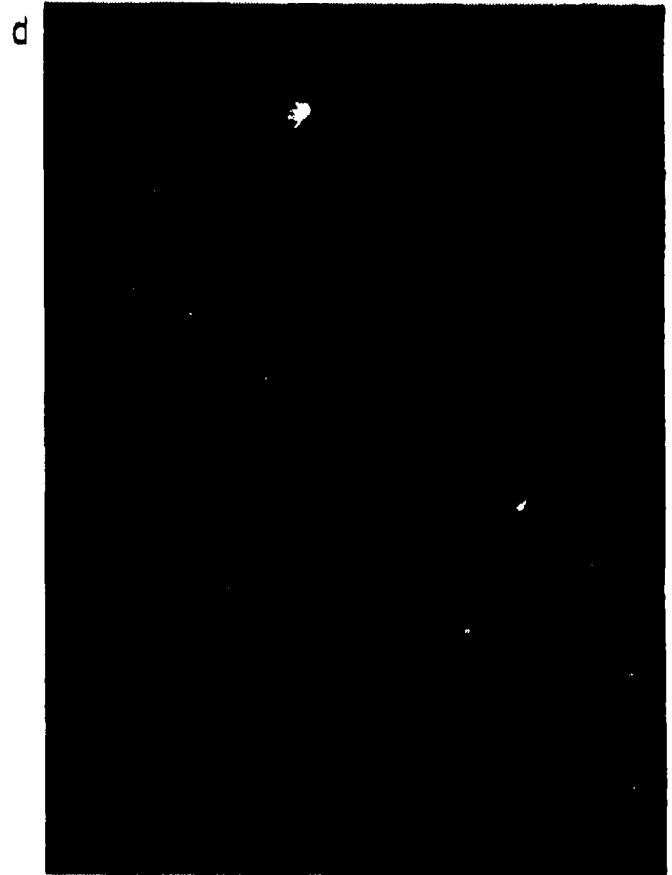
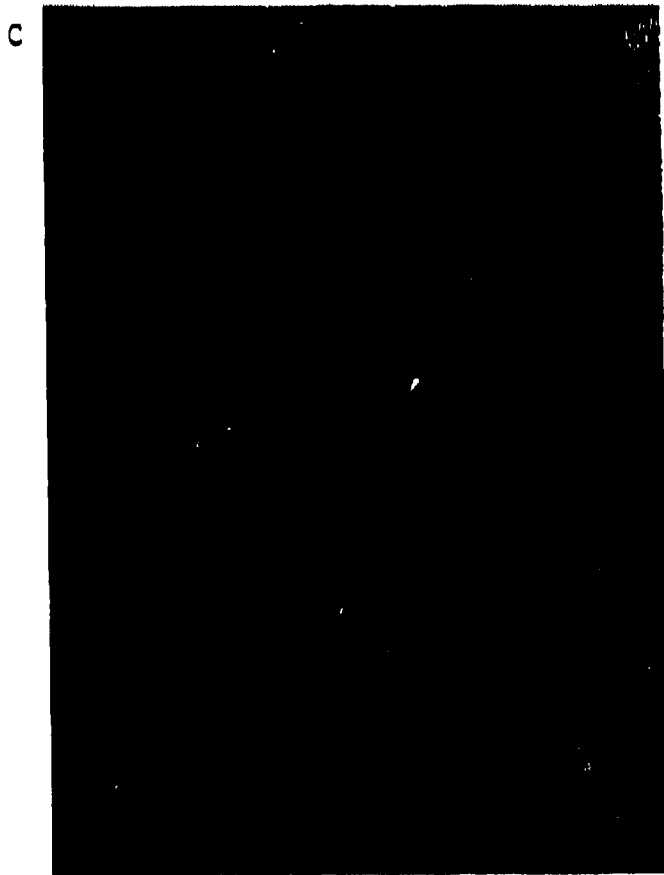
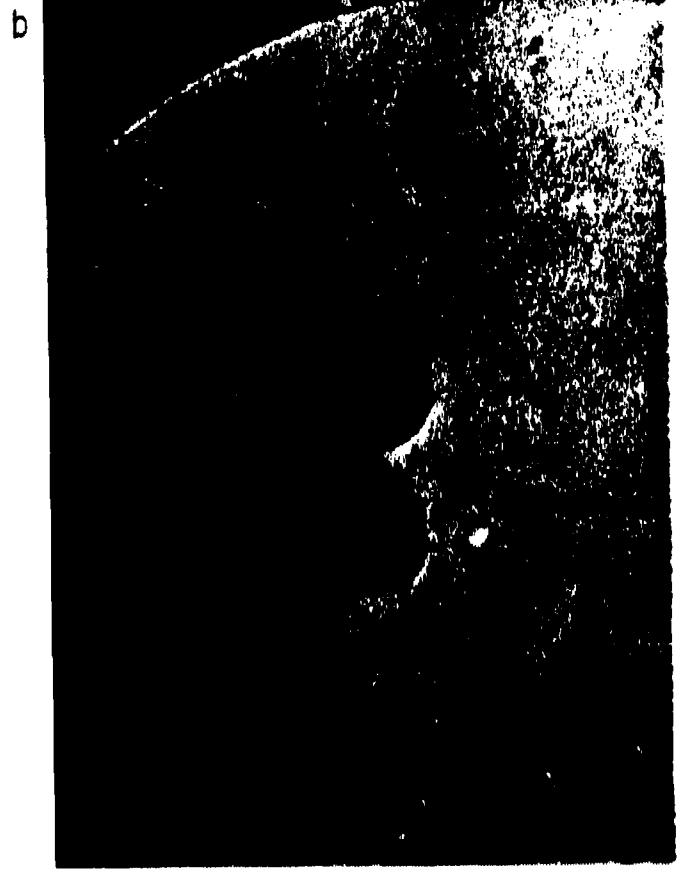
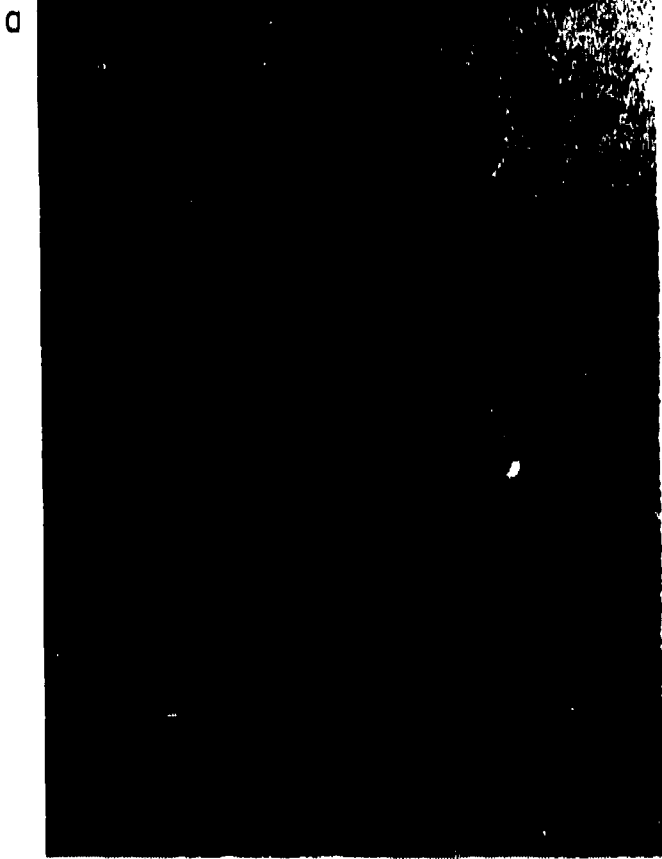


Figure 26. Droplets from Figure 25 Enlarged. d) Shows evidence of a droplet Collision.



c

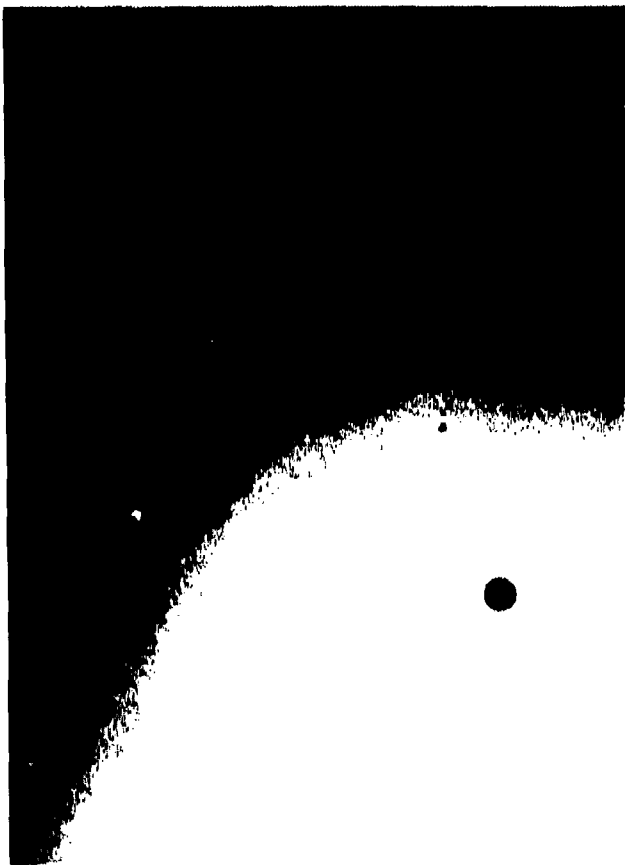


Figure 27. Droplets after Passage Through Heated Tube at 800°C.  
a) and b) 20 cm, c) 50 cm.

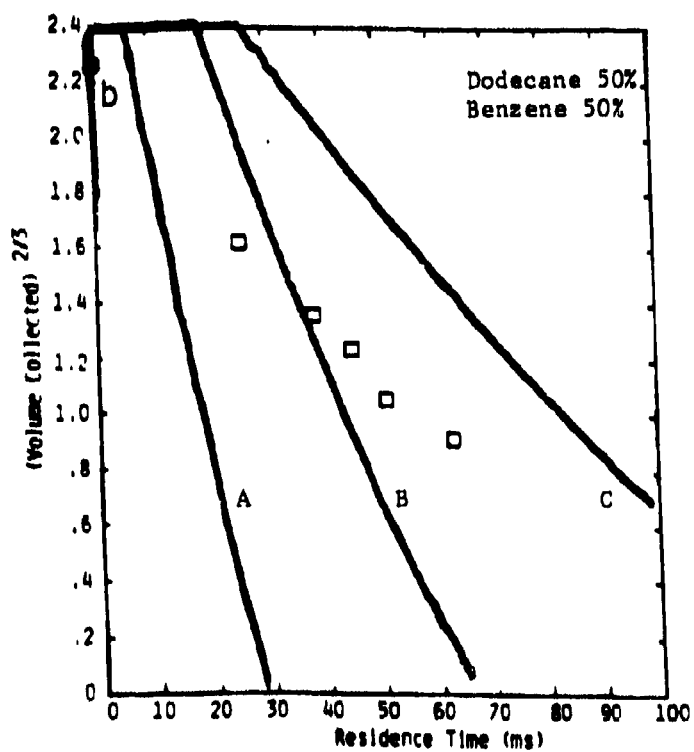
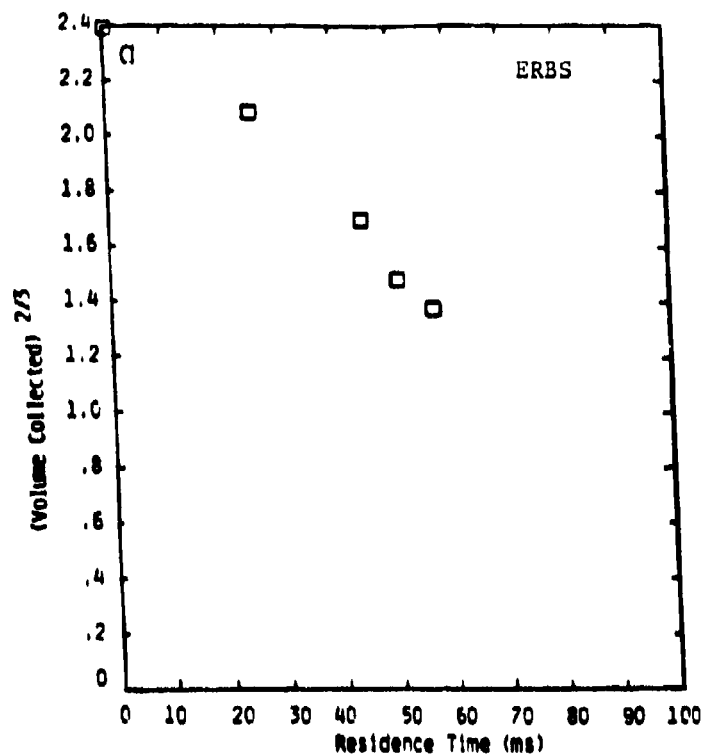


Figure 28. Droplet Vaporization in Helium at 800°C. Lines are Theory for a) Dodecane in Helium, b) Dodecane in Fuel Vapor, c) Benzene in Nitrogen.

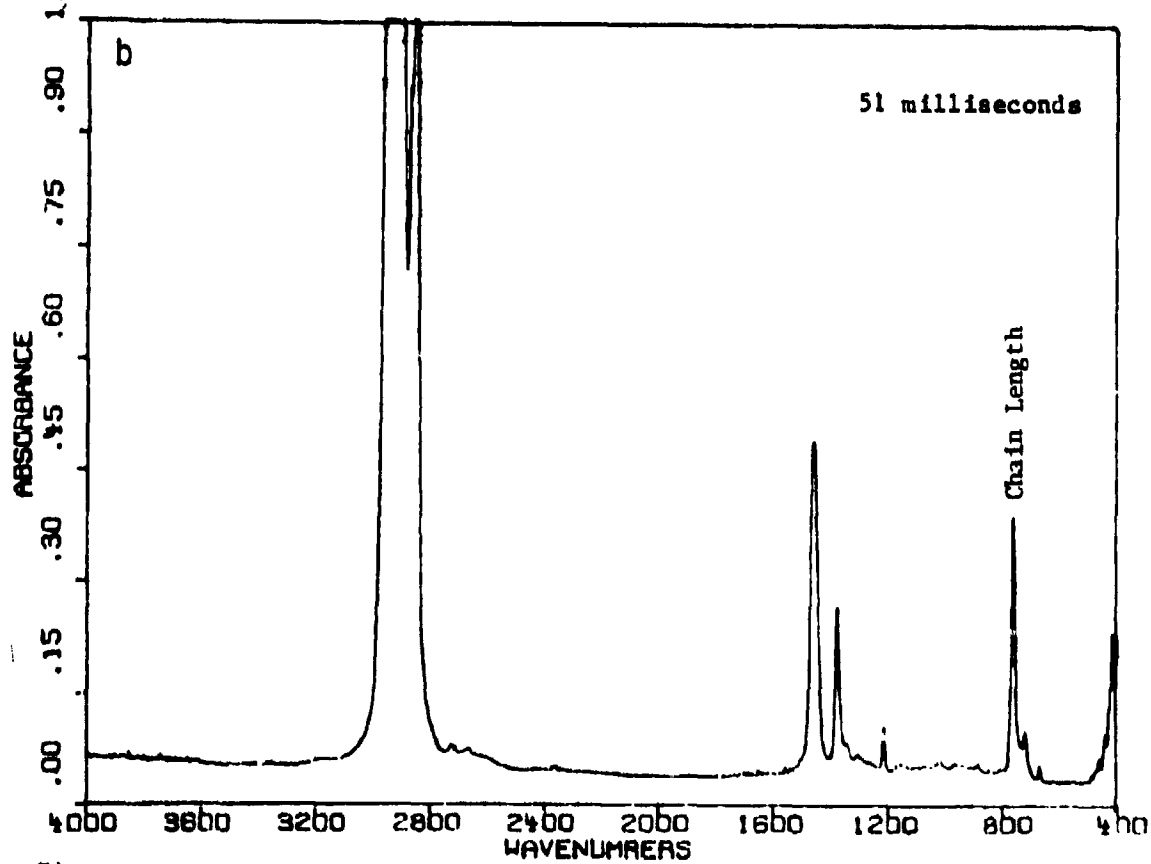
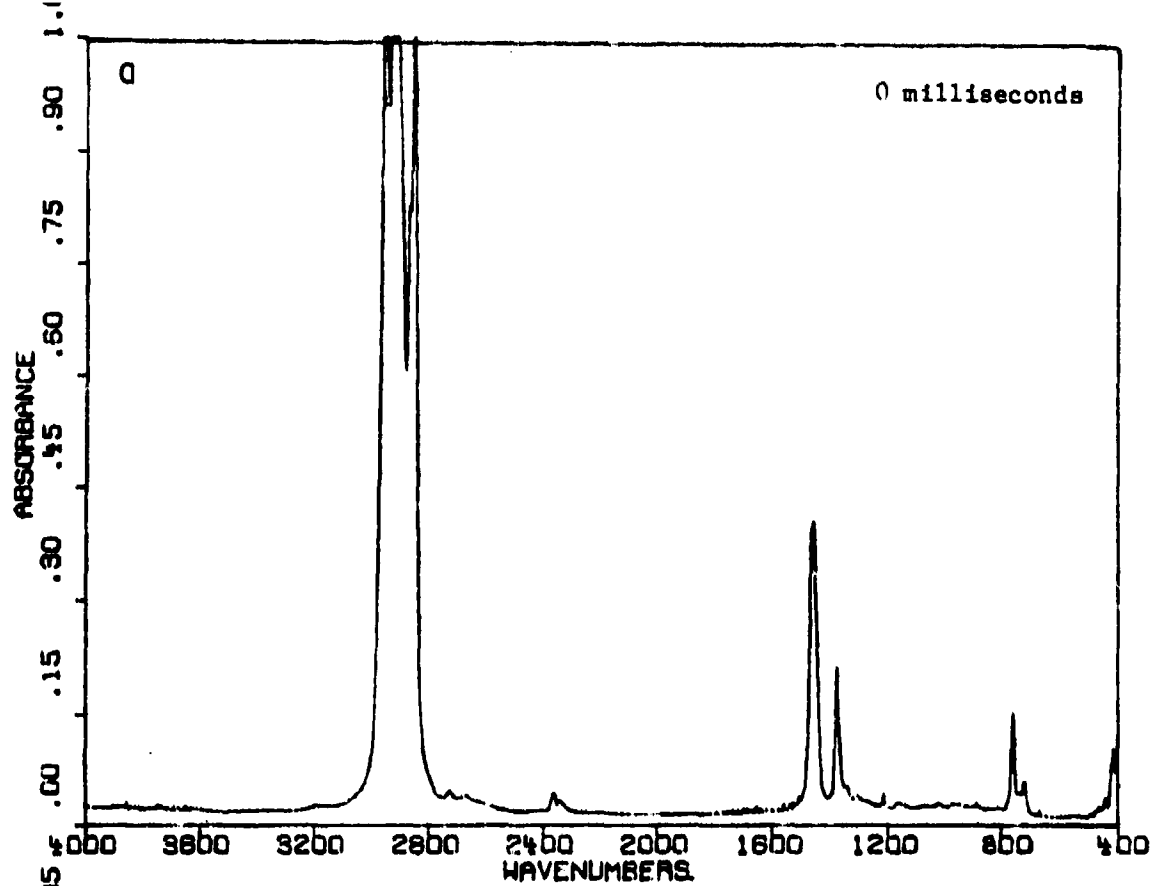


Figure 29. Comparison of FT-IR Spectra for Initial and Partially Vaporized Droplets of JP-7 in Helium at 800°C.

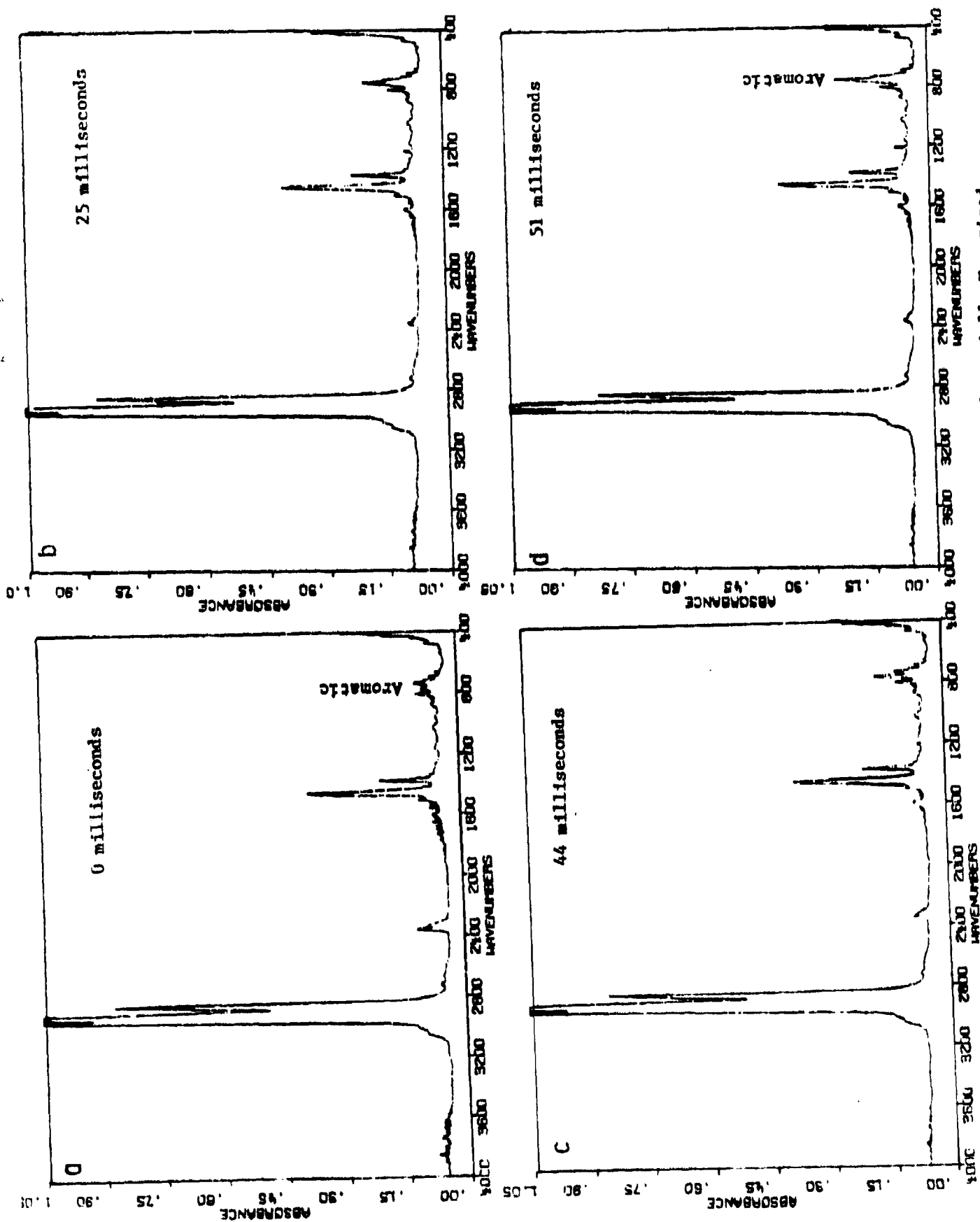


Figure 30. Comparison of FT-IR Spectra for Initial and Partially Vaporized Droplets of ERBS in Helium at 800°C.

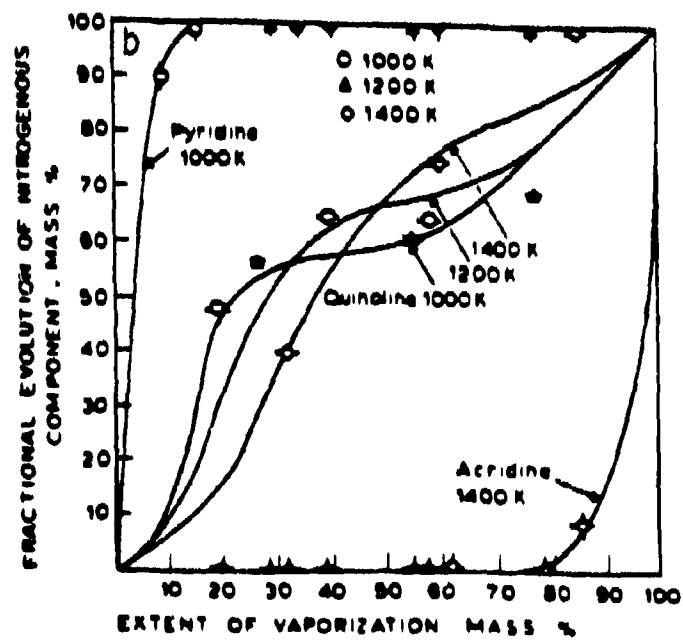
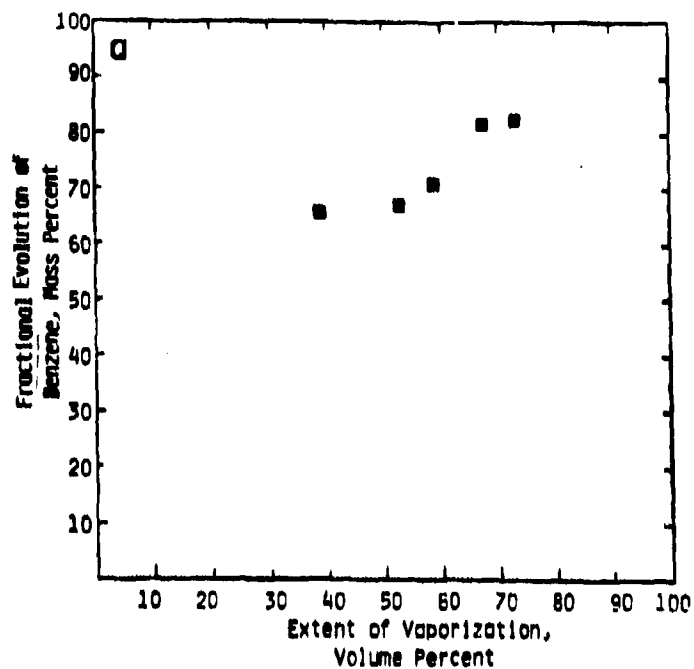


Figure 31. Separation of Components During Vaporization of Fuel Droplets. a) Benzene in Dodecane, b) Pyridine, Quinoline and Acridine in Dodecane, (Nitrogen Data from Hansen et al 48).

### Droplet Heating and Vaporization

The vaporization of the fuel droplets was modeled using the methods of Reference (51). This model considers the energy balance to a droplet which is stationary relative to an ambient gas stream. The heat into the droplet is by radiation from the furnace walls, and by conduction through a layer of fuel vapor and ambient gas surrounding the droplet. The absorption of thermal radiation is negligible for the conditions of the experiment since the absorptivity as measured by FT-IR (Fig. 32e) is essentially zero except in a few wavelength regions. Thus, the energy transport is dominated by the conductivity of the gas surrounding the droplet.

In Figure 32 are the results of our modeling calculations, showing the manner in which velocity, temperature and (diameter)<sup>2</sup> vary with time for 200 micron dodecane droplets injected into a 800 K furnace at an initial relative velocity of 200 cm/sec. The droplet velocity (Fig. 32f) is determined by the force balance between Stoke's Law and the force due to acceleration.

On the left of Fig. 32 can be seen the most significant features of the model. The initial portion of the process is simply heating the droplet up to its boiling point (Fig. 32c), followed by an almost isothermal vaporization of the droplet (Fig. 32d). This vaporization stage is an equilibrium between heat transported into the droplet to vaporize it, and mass transport out from the particle. Much of the heat conducted into the particle is used to heat up the outgoing fuel vapor.

On the Figs. 32f,g,h one can discern the warm-up period, followed by evaporation at the boiling point.

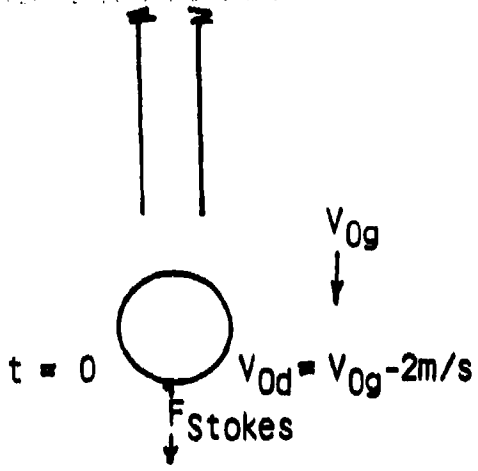
The most serious limitations of the model that we used were as follows: a) the droplet was assumed to be isothermal at all times and b) transport and thermal properties for the "film" were evaluated at the "mid" film temperature and composition, respectively. A better correlation with experiment has been obtained using temperatures and compositions evaluated closer to the droplet (52). We will use this scheme in future calculations.

For the low Reynolds number situations corresponding to our observations, the model gives the value of K (Fig. 32d), the "burning rate" constant for the "d<sup>2</sup>" law, as

$$K = 8k/\rho_L c_p \ln(1 + c_p \cdot \Delta T/L)$$

the well-known rate for stagnant conditions (8,10,11) where k is the "film" thermal conductivity, c<sub>p</sub> the specific heat of the "film", ρ<sub>L</sub> the liquid density, and ΔT the "driving" temperature difference across the film.

The theory for pure components was compared to the data of Fig. 28b for vaporization of a dodecane/benzene mixture. Line A is the prediction for dodecane in helium. The high thermal conductivity of helium results in too high a heat transfer rate. When the thermal properties of dodecane were used for the "film" surrounding the drop, the heat transfer rate is more reasonable. For benzene in nitrogen the heat transfer rate is too low. The theory appears to give reasonable predictions.



b

radiation

Initial Energy Balance

conduction/convection (dominant)

limited mass transport

c

$t = t_{w.b.}$

Wet Bulb Condition

mass transport limited by energy transport

d

$t$

$d_t$

$d_t^2 = d_1^2 - K(t - t_{w.b.})$

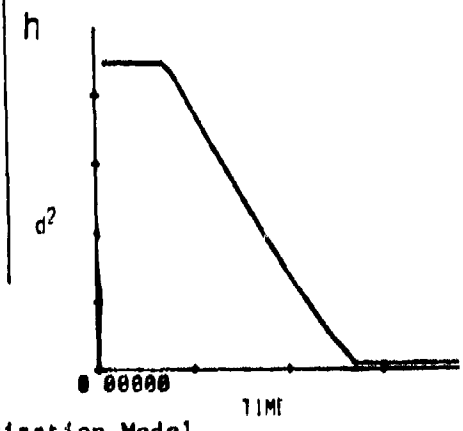
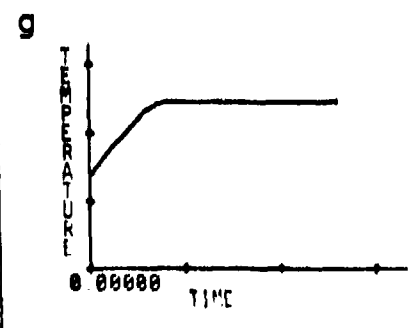
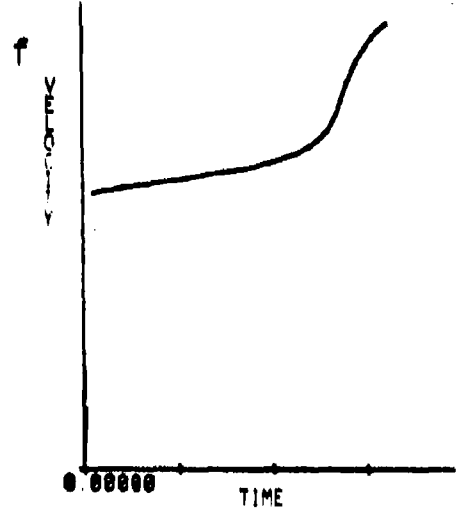
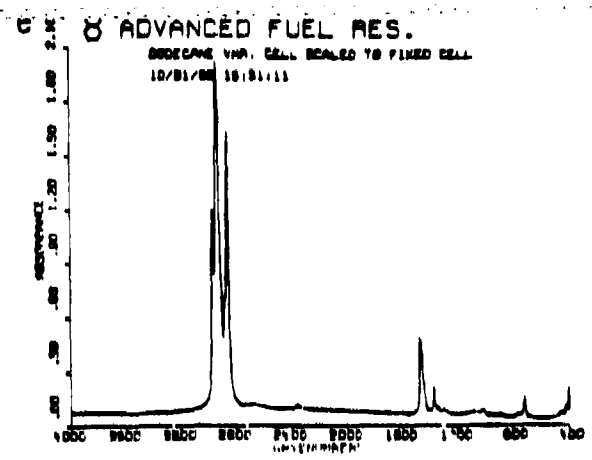
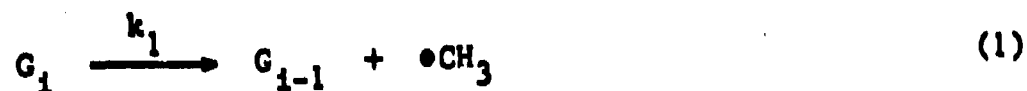


Figure 32. Effects Considered in Droplet Evaporization Model.

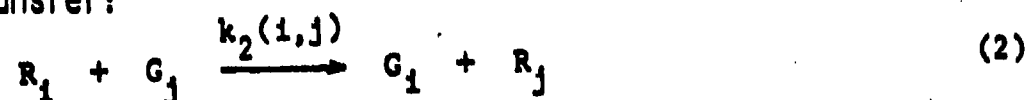
## Gas Phase Cracking

A kinetic model has been developed using some of the free radical reactions known to be important in hydrocarbon cracking theories. Specifically, free radical initiation (Eq. 1), recombination (Eq. 5), radical decomposition (Eqs. 3&4), and H transfer reactions (Eq. 2) have been included.

Initiation:



Hydrogen Transfer:



Decomposition:



Termination:





The model can treat mixtures of straight chain olefins and paraffins with up to 20 carbons. To reduce computational times, the hydrocarbons with lengths greater than three carbons were assumed to rapidly exchange hydrogens. Thus, radical and hydrocarbon populations were always assumed to be in equilibrium and only total heavy radicals needed to be calculated (this approximation is not accurate for many circumstances and will be improved. The remaining equations for radical populations were solved algebraically after making the steady state approximation. That is, for each iteration, the gas populations were held fixed and the equilibrium radical populations were calculated. This technique allows rapid calculations for a set of differential equations with widely varying rates. To reduce the number of parameters appearing in the model, only single initiation and recombination rate constants were used, and it was assumed that radical decomposition rates for the large hydrocarbons depended only on chain position, not on chain lengths. Rate constants were taken unchanged from papers by Doolan and Mackie (53) and by Allara and Shaw (54). The frequency factors for the initiation and recombination rates were then adjusted to give decompositions on the right time scales. The model can be solved in approximately 5 minutes on a PDP 11/23 laboratory computer.

A typical calculation is shown in Fig. 33 for octane decomposition. At short reaction times (Fig. 33a) most of the octane remains uncracked. As time progresses, cracking occurs, resulting in the formation of hydrogen, ethylene, methane and larger products. By 700 milliseconds (Fig. 33f) the octane is almost completely cracked. Methane, ethylene and hydrogen are the dominant products. The results are presented as a function of reaction distance in Fig. 9 for comparison with the entrained flow research data. There is reasonable agreement for both the amount and shape of the predictions. The methane is underpredicted, but as discussed earlier, the JP-4 fuel produces about twice as much methane as a typical paraffin suggesting additional methane sources.

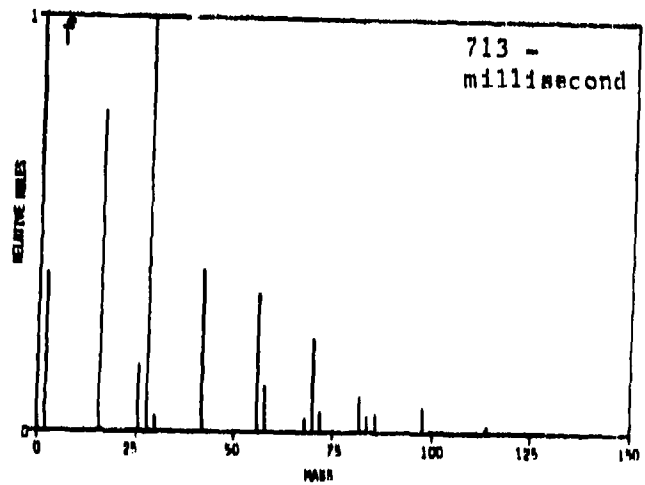
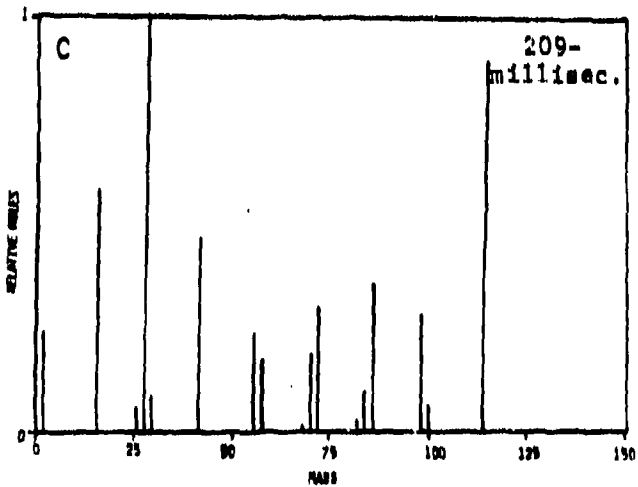
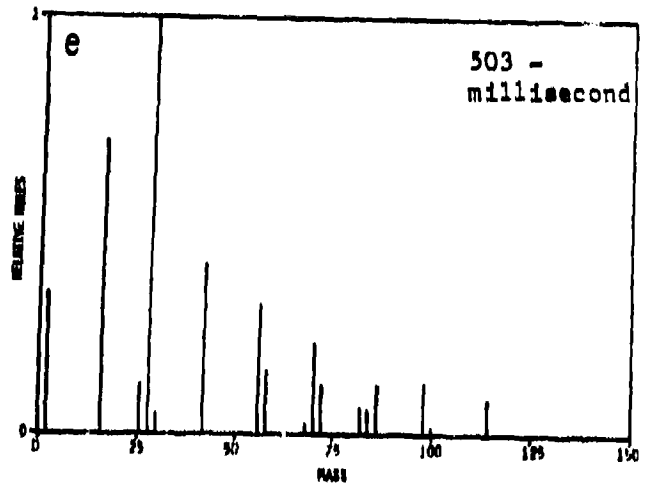
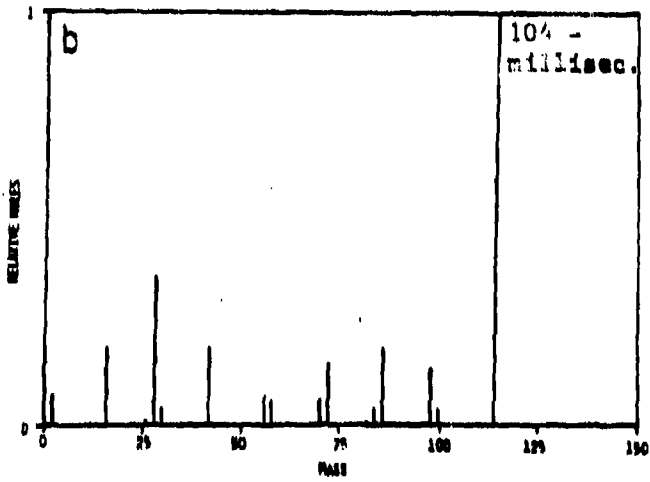
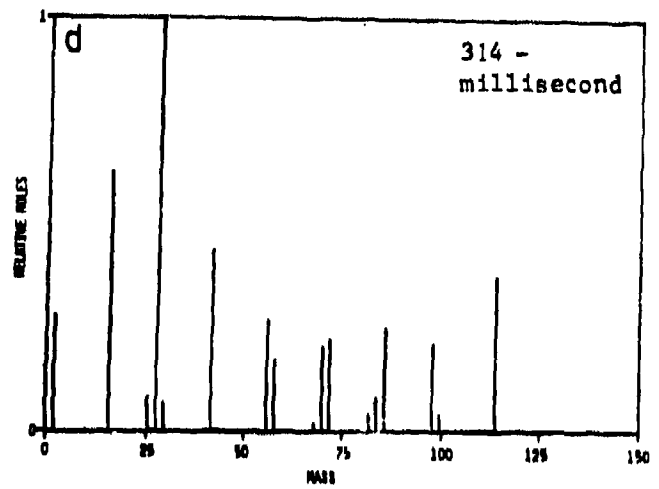
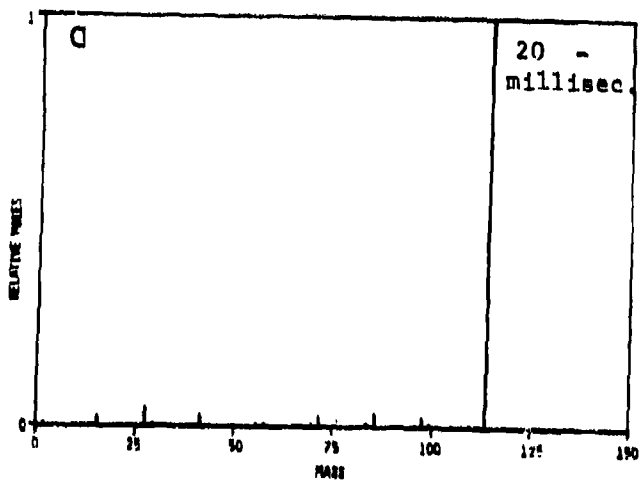


Figure 33. Calculated Species Concentrations from Pyrolysis of Octane at Various Residence Times at 1100°C.

### 3. DISCUSSION

#### Soot Formation

A major objective of this work is to understand the interaction between pyrolysis, combustion and soot formation. In attempting to relate sooting potential to the characteristics of the fuel, Glassman has argued that there are a number of complications caused by studying soot production under combustion conditions (25-27). In this case the level of soot is a balance between soot formation (in fuel rich regions where pyrolysis occurs) and soot destruction by oxidation. It is clear that the competing processes which control soot production in flames provide substantial complications which have limited progress in understanding the mechanisms of soot formation and its relation to fuel properties. To solve the problem the experiments in Task I will be performed under conditions which allow independent control of the important variables affecting soot formation (temperature, residence time, fuel concentration, fuel type, ion concentration and oxygen concentration) and which eliminate the complications of fuel vaporization, fuel mixing, and destruction of soot by oxidation.

The study of soot formation in pyrolysis may simplify the problem, but is it relevant to combustion? Results from Phase I suggest that this is so. Figure 34 compares the soot emission intensities from Figs. 11 and 12 to the measured smoke point for several fuels (55). There is an excellent correlation between the parameters measured in pyrolysis and in combustion. Another good correlation was made in Fig. 35 with the soot emission from four liquid fuels in pyrolysis and soot measured for fuels of comparable aromaticity in a jet engine under take-off conditions (2).

\* The study of soot produced in pyrolysis has provided some important observations in Phase I relating to the influence of hydrogen in suppressing soot formation. In obtaining the emission data for ethane and acetylene (Fig. 12) it was found that the pyrolysis gas composition for ethane (Fig. 36b) contained much more acetylene than the pyrolysis gas of acetylene itself (Fig. 36a). This was so, even though the ethane produces about 1/7 the amount of soot produced by the acetylene. A possible explanation was that the more hydrogen-rich ethane provided certain pyrolysis products which inhibited soot formation. To test this hypothesis, the soot emission from benzene was measured with and without ethane addition. The results in Fig. 37 show that the ethane addition reduced soot, even though the carbon density in the reactor increased.

\* A candidate pyrolysis product which may inhibit soot formation is hydrogen. Wang et al (56) found that soot from acetylene was reduced in the presence of hydrogen. To test this, hydrogen was added to the benzene. The emission spectra of Fig. 38 shows the reduction of soot emission with hydrogen addition.

\* Based on these results, the suggestion is made that the hydrogen released by a fuel in pyrolysis may be an important factor in soot production. This concept is in accord with the correlations which have been made with regard to soot yields versus aromaticity and hydrogen. The more aromatic a fuel, the less hydrogen it can release in pyrolysis. Thus, ERBS and benzene are high sooting fuels. In general, the more aromatic a fuel, the lower its total hydrogen, so low hydrogen and high aromaticity go together. But what about JP-4 which has 15% aromatics but a hydrogen value greater than JP-7 with 2.5% aromatics. A clue is that JP-4 produces about twice the methane of JP-7 (Figs. 7b and 8b). A plausible explanation is that JP-4 is highly branched with a high concentration of methyl groups. In pyrolysis, these groups form methane, not hydrogen, so that while JP-4 has a high hydrogen concentration, its hydrogen released in pyrolysis is low, leading to high soot yields.

\*Use or disclosure of the proposal data on lines specifically identified by asterisk (\*) are subject to the restriction on the cover page of this proposal.\*

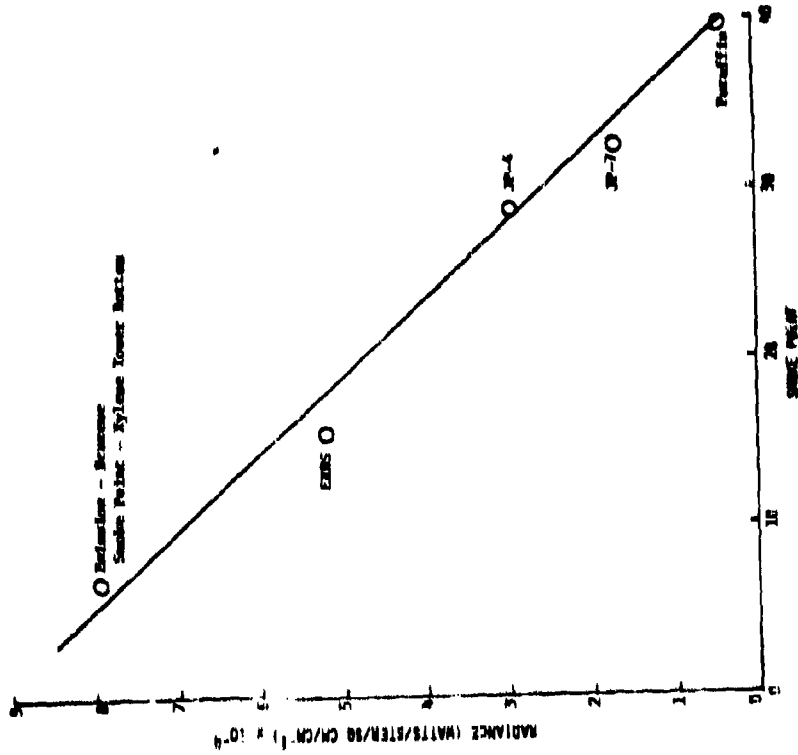


Figure 34. Correlation of Soot Emission in Pyrolysis with Measured Smoke Point. (Smoke Point Data from Rosfjord, 55).

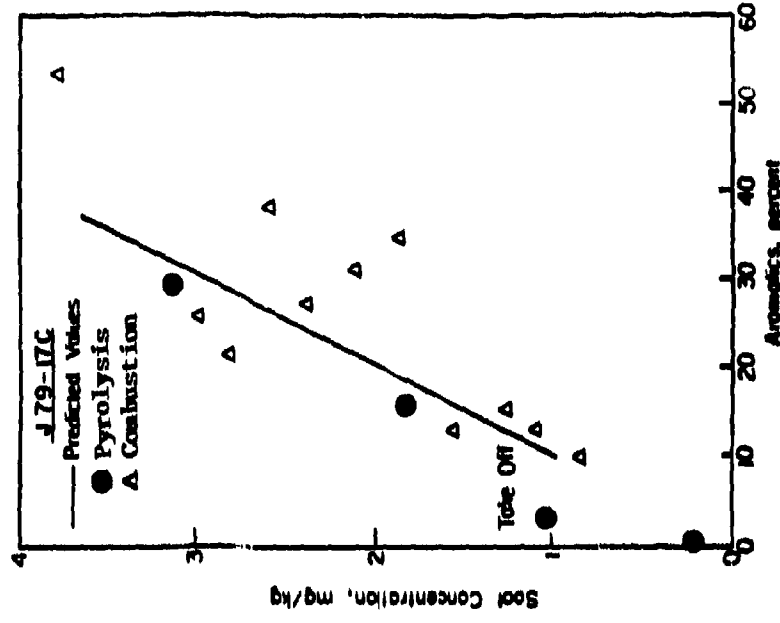


Figure 35. Correlation of Soot Production with Aromatic Content. Circles are Soot Measured in Pyrolysis, in Phase I, Triangles are Soot Measured at Take off Conditions. From Lefebvre (2).

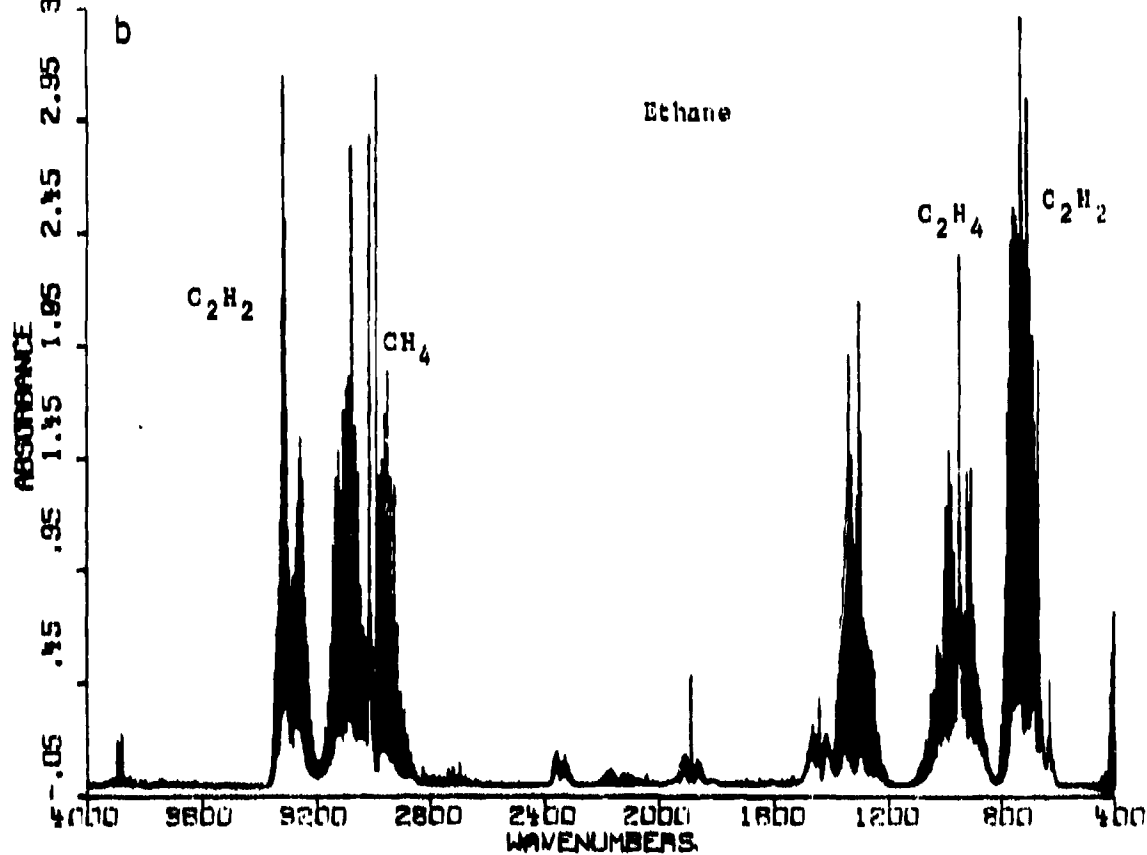
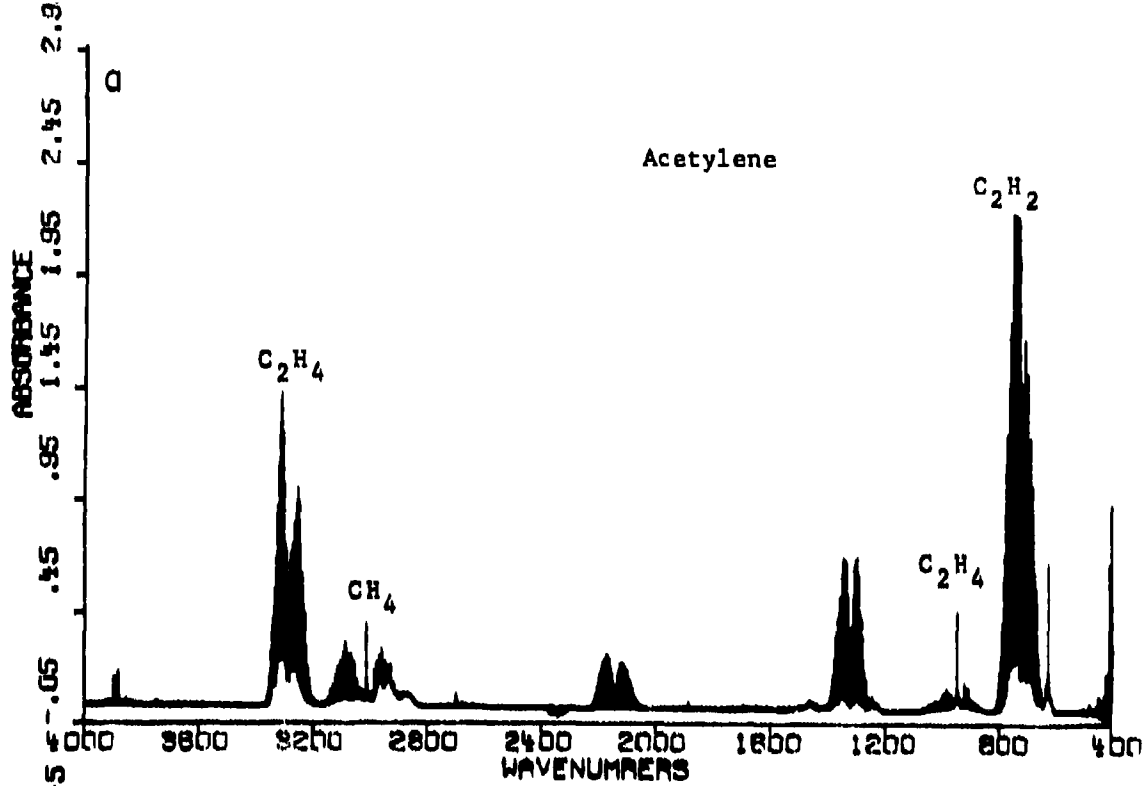


Figure 36. Spectra of Pyrolysis Gas From Ethane and Acetylene at 1300°C for 56 cm Reaction Distance.

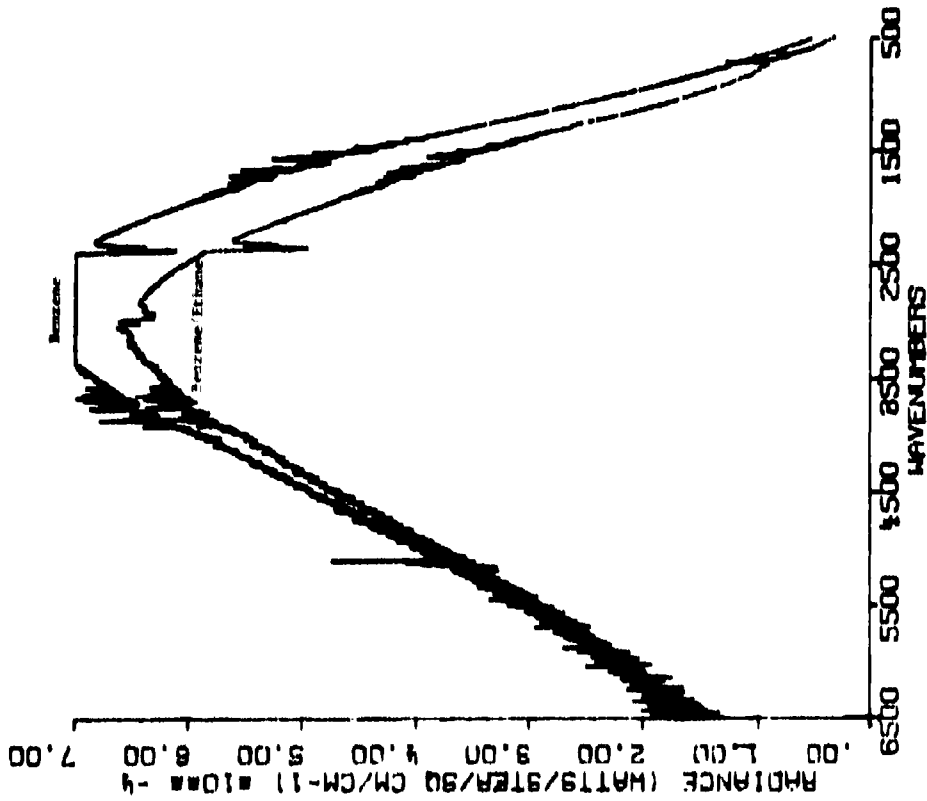


Figure 37. Emission Spectra for Benzene and Benzene Plus Ethane at 1300°C for 56 cm Reaction Distance.

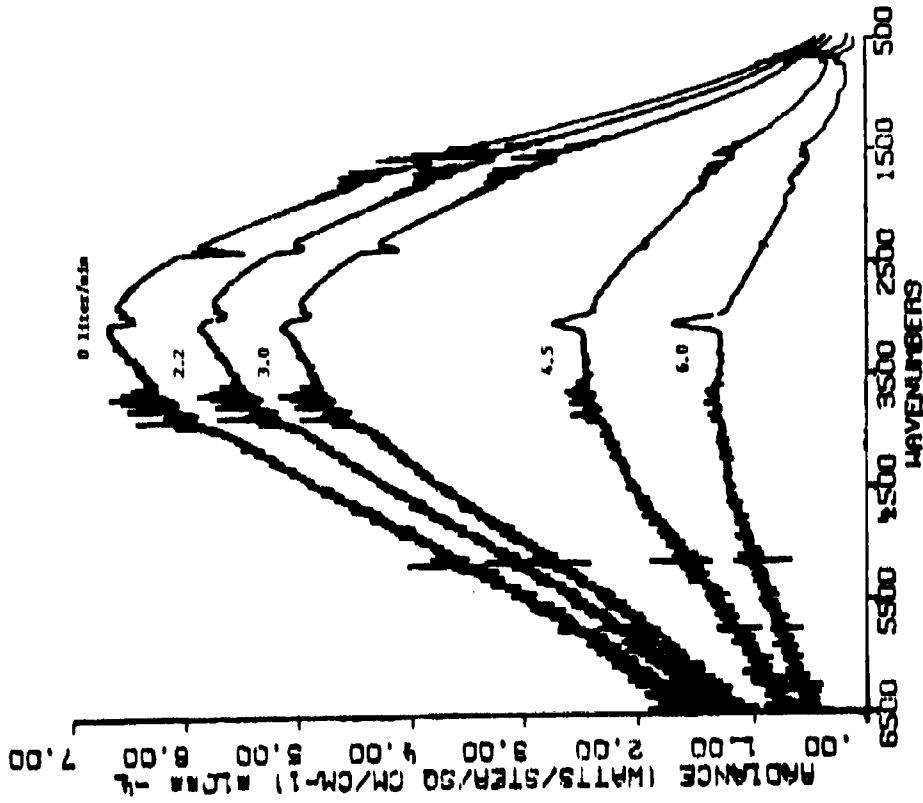


Figure 38. Emission Spectra for Benzene and Benzene Plus Hydrogen at 1300°C for 56 cm Reaction Distance.

\* As indicated in Fig. 18, the addition of oxygen also dramatically effects the  
\* production of soot. This variation appears to occur because of the increase of the  
\* pyrolysis rate in the presence of oxygen. This is expected since oxygen will  
\* increase the free radical concentration which controls the pyrolysis rate. It also  
\* reduces the available hydrogen. It represents another important variable in  
\* identifying the soot production mechanisms.

\* The mechanisms of soot formation have been discussed by a number of authors (25-27,  
\* 57-75). An excellent collection of reviews appears in "Soot in Combustion Systems"  
\* (57) which contain many of the articles referred to herein. Soot formation is  
\* considered to be a series of processes which starts with the growth of large  
\* molecules (the soot precursors) followed by the nucleation of small particles  
\* (larger than 1.5 nm). The small particles grow first by consuming molecular species  
\* and by coagulation to sizes of 20 to 100 nm and finally by agglomeration (up to 1000  
\* nm). There is reasonable agreement that the coagulation can be treated by collision  
\* theory as discussed by Prado and co-workers (68,69), and Howard and co-workers (62).  
\* The major question is the mechanism of large molecule formation and particulate  
\* nucleation, and whether there are different paths for paraffins and aromatics.  
\* Several features of the nucleation process have been identified. J.B. Howard, J.P.  
\* Longwell and co-workers (59,61,65,71,72) have demonstrated that the growth of large  
\* polycyclic aromatic hydrocarbons (PAH), many of which are charged, precede the  
\* appearance of soot. Howard has discussed possible mechanisms for PAH growth which  
\* involve aromatic radicals, unsaturated aliphatics such as acetylene and H atoms.  
\* Calcote (66,67) has argued that radical mechanisms are too slow to explain the rapid  
\* appearance of PAH and that ionic species are present in sufficient quantities, and  
\* have sufficiently fast reaction rates to be the primary ingredient of soot  
\* formation. Glassman and co-workers (25-27) point out that pyrolysis kinetics play a  
\* dominant role in the sooting tendencies of flames.

\* Pyrolysis of hydrocarbon fuels produces small stable species such as methane,  
\* acetylene and benzene as well as large species. The capture and analysis of the  
\* large molecules will be particularly important. While these molecules were not  
\* specifically identified in Phase I, their presence can be inferred. The data for  
\* pyrolysis at 1100°C show a loss from total gas species above 50 cm (Fig. 9a).  
\* There is no corresponding increase in the soot emission (Figs. 5 and 6) and it is  
\* likely that the loss of material is going to build heavier molecules not detected by  
\* FT-IR in the gas phase. A cooled trap will be used to collect this material for  
\* analysis by FT-IR, GC and FIMS.

\* In future studies, the relationship between pyrolysis, combustion and soot formation  
\* should be examined by measuring the growth of small pyrolysis products, of large  
\* molecules and of soot for a variety of fuels and additives (oxygen, hydrogen and  
\* ions) which affect soot formation.

#### Correlation of Soot Formation with FT-IR Spectra of Fuels

\* The methodology for FT-IR analysis was discussed in Sec. 2.2. The purpose of the  
\* analysis is to correlate FT-IR properties with combustion behavior. Properties of  
\* interest include i) the aromaticity and chain length indicator as illustrated in  
\* Fig. 39c (dodecane has the longest and JP-4 the shortest chains and ERBS is most  
\* aromatic). ii) the  $\text{CH}_3$  and  $\text{CH}_2$  wag in Fig. 39b (JP-4 has the highest methyl and  
\* dodecane the lowest, ERBS has the lowest  $\text{CH}_2$  peak). iii) the  $\text{CH}_3$  and  $\text{CH}_2$  stretch in  
\* Fig. 39a (JP-4 has the highest  $\text{CH}_3$  and ERBS the lowest  $\text{CH}_2$ ).

\* The higher methyl group concentration for JP-4 is in agreement with its high methane  
\* yield and high soot production. An indication of hydrogen release in pyrolysis may

\* "Use or disclosure of the proposal data on lines specifically identified by asterisk (\*) are  
\* subject to the restriction on the cover page of this proposal."

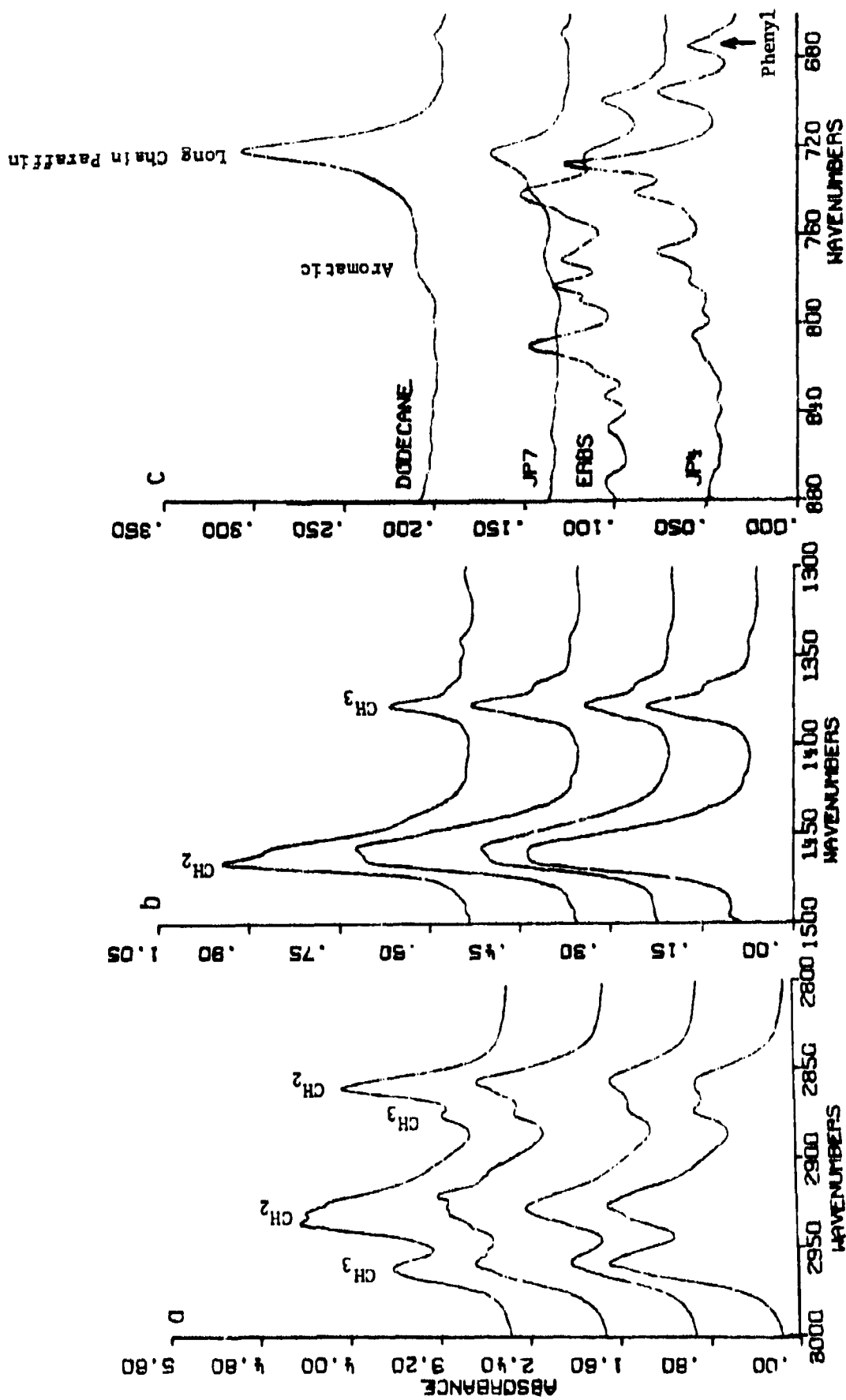


Figure 39. Comparison of FT-IR Spectra for Four Fuels. a) Aliphatic Stretch Region, b) Aliphatic Wag Region, c) Aromatic Wag Region.





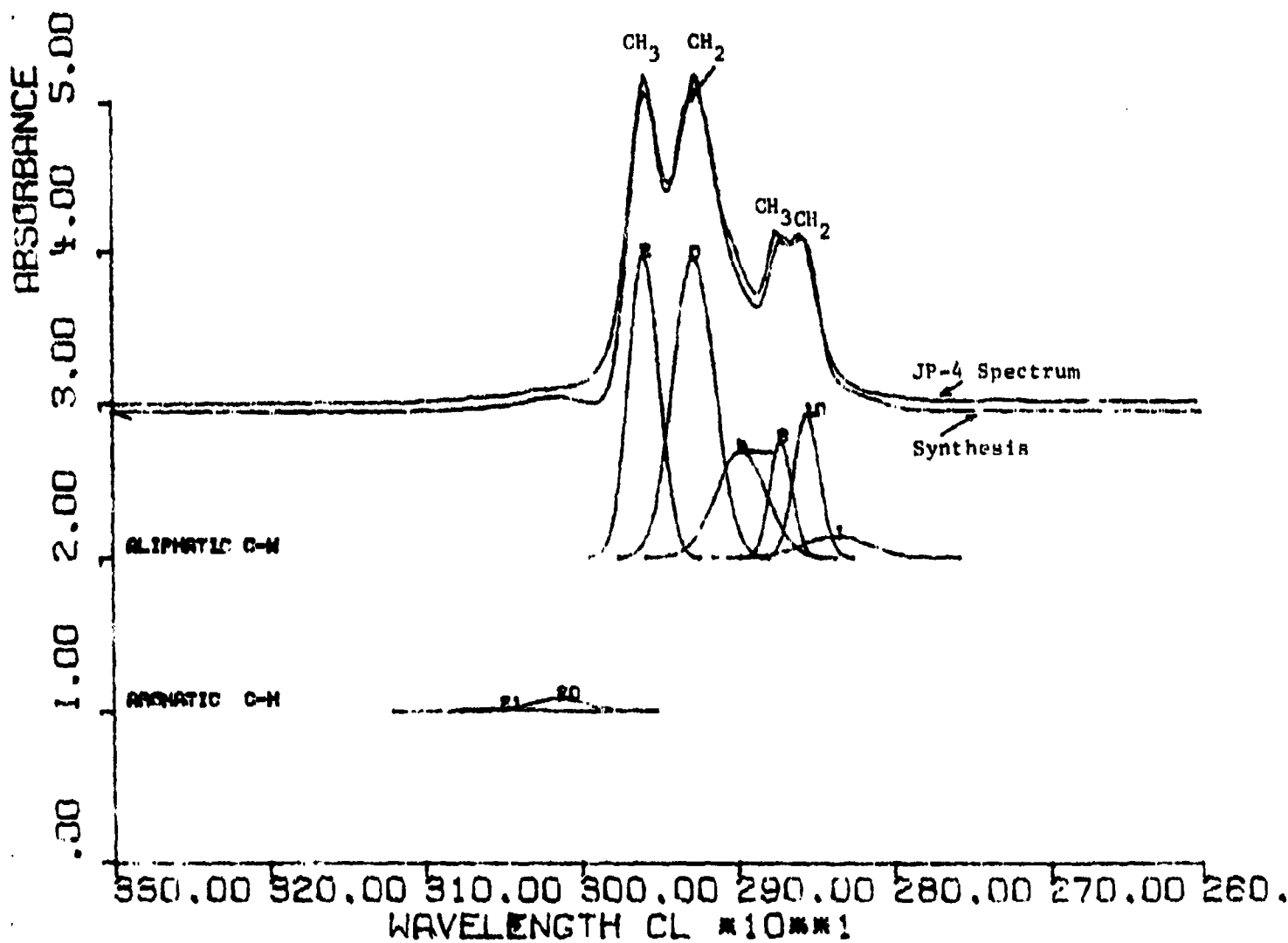


Figure 40. Automated Curve Analysis Routine for Quantitative Analysis of Specific Functional Groups.

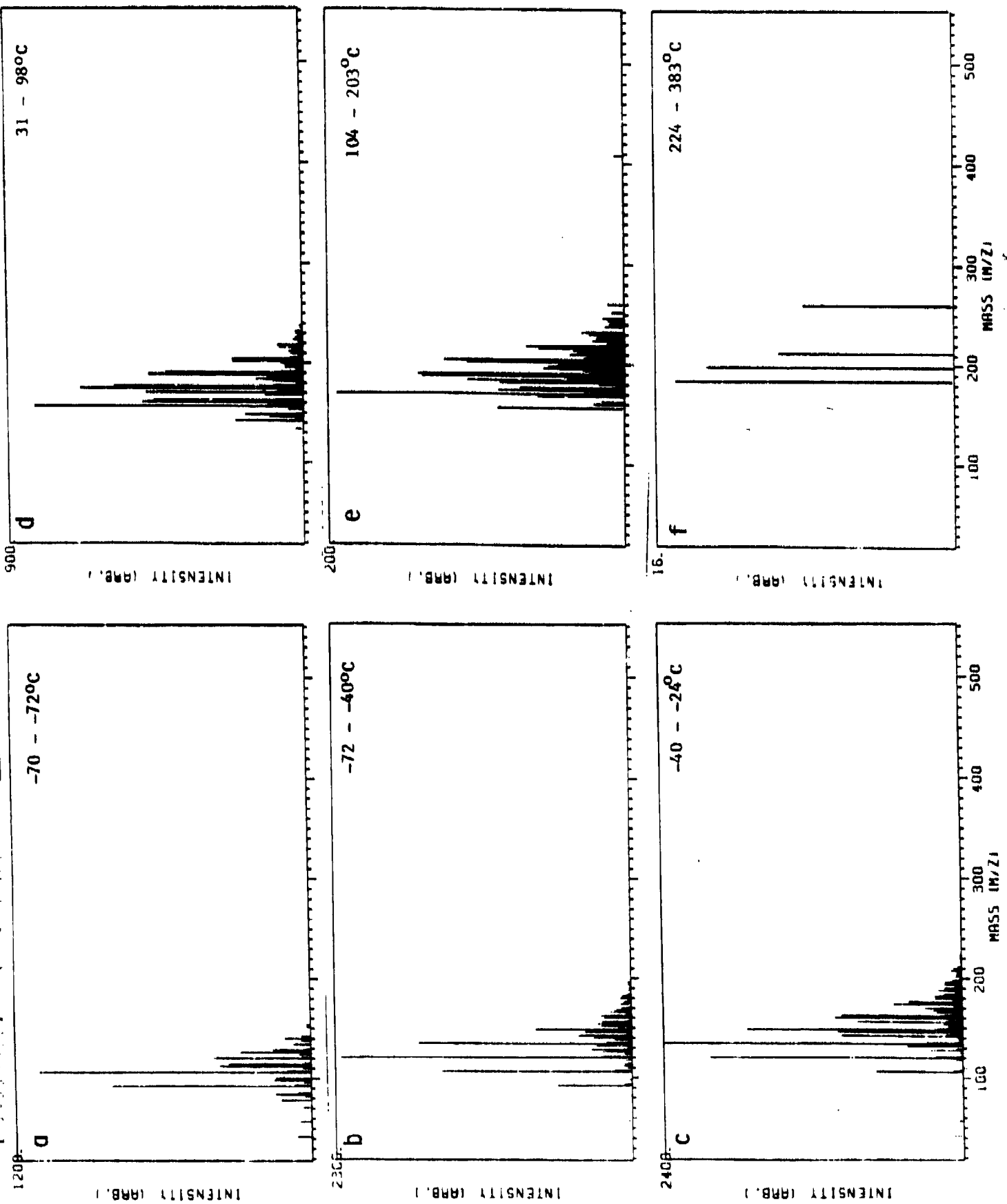


Figure 41. FIMS Spectra of JP-4 Fuel at Several Sample Temperatures.

#### 4. CONCLUSIONS AND RECOMMENDATIONS

\* The major objective of this work was to determine how the fuel characteristics  
\* influence combustion behavior including atomization, vaporization, pyrolysis,  
\* ignition and soot formation. The Phase I program has demonstrated the effectiveness  
\* of mechanistic studies in a well controlled laboratory reactor with in-situ FT-IR  
\* diagnostics. It has further demonstrated the usefulness of using FT-IR and FIMS to  
\* characterize the initial fuel and follow changes during vaporization and pyrolysis.  
\* Applying these techniques in Phase I has allowed identification of the "hydrogen  
\* release potential" of fuel as possibly the most important factor affecting soot  
\* formation. The effect of low concentration of oxygen in increasing soot has also  
\* been demonstrated. Mechanistic studies should proceed to elucidate the fundamental  
\* mechanisms, the role of hydrogen (in soot suppression), and the role of oxygen (in  
\* soot enhancement and oxidation) and should also extend the studies to conditions  
\* closer to combustion in a jet engine. The following questions raised in Phase I  
\* should be addressed.

- \*  
\*     • The interesting observation that soot formation in pyrolysis appears to  
\* depend on the  $H_2$  released from the fuel in pyrolysis must be investigated  
\* to quantify the result and determine whether it applies for oxidative  
\* conditions and high pressures.  
\*  
\*     • If  $H_2$  released during pyrolysis is the chief factor controlling soot  
\* formation, correlations must be developed to predict  $H_2$  released using  
\* fuel characteristics and combustion conditions. Also, what does this  
\* result tell us about the soot formation process?  
\*  
\*     • The increase in soot production with oxygen will have to be investigated  
\* to determine the mechanisms and fit it into the model for pyrolysis and  
\* soot production.  
\*  
\*     • Several changes in experimental techniques are needed to improve the  
\* mechanistic studies. Variations in droplet size and droplet collisions  
\* were observed using a vibrating tube droplet generator. An improved  
\* piezoelectric droplet generator to provide more regular droplet sizes and  
\* wider spacing should be employed for the additional mechanistic studies.  
\* The in-situ emission and transmission measurements were subject to  
\* variation caused by variations in flow homogeneity. A better controlled  
\* flow in front of the optical window should be provided.  
\*  
\*     • The gas phase reaction model has been developed for cracking reactions  
\* with hydrocarbon radicals only. Further work is needed to optimize the  
\* reaction kinetics, add oxygen containing radicals and expand the model to  
\* describe large molecule building which occurs in soot formation.  
\*  
\*     • Fuel composition variations were observed during vaporization. The  
\* results suggest that component separation falls between the extremes  
\* expected for complete mixing and equilibrium distillation. To provide an  
\* adequate test of drop vaporization theories, experiments must be performed  
\* as a function of relative drop velocity.  
\*  
\*     • The experiments at one atmosphere must be extended to characterize the  
\* behavior at typical engine pressures.  
\*

"Use or disclosure of the proposal data on lines specifically identified by asterisk (\*) are subject to the restriction on the cover page of this proposal."

1. T.L. Oller, Gleason, C.C., Kenworthy, M.J., Cohen, J.D., and Bahr, D.W., "Fuel Mainburner/Turbine Effects", Final Report, AFWAL-TR-81-2100, General Electric Company, (June 1979-May 1981).
2. Lefebvre, A.H., "Fuel Effects on Gas Turbine Combustion", Final Report, AFWAL-TR-83-2004, Purdue University, (September 1981-December 1982).
3. Abbas, A.S., Koussa, S.S. and Lockwood, F.C., 18th Symposium (Int) on Combustion, The Combustion Institute p. 1427 (1981).
4. Spalding, D.B., Numerical Computation of Two-Phase Flow, Second International Conference on Physicochemical Hydrodynamics (1978).
5. Edelman, R.B. and Harsha, P.T., Prog. Energy Comb Sci 4, 1, (1978).
6. McDonald, H. Prog. Energy Comb Sci 5, 97, (1979).
7. Oran, E.S. and Boris, J.P., Prog. Energy Comb Sci 7, 1, (1981).
8. Faeth, G.M., Prog. Energy Combustion Science, 3, 191 (1977).
9. Chigier, N.A., "Energy, Combustion and Environment", McGraw-Hill, NY (1981).
10. Williams, A., Prog. Energy Combustion Science, 2, 167 (1976).
11. Law, C.K., Prog. Energy Combustion Science, 8, 171 (1982).
12. Sirignano, W.A., Fuel Vaporization and Spray Combustion Theory, to be published in Prog. Energy Comb. Sci (1983).
13. Sirignano, W.A., Law, C.K., Adv. in Chem. Series 166, pp. 1-26 (1978).
14. Solomon, P.R., and Hamblen, D.G., Quarterly Reports, DOE Contract #DE-AC21-FE05122, Coal Gasification Reactions With On-Line In-Situ FT-IR Analysis, (1981).
15. Solomon, P.R. and Hamblen, D.G., Quarterly Reports, DOE Contract #DE-AC22-82PC50254, An Investigation of Vaporization and Devolatilization of Coal/Water Mixtures, (1982-1984).
16. King, H.H., Solomon, P.R., Avni, E. and Coughlin, R., Modeling Tar Composition in Lignin Pyrolysis, ACS Div Fuel Chem., 319, (1983).
17. Avni, E., Coughlin, R., Solomon, P.R. and King, H.H., Lignin Pyrolysis in Heated Grid Apparatus: Experiment and Theory, ACS Div Fuel Chem., Preprints, 307, (1983).
18. Solomon, P.R. and Hamblen, D.G., Final Report, EPRI Project No. 1654-7, Characterization of Thermal Decomposition of Coal in Experimental Reactors, (1982).
19. Solomon, P.R. and Hamblen, D.G., Measurement and Theory of Coal Pyrolysis Kinetics in an Entrained Flow Reactor, EPRI Final Report for Project RP 1654-8, (1983).
20. Solomon, P.R., The Synthesis and Study of Polymer Models Representative of Coal Structure, Final Rep. GRI, Cont #5081-260-0582, , (April, 1983).
21. Solomon, P.R. and King, H.H., Pyrolysis of Models Polymers: Theory and Experiments, Accepted for publication in Fuel.
22. Solomon, P.R., Hamblen, D.G., Carangelo, R.M., and Krause, J.L., Coal Thermal Decomposition in an Entrained Flow Reactor; Experiments and Theory, 19th Symposium (Int) on Combustion, The Combustion Institute, Pittsburgh, PA, p. 1130 (1982).
23. Solomon, P.R., Hamblen, D.G. and Carangelo, R.M., Analytical Pyrolysis of Coal Using FT-IR, 5th Int. Symp on Analyt. Pyrolysis, Vail, CO (Sept. 1982).
24. Solomon, P.R. and Hamblen, D.G., ACS Preprints, Division of Fuel Chemistry 27, p 41 (1982).
25. Takahashi, F. and Glassman, I., Sooting Correlations for Premixed Flames, (to be published).
26. Glassman, I., Soot Reduction in Power Plants, Engineering Report 1632, AFOSTR TR No. (applied for).
27. Glassman, I., Brezinsky, K., Gomer, A. and Takahashi, F., Physical and Chemical Kinetic Effects in Soot Formation, Annual Meeting of The Combustion Institute, Sezione Italiana Ischia (July 2, 1982).
28. Solomon, P.R., Advances in Chemistry, 193, 95 (1981).

29. Solomon, P.R., Hamblen, D.G. and Carangelo, R.M., Applications of FT-IR in Fuel Science, ACS Symposium Series 205, (1981) pg. 77.
30. Solomon, P.R. and Carangelo, R.M., Fuel, 61, 663, (1982).
31. Solomon, P.R. and Hamblen, D.G., Finding Order in Coal Pyrolysis Kinetics, Progr. in Energy and Comb. Sci. (1984).
32. Solomon, P.R. and Colket, M.B., Fuel 57, 749, (1978).
33. Solomon, P.R., Hobbs, R.H., Hamblen, D.G., Chen, W.Y., La Cava, A., and Graff, R.S., Fuel, 60, 342, (1981).
34. Solomon, P.R., and Colket, M.B., 17th Symposium (International) on Combustion, p. 131, The Combustion Institute, Pittsburgh, PA, (1979).
35. Best, P.E., Carangelo, R.M., and Solomon, P.R., Use of Fourier Transform Infrared Emission to Study Pyrolysis, (submitted to 20th Symposium (Int) on Combustion (1984)).
36. Gardner, J.L., Jones, T.P. and Davies M.R., "Temperature", Vol. 5, Part 1, Ed. by J.F. Schooley, (Am. Inst. Phys.), 1982 p. 409.
37. Vervisch, P. and Coppalle, A., Combustion and Flame, 52, 127 (1983).
38. Buckius, R.O. and Tien, C.L., Inst. J. Heat Mass Transfer, 20, 93, (1977).
39. D'Alessio, A.D., Beretta, F. Cavalliere, A. and Menna, "Soot in Combustion Systems", Ed. by Lahaye, J. and Prado, G. pg. 30, Plenum Press (1983).
40. Van de Hulst, H.C., "Light Scattering by Small Particles", Dover Publications, NY, (1981).
41. Lee, S.C. and Tien, C.L., 18th Symposium (Int) in Combustion, p. 1159, (1981) and references therein.
42. Stull, V.R. and Plass, G.N., J. Optical Soc. Am., 50, 121, (1960).
43. The analysis requires that the soot in the path be at one temperature, but does not require constant soot density.
44. Pagni, P.J. and Bard, S., 17th Symposium (Int) in Combustion, p. 1017, (1978).
45. Schack, A., Z. Tech. Phys., 6, 530, (1925).
46. Schug, K.P., Mannheimer-Timnat, Y., Yaccarino, P., and Glassman, I., Sooting Behavior of Gaseous Hydrocarbon Diffusion Flames and the Influence of Additives, Comb. Sci. and Tech. 22, 235 (1975).
47. St. John, G.A., Buttrill, S.E., Jr. and Anbar, M., "Field Ionization and Field Desorption Mass Spectroscopy Applied to Coal Research", in Organic Chemistry of Coal, (Ed J. Larsen) ACS Symposium Series 71, 1978, p. 223.
48. Hansen, S.P., Beer, J.M. and Sarofim, A.F., 19th Symposium (Int) on Combustion, The Combustion Institute, p. 1029 (1982).
49. Sirignano, W.A. and Yao, S.C., Vaporization of Synthetic Fuels, Proceedings Direct Utilization AR&TD Contractors Review Meeting, p. 20, Pittsburgh, PA, April 5-8 (1981).
50. Prakash, S. and Sirignano, W.S., Int. J. Heat and Mass Transfer, 23, 253-268 (1980).
51. Bird, R.B., Stewart, W.E. and Lightfoot, E.N., Transport Phenomena, John Wiley & Sons, New York, 1960.
52. Hubbard, G.L., Denny, V.E. and Mills, A.F., Int. J. Heat and Mass Transfer, 18, 1003-1008 (1975).
53. Doolan, K.R. and Mackie, J.C., Combustion and Flame 50, 29, (1983).
54. Allara, D.L. and Shaw, R., J. Phys. Chem. Ref. Data, 9, (3), 523 (1980).
55. Rosfjord, T.J., NASA Contractor Report #168334, "Aviation-Fuel Property Effects on Combustion", February (1984).

56. Wang, T.S., Matula, R.A. and Faryner, R.C., Eighteenth Symposium (Int) on Combustion, The Combustion Institute, Pittsburgh, PA, p. 1149 (1981).
57. Lahaye, J. and Prado, G. "Soot in Combustion Systems", NATO Conference Series, 7, Plenum Press, NY (1983).
58. Wagner, H. GG, Seventeenth Symposium (Int) on Combustion, The Combustion Institute, Pittsburgh, PA, p. 3 (1978).
59. Howard, J., ACS Fuel Division Preprints, 28, #4, p. 241, (1983).
60. Palmer, H.B. and Cullis, H.F., "The Formation of Carbon from Gases in Chemistry and Physics of Carbon", Vol. 1, 265 Marcel Dekker, NY (1965).
61. Howard, J.B. and Longwell, J.P., "Formation Mechanisms of PAH and Soot in Flames", Presented at the Seventh International Symposium on Polynuclear Aromatic Hydrocarbons, Oct. 1982.
62. Howard, J.B., and Williams, G.C., Fourteenth Symposium (International) on Combustion, Pittsburgh, PA p. 929 (1973).
63. Howard, J.B., Twelveth Symposium (International) on Combustion, Pittsburgh, PA, p. 877 (1969).
64. D'Alessio, A, DiLorenzo, A. Beratta, F. Venitozzi, C., Fourteenth Symposium (International) on Combustion, Pittsburgh, PA p. 941 (1973).
65. Longwell, J.P., Reference 57, pg. 37.
66. Calcote, H.F., Reference 57, pg. 197.
67. Calcote, H.F., Combustion and Flame, 42, 215, (1981).
68. Prado, G., Lahaye, J. and Haynes, B.S., Reference, 57, pg. 45.
69. Lahaye, J. and Prado, G., Carbon, 12, 24 (1974).
70. Wagner, H.GG., Reference 57, pg. 77
71. Longwell, J.P. Nineteenth Symposium (International) on Combustion, Pittsburgh, PA p. 1339 (1982).
72. Bittner, J.D., Howard, J.B., Palmer, H.B., Reference 3, pg. 45.
73. Lester, J.W. and Wittis, S.L. Sixteenth Symposium (International) on Combustion, Pittsburgh, PA, pg. 671, (1976).
74. Graham, S.C., Sixteenth Symposium (International) on Combustion, Pittsburgh, PA, pg. 663, (1976).
75. Cundall, R.B., Fussey, D.E., Harrison, A.J. and Lampard, D., 11th International Shock Tube Symposium, Seattle, WA (1977).
76. Kausch, W.J., Clampitt, C.M., Prado, G., Hites, R.A. and Howard, J.B., 18th Symposium (Int) on Combust., The Combust. Institute, p. 1097 (1981).
77. Longanbach, J. and Levy, A., Formation and Oxidation of Synfuel Pyrolysis Products, Proceedings Direct Utilization AR&TD Contractors Review Meeting, p. 43, Pittsburgh, PA April 5-8 (1983).
78. Vranos, A. and Liscinsky, D.S., Fuel, 63, 185, (1984).
79. Law, C.K. and Law, H.K., Combust. Sci. Tech. 12, 207 (1976).
80. Law, C.K. and Law, H.K., Combust. Flame 29, 269-275 (1977).
81. Glassman, I. Brezinsky, K, Gomez, A. and Takahashi, F., ACS, Division of Fuel Chemistry 28, p 252 (1983).
82. Bockhorn, H., Fetting, F., Meyer, U., Reck, R. and Wannemacher, G., 18th Symposium (Int) on Combustion, The Combustion Institute, p. 1137 (1981).
83. Kent, J.H., Jander, H. and Wagner, H., GG., 18th Symposium (Int) on Combustion, The Combustion Institute, p. 1117, (1981).
84. Ottesen, D.K. and Stephenson, D.A., Combustion and Flame, 46, p. 95 (April 1982).
85. Beretta, F. Cavaliere, A., Ciajolo, A., D'Alessio, A., Langella, C., DiLorenzo, A., and Noviello, C., 18th Symposium (Int) on Combustion, The Combustion Institute, p. 1091, (1981).

REPORT HAS BEEN DELIMITED  
AND CLEARED FOR PUBLIC RELEASE  
UNDER DOD DIRECTIVE 5200.20 AND  
RESTRICTIONS ARE IMPOSED UPON  
USE AND DISCLOSURE.

TRIBUTION STATEMENT A  
APPROVED FOR PUBLIC RELEASE,  
TRIBUTION UNLIMITED.